The (Mis)Allocation Channel of Climate Change

Evidence from Global Firm-level Microdata *

Tianzi Liu †
Cornell University

Zebang Xu ‡
Cornell University

Job Market Paper, 2026-2027

December 2025, Updated Regularly

Abstract

Macroeconomic estimates of climate damages are large, yet firm-level micro estimates often appear modest. We reconcile this gap by uncovering a powerful channel—*the impact of extreme temperatures on capital misallocation*—as the major driver of aggregate climate damage. Using global firm-level microdata from 32 countries, we provide causal evidence that a day of extreme heat ($>$ 30°C) increases the dispersion of returns to capital across firms by 0.31 log points, implying a 0.11% annual aggregate TFP loss for the average region–sector. The effect is more pronounced in hotter and more economically developed regions. To explain these mechanisms, we develop a tractable general-equilibrium model of firm dynamics with heterogeneous temperature sensitivities, endogenous adaptation, and time-to-build capital. The model shows that higher climate volatility increases regional dispersion in returns to capital, with amplification driven by heterogeneity in firms' temperature exposure, adaptation, and capital wedges. When estimated by the microdata, climate-induced misallocation lowers global TFP by 12% and accounts for 9% of cross-country productivity differences. Our results shift the focus of climate damage from direct physical productivity losses to *allocative efficiency losses in the cross-section*, highlighting firm heterogeneity as central for measuring aggregate damages and designing effective mitigation and adaptation policy.

*We thank Ryan Chahrour, Kristoffer Nimark, Ivan Rudik, Ezra Oberfield and Mathieu Taschereau-Dumouchel for their continued guidance and support. This paper has also benefited from discussions with Doug Almond, Levon Barseghyan, Johannes Boehm, Tamma Carleton, Julieta Caunedo, Luming Chen, Tomás Domínguez-Iino, Caroline Flammer, Todd Gerarden, Cathy Kling, Kyle Meng, Pablo Ottonello, Will Rafey, Diego Restuccia, Jeffrey Shrader, and seminar participants at Columbia Climate School, Cornell Macro Lunch and Cornell SEERE Seminar, the 2024 Econometric Society NASM, CU Environmental & Resource Economics Workshop, the 2025 NBER Climate Finance PhD Workshop and ASSA 2026. We thank the Structural Transformation and Economic Growth (STEG) Research programme for supporting this research. First draft was circulated on February 16th, 2024.

†Department of Applied Economics and Management, Cornell University (email:tl567@cornell.edu).

‡Department of Economics, Cornell University (email:zx88@cornell.edu).

1 Introduction

Rising temperatures due to climate change are projected to impose very large macroeconomic costs. For example, Burke, Hsiang, and Miguel (2015) estimate losses on the order of roughly 23% of global GDP by 2100, while more recent work finds even larger damages (e.g. about 50% in Bilal and Känzig 2024). These aggregate damages are typically summarized as a deterioration in economy-wide productivity—often modeled or interpreted as losses in aggregate TFP since the early integrated assessment and macro-climate frameworks (e.g. Nordhaus 1992). Meanwhile, direct estimates of firm-level (or plant-level) productivity damages from temperature are much smaller. Addoum, Ng, and Ortiz-Bobea (2020) uses US plant data and finds effects close to zero; the more recent global manufacturing evidence in Nath (2025) suggests modest losses on the order of 1–2% once accounting for adaptation.

Such contrasting magnitude between micro and macro estimates seems puzzling: if average within-firm productivity damage is limited, what microeconomic mechanisms can generate the large aggregate TFP losses implied by macro estimates? In other words, what are the micro channels that map temperature shocks into depressed aggregate productivity?

Our paper proposes and quantifies one such channel: climate-induced *across-firm* capital misallocation. Rather than viewing temperature shocks primarily shifting down the physical productivity frontier, we study how temperature shocks and a warming climate reduce aggregate TFP by increasing dispersion among firms' marginal revenue products of capital (MRPK). To fix ideas, consider a region with two firms: one benefits from heat and one is harmed by it. When an unexpected heat shock arrives, capital input cannot adjust immediately. The heat-loving firm cannot install more capital input fast enough to expand and its MRPK rises; while the heat-averse firm cannot unwind its capital input and its MRPK falls. Therefore dispersion in capital returns increases, and the aggregate output is lower than in a counterfactual world where capital could be adjusted immediately. This two-firm example conveys the basic intuition on climate-induced misallocation: the allocative efficiency and aggregate TFP could increase if more capital is adjusted towards the heat-loving firm.

Our goals in this paper are threefold: first, to causally identify the misallocation channel using temperature shocks and assess its quantitative impact under future climate change scenarios; second, to understand the drivers of climate-induced misallocation from a firm dynamics perspective; and third, to uncover novel implications for climate mitigation and adaptation policies suggested by the misallocation channel.

We begin by developing a climate-TFP accounting framework that allows us to decompose the region-sector level aggregate TFP into the efficient frontier (i.e., technology) and losses from capital misallocation (i.e., allocative inefficiency). The loss of capital misallocation is causally identified from variations in variance of (log) MRPK across firms from exogenous temperature shocks in a given year at the region-sector level. We measure the dispersion in the marginal products within individual sectors from each sub-national region in 30 European countries from the BvD Orbis dataset, and China and India from government-conducted surveys. We construct historical temperature variables using the ERA5-Land gridded daily weather data from the European Centre for Medium-Range Weather Forecasts (ECMWF).

Our estimation reveals a U-shaped pattern: both extreme heat and cold increase measured capital misallocation. Notably, an extra hot day with a temperature above 30°C (86°F) relative to a day in the 5-10°C (41-50°F) range within a year increases MRPK dispersion by about 0.31 log points, which translates to a 0.11% annual aggregate TFP loss. Our findings also suggest that the misallocation channel is a dominant force in aggregate climate damage, given that technical efficiency losses from heat are estimated to be only one-fifth as large as misallocation losses.

Importantly, we estimate the heterogeneous effects of temperature on misallocation and find that the effect of heat shocks on capital misallocation is more pronounced in hotter and more economically developed regions, indicating limited potential for market adaptation to mitigate aggregate misallocation losses as economies develop and climates warm over the long run.

We use our causal estimates to project the impact of global warming on misallocation-induced TFP loss by the end of the century. Under a moderate warming scenario, our estimates indicate that, compared to current income and climate levels, the global cost of climate-induced misallocation will amount to 36.73% of aggregate TFP by the end of the century. Empirically, the projected losses are mostly driven by projected economic development and long-run average temperature increase. The projected losses grow over time as more regions transition into richer and hotter economies with more extreme temperature realizations.

To study the frictions that impede the (ex-post) allocative efficiency of capital under climate change and the role of adaptation, we develop a tractable general-equilibrium model with heterogeneous firms facing time-to-build capital, pre-existing capital wedges, and costly climate adaptation in Section 5. In the model, firms produce differentiated varieties under monopolistic competition. Firms choose next-period capital and adapt production technology endogenously before temperature and idiosyncratic shocks are realized. Specifically, firms adapt by improving on its temperature sensitivity and productivity. The three components of the temperature sensitivity are (i) a persistent product/technology exposure known to the firm; (ii) an endogenous resilience margin chosen by purchasing adaptation resources subject to convex costs; and (iii) an idiosyncratic "random sensitivity" component that captures unpredictable firm-specific disruptions. Temperature affects the log productivity through the deviation from the bliss point, scaled by the firm-specific sensitivity. The household is representative and risk-averse. Every period, the household inelastically supplies labor and elastically supply aggregate adaptation which is costly and scales down the utility from consumption. By assuming markets are complete with respect to aggregate risk, firms discount future cash flows using the households' stochastic discount factor. We then solve the model in closed form using a risk-adjusted perturbation approach around the homogeneous steady state.

The optimality conditions show that in warm regions, a positive heat surprise raises a firm's expected productivity. The gain is larger for firms that produce heat-loving products, or have a higher endogenous sensitivity to temperature; together, these components increase the firm's effective exposure to heat. The cross-sectional differences in firms' capital and adaptation are governed by expected productivity and profitability. Firms anticipating a larger profit base will adapt more and invest more capital. Higher capital wedges reduce capital investment; but the increased capital cost tilts firms toward relatively greater adaptation. Interestingly, firms whose productivity is high when the climate is hot and marginal utility is high, face stronger risk-adjusted

incentives to invest and adapt more.

Solving the model yields a transparent equilibrium decomposition of capital misallocation into a small set of climate-related forces that map directly into cross-firm dispersion in realized returns. A key object is each firm's *effective exposure* to temperature, which combines intrinsic product sensitivity with endogenous resilience chosen through adaptation. Two components then matter for how climate translates into MRPK dispersion. First, a *level (damage-volatility) channel* arises because idiosyncratic climate disruptions become more consequential as a region's climate moves away from the bliss point T^*: the same cross-firm dispersion in disruption risk produces larger realized productivity gaps when temperature is persistently too hot or too cold. Second, a *forecast-and-risk channel* operates because temperature is only imperfectly predictable. Common temperature surprises (forecast errors) and common forecast uncertainty are multiplied by heterogeneous effective exposure, so aggregate "temperature news" becomes heterogeneous realized productivity shocks and heterogeneous risk premia. Finally, pre-existing capital wedges interact with exposure: for a given climate shock, misallocation is larger when high-exposure firms are also the firms facing tighter wedges, and smaller when exposure and wedges are negatively aligned. An important implication is that the same realized heat shock can generate very different increases in misallocation across otherwise similar warm regions, depending on the dispersion of effective exposure and its covariance with wedges.

We discipline these mechanisms using variation at both the firm and the region–sector level. Within region–sector–years, the model predicts that adaptation is *non-homothetic*: the payoff to temperature resilience scales with operating scale, and wedges tilt firms toward adaptation relative to capital. Using the Indian ASI measure of computerized air-conditioning adoption as a proxy for adaptation, we show that adaptation rises with firm capital and with lagged MRPK (our proxy for capital wedges), conditional on common local conditions. We then test the model's heterogeneous-exposure prediction directly by estimating differential MRPK responses to identical heat realizations: interacting temperature bins with firm capital and with lagged MRPK reveals that extreme heat shifts MRPK differentially across firms in ways that line up with the model's exposure-and-adaptation logic. Across region–sectors, the equilibrium decomposition implies two reduced-form patterns. First, TFP volatility is U-shaped in long-run temperature: volatility is minimized in the empirically relevant bliss-point range and rises as climates become more extreme, consistent with the level/damage-volatility channel. Second, imperfect predictability amplifies dispersion: larger mid-range forecast errors and greater forecast uncertainty are both associated with higher MRPK dispersion, consistent with common temperature news being mapped into heterogeneous realized returns through dispersion in effective exposure. Both mechanisms are stronger in hotter and more economically developed regions, consistent with lower adaptation costs raising average adaptation but also steepening the mapping from common temperature risk into dispersion by increasing heterogeneity in effective exposure.

We then estimate the model and quantify the aggregate importance of these channels. We bring the model to firm-level data using a GMM procedure on panels spanning 1,916 regions in the EU, China, and India. The closed-form solution delivers explicit policy rules and an accounting decomposition of MRPK dispersion into (i) wedge-driven dispersion, (ii) idiosyncratic climate damages that scale with distance from T^*, and (iii) forecast-error and forecast-uncertainty

components that are amplified by heterogeneity in effective exposure. The estimation recovers a model-consistent bliss point (around 11°C) and disciplines the dispersion in random climate sensitivity and the regional strength of endogenous adaptation as a function of long-run climate and development. We then combine the estimated mapping with granular climate and mid-range forecast data to extend the sufficient statistics globally (partitioning the world into 4,894 regions) and to trace the evolution of misallocation over time.

Quantitatively, the estimated model implies that climate-induced misallocation is large and is driven primarily by persistent climate differences rather than by short-run forecast errors. Averaged over 1981–2019, the model-implied sufficient-statistics decomposition implies that climate-induced MRPK dispersion lowers global TFP by about *12.5%* in an average year. Roughly *10.38* percentage points of this loss come from the level/random-damage channel (persistent displacement from T^* that magnifies heterogeneous, unpredictable firm-level disruptions), while *2.11* percentage points come from exposure-amplified forecast errors and forecast uncertainty; the wedge–exposure interaction, while potentially important in particular regions, is quantitatively negligible in the global aggregate. Moreover, feeding observed temperature paths and forecast moments into the decomposition shows that warming since 1981 has made the misallocation cost more severe: between 1981 and 2019, climate-induced misallocation lowers global TFP by an additional *4.81* percentage points, with the increase driven overwhelmingly by the level/random-damage channel. Finally, when aggregated to the country-year level, the model-implied misallocation losses track measured TFP in the Penn World Table: the climate-misallocation channel accounts for about 9% of cross-country TFP differences. These findings sharpen the policy takeaway from the model. Because long-run climate displacement and disruption-driven volatility dominate the global misallocation cost, limiting persistent warming is central for protecting allocative efficiency.

We conclude that capital misallocation is a quantitatively important channel through which climate change affects the aggregate economy. Climate-induced misallocation stems from substantial cross-sectional firm-level heterogeneity in temperature sensitivity. The estimated loss due to misallocation across firms is considerable, indicating that the average effect of firm-level productivity loss alone is insufficient to capture the aggregate cost of climate change in the economy. Our results suggest that climate policies that solely target the average effect, while overlooking firm heterogeneity, may have limited efficacy.

Contributions to the Literature. This paper relates to a large literature on measuring the economic damages from temperature shocks and climate change. One canonical approach directly estimates the effect of temperature shocks on aggregate region–sector, country, or global outcomes (see Dell, Jones, and Olken 2012; Burke, Hsiang, and Miguel 2015; Lemoine 2018; Carleton et al. 2022; Nath, Ramey, and Klenow 2023; Bilal and Känzig 2024, among others). Another strand of work estimates average firm- or worker-level productivity losses from climate change (e.g., Zhang et al. 2018; Somanathan et al. 2021), and, more recently, contemporaneous work by Tarsia (2023) and Ponticelli, Xu, and Zeume (2023) examines the heterogeneous effect of heat shocks across firm sizes.[1] Most existing studies interpret their findings as physical productivity losses

1. Studies that focus on other micro-level outcomes and mechanisms include Acharya, Bhardwaj, and Tomunen (2023) on employment, Rode et al. (2022) on labor supply, and Erda (2024) on capital.

resulting from climate shocks. This paper contributes to the literature by taking a conceptually different approach: we focus on how climate change can depress aggregate productivity by causing *across-firm* misallocation of capital. We show that a sizable portion of the aggregate climate impact is *allocative* rather than purely *physical*. At the macro level, our approach uncovers a large causal effect of the misallocation channel induced by climate shocks and projects substantial TFP losses across all future climate-change scenarios. Quantitatively, we document novel heterogeneity in climate-induced misallocation losses across regions with different levels of development and climate conditions. At the micro level, we provide a complementary view to the existing work, showing that key dimensions of firm heterogeneity (e.g., size and distortions) also determine climate-induced allocative frictions in the cross-section.

Second, regarding the macroeconomic modeling of climate change, the existing studies have incorporated climate change into workhorse macro and trade models of efficient economies (Nath 2025; Cruz and Rossi-Hansberg 2023; Bakkensen and Barrage 2021; Casey, Fried, and Gibson 2022; Rudik et al. 2021). Naturally, these models remain silent on the causes and effects of how climate change drives distortions and misallocation of productive factors in the economy. This paper provides a static general equilibrium framework to measure the costs of the temperature-induced misallocation channel using an easy-to-implement sufficient statistics approach. We also build a firm dynamics model to better understand the endogenous mechanisms behind climate-induced misallocation, which stem from *firm-level heterogeneity*, a previously overlooked but quantitatively significant dimension in the climate-macro literature. Very few studies have explored the allocative effect of climate change. Perhaps the closest to our paper is the contemporaneous work by Caggese et al. (2023). They project how the future geographical distribution of temperature shocks in Italy might lead to differential factor productivity of firms across micro-regions under future global warming, and thus allocative efficiency losses could be predicted. In contrast, our paper provides a direct causal estimate of climate impacts on within-region *marginal product dispersion* across firms using historical regional climate variations and firm-level data drom 32 countries globally. It is a direct measure of misallocation (as in Hsieh and Klenow 2009 and Sraer and Thesmar 2023) and captures *all channels* of climate-induced misallocation, not just those stemming from the geographical distribution of temperature.

Finally, we contribute to the literature on misallocation. Since the seminal contributions by Restuccia and Rogerson (2008) and Hsieh and Klenow (2009), a large body of work has studied the aggregate (e.g., Gopinath et al. 2017, David and Zeke 2021) and firm-level (e.g., Asker, Collard-Wexler, and De Loecker 2014, David and Venkateswaran 2019, Baqaee and Farhi 2019) drivers of misallocation. Our paper adds to this literature by demonstrating that environmental factors, such as temperature variations and climate change, are also sources of misallocation and might become increasingly important as global warming worsens. Additionally, our paper connects to a small but growing body of literature that studies the causal identification of the drivers of misallocation using (quasi-)natural experiments (Sraer and Thesmar 2023, Bau and Matray 2023, among others). These studies employ exogenous shocks to explore the causes and consequences of misallocation. We expand on this literature by using exogenous temperature variations to examine the impacts of climate change as a driver of misallocation.

The structure of the paper is organized as follows. Section 2 develops the climate–TFP ac-

counting framework that links temperature shocks to aggregate TFP through technology and capital misallocation. Section 3 describes the firm-level, climate, and forecast datasets and the construction of our key variables. Section 4 presents the empirical strategy and evidence, including average and heterogeneous effects, the technology–versus–misallocation decomposition, and end-of-century projections. Section 5 introduces a firm dynamics model with endogenous adaptation and temperature risk to rationalize the mechanisms. Section 6 tests the model's key implications using firm-level and region–sector evidence. Section 7 estimates the model and quantifies the aggregate importance of the misallocation channel. Section 8 concludes.

2 A Framework for Climate TFP Accounting

In this section, we develop a climate-TFP accounting framework by extending Hsieh and Klenow (2009)'s distorted closed-economy model of heterogeneous firms to flexibly capture climate's firm-specific effects on productivity, demand, and wedges, and to quantify their aggregate implications. We show how climate shocks might affect aggregate productivity through two distinct channels in a distorted economy: lowering micro-level productivity (technology) and increasing the dispersion in marginal products (misallocation). We derive measurable sufficient statistics for both channels, guiding our empirical strategy in Section 4. We deliberately abstract from the exact mechanisms driving climate-related wedges to keep the accounting framework general. Besides the demand and production functional forms, we allow for *arbitrary* climate-impact heterogeneity at the firm-year level. This allows our empirical strategy to measure *all* channels through which climate might lead to aggregate TFP losses without taking a stance on the exact mechanism. We will return to the question of *why* in Section 5.

2.1 Model Preliminaries

Consider an economy comprised of R regions indexed by r, and S sectors indexed by s. We use $n = (r, s)$ to denote a region-sector pair and there are $N = R \cdot S$ region-sector pairs. We focus on the aggregation of firm-level economic activities within a region-sector pair. We allow all fundamentals of firm i in the market $n = (r, s)$ to be arbitrary functions of a general array of (current and past) regional climate conditions, $\tilde{\mathbf{T}}_{rt}$, the aggregate states of the economy, $\tilde{\mathbf{X}}_{nt}$, and the idiosyncratic states of firm i, $\tilde{\mathbf{Z}}_{nit}$. [2] This general representation accommodates a wide range of structural models in our accounting framework.

2.2 Aggregation Model with Micro Effects of Climate Conditions

We now describe the aggregation model and how we incorporate the micro effects of climate conditions into the model.

2. For concreteness, one can think of current climate conditions, $\mathbf{T}_{rt}$, as realizations of daily temperature, precipitation, and other types of extreme weather events. $\mathbf{X}_{nt}$ and $\mathbf{Z}_{nit}$ can be interpreted as other aggregate and firm-specific productivity or demand shocks. The data generating process of $(\tilde{\mathbf{T}}_{rt}, \tilde{\mathbf{X}}_{nt}, \tilde{\mathbf{Z}}_{nit})$ could be stochastic. We use the tilde notation, $(\tilde{\mathbf{T}}_{rt}, \tilde{\mathbf{X}}_{nt}, \tilde{\mathbf{Z}}_{nit})$, to denote the history of realizations up to date t. Also, we do not take a stance on whether $\mathbf{X}_{nt}$ and $\mathbf{Z}_{nit}$ depend on $\mathbf{T}_{rt}$.

Aggregate Region-Sector Production. Total output Y_{nt} for region-sector n is given by a constant elasticity of substitution (CES) production function of differentiated products of measure J_n:[3]

$$Y_{nt} = \left(\int_0^{J_n} B_{nit}^{\frac{1}{\sigma_n}} Y_{nit}^{\frac{\sigma_n - 1}{\sigma_n}} di \right)^{\frac{\sigma_n}{\sigma_n - 1}}, \tag{1}$$

where B_{nit} is a good-specific preference shifter, Y_{nit} denotes the output of firm i and $\sigma_n > 1$ is the elasticity of substitution between products within region-sector n. Profit maximization of industry output producers leads to the inverse demand function for the output of each firm, Y_{nit}:

$$Y_{nit} = B_{nit} Y_{nt} \left[\frac{P_{nit}}{P_{nt}} \right]^{-\sigma_n}, \tag{2}$$

where $P_{nt} = \left(\int_0^{J_n} B_{nit} P_{nit}^{1-\sigma_n} di \right)^{\frac{1}{1-\sigma_n}}$ is the price index in region-sector n. The demand shifter $B_{nit} \equiv B_{ni}(\tilde{\mathbf{T}}_{rt}, \tilde{\mathbf{X}}_{nt}, \tilde{\mathbf{Z}}_{nit})$ is a firm-specific function of climate and economic conditions, capturing how certain goods or services may be less desirable in hotter climates.[4]

Firm-level Production. Each product is produced by a single firm with a constant returns-to-scale Cobb-Douglas production function

$$Y_{nit} = A_{nit} \, K_{nit}^{\alpha_{Kn}} L_{nit}^{\alpha_{Ln}}, \tag{3}$$

where $A_{nit} \equiv A_{ni}(\tilde{\mathbf{T}}_{rt}, \tilde{\mathbf{X}}_{nt}, \tilde{\mathbf{Z}}_{nit})$ denotes physical productivity of firm i, and K_{nit} and L_{nit} are capital stock and labor input employed by i.[5] The parameters satisfy $\alpha_{Kn} + \alpha_{Ln} = 1$. The physical productivity of firm i is modeled as a firm-specific function, $A_{nit} \equiv A_{ni}(\tilde{\mathbf{T}}_{rt}, \tilde{\mathbf{X}}_{nt}, \tilde{\mathbf{Z}}_{nit})$, to capture the different sensitivity to heat (or cold) among different firms within and across various region-sectors. Such heterogeneity can be potentially attributed to the distinct nature of production processes across firms and varying levels of adaptability to climate conditions.[6] Even within the same region-sector, heterogeneity arises: in agriculture, rainfed farms endure more heat stress than irrigated farms (Piao et al. 2010), while in manufacturing, workers with AC installations are less vulnerable to heat than those without (Somanathan et al. 2021).

Wedges. Each firm faces a variety of frictions, including climate-related ones. Regardless of their structural origins and for pure accounting purposes, we describe them as time-varying and firm-specific wedges that distort the static equilibrium decisions of firms operating in otherwise (monopolistically) competitive markets. Subject to the inverse demand and wedges, each firm

3. In theory, J_n, the local variety, could also vary over time to capture how climate might affect firm entry and exit. However, accurately measuring these dynamics within a granular region-sector pair over time is challenging due to data limitations, particularly for cross-country analysis. Therefore, the model does not address this aspect.

4. This is particularly evident in service industries where climate can sharply affect consumer behavior. For example, Zivin and Neidell (2014) find that heat shocks shift Americans from outdoor to indoor recreational activities (e.g., away from recreational fishing as found by Dundas and Haefen 2020). Anecdotal examples in food services include ice-cream parlors versus hot tea shops.

5. A_{nit} is a measure of quantity-based total factor productivity (TFPQ), reflecting the overall efficiency with which the firm uses its inputs to produce units of *physical output*. TFPQ cannot be directly measured in the absence of price or quantity data, barring any additional structural assumptions (see, for example, Bils, Klenow, and Ruane 2021).

6. For the cross-country heterogeneity in productivity damage due to adaptation, see Nath (2025).

i engages in monopolistic competition and optimally chooses its quantity of inputs and price to maximize profits:

$$\max_{P_{nit},K_{nit},L_{nit}} \left(1-\tau_{nit}^{Y}\right)P_{nit}\underbrace{A_{nit}K_{nit}^{\alpha_{Kn}}L_{nit}^{\alpha_{Ln}}}_{Y_{nit}} - \left(1+\tau_{nit}^{K}\right)R_{nt}K_{nit} - \left(1+\tau_{nit}^{L}\right)W_{nt}L_{nit} \tag{4}$$

$$\text{subject to}: Y_{nit} = B_{nit}Y_{nt}\left[\frac{P_{nit}}{P_{nt}}\right]^{-\sigma_n},$$

where R_{nt} is the user cost of capital and W_{nt} is the wage. The output wedge τ_{nit}^{Y} distorts output prices, while the input wedges τ_{nit}^{F} for $F \in \{K, L\}$ changes the effective marginal cost of each factor from its market rate. We assume all firms take these wedges as given for now and turn to model the endogenous nature of these frictions and their relationship with climate change in Section 5. As with demand shifters and productivity, we assume they are firm-specific functions of climate and of the region-sector and firm states.

What might appear as wedges in this accounting exercise? For instance, the output wedge $\tau_{nit}^{Y} \equiv \tau_{ni}^{Y}(\tilde{\mathbf{T}}_{rt}, \tilde{\mathbf{X}}_{nt}, \tilde{\mathbf{Z}}_{nit})$ reflects potential heterogeneity in revenue taxes and markups relative to the Dixit-Stigliz benchmark. These market imperfections could potentially be amplified by temperature shocks changing the local market structure (Ponticelli, Xu, and Zeume 2023). Similarly, input wedges, $\tau_{nit}^{F} \equiv \tau_{ni}^{F}(\tilde{\mathbf{T}}_{rt}, \tilde{\mathbf{X}}_{nt}, \tilde{\mathbf{Z}}_{nit})$, capture all channels through which firms are disincentivized from using inputs $F \in \{K, L\}$, as if they were effectively paying higher factor prices.[7] For instance, firms with more exposure to adverse climate conditions may encounter worse financing frictions (Ginglinger and Moreau 2023). Importantly, in the context of dynamic input choices with adjustment frictions, such as capital, the wedge function $\tau_{ni}^{K}(\tilde{\mathbf{T}}_{rt}, \cdot)$ also accounts for ex-post investment mistakes triggered by unanticipated temperature shocks (e.g. when a heat-averse firm invested too much capital before a severe heat wave), in reminiscence of Asker, Collard-Wexler, and De Loecker (2014) and David, Hopenhayn, and Venkateswaran (2016).

Equilibrium. The total factor supply in the region-sector n are given by $K_{nt} = \sum_i K_{nit}$ and $L_{nt} = \sum_i L_{nit}$.[8] The equilibrium allocations in a region-sector depend on the set of fundamentals $(\{B_{nit}\}_i, \{A_{nit}\}_i, \{\tau_{nit}^{Y}\}_i, \{\tau_{nit}\}_{F;i}, \{F_{nt}\}_F)$. Given preference shifter B_{nit}, physical productivity A_{nit}, output distortions τ_{nit}^{Y}, factor distortions $\{\tau_{nit}^{F}\}_F$ for all firms i, aggregate prices P_{nt}, and total factor supply of K_{nt} and L_{nt}, an equilibrium in region-sector n consists of goods prices P_{nit}, factor prices $\{P_{nt}^{F}\}_F$, and a set of factor allocation $\{F_{nit}\}_{F,i}$ that solves all firms' problems in (4) and all markets clear. We call the equilibrium defined by $(\{B_{nit}\}_i, \{A_{nit}\}_i, \{\tau_{nit}^{Y}\}_i, \{\tau_{nit}\}_{F;i}, \{F_{nt}\}_F)$ the *distorted equilibrium* and the equilibrium defined by $(\{B_{nit}\}_i, \{A_{nit}\}_i, \{0\}_i, \{0\}_{F;i}, \{F_{nt}\}_F)$ the *efficient equilibrium*.[9] We will use an asterisk (*) to denote the efficient equilibrium outcomes.

7. Naturally, for a firm to be active, it is necessary that all prices are positive, which requires $1 - \tau_{nit}^{Y} > 0$ and $1 + \tau_{nit}^{F} > 0$.

8. The total factor supply is treated as exogenously given every period. We could also model the total factor supply to be region-sector specific functions of the form: $L_{nt} := L_n(\tilde{\mathbf{T}}_{rt}, \cdot), K_{nt} := K_n(\tilde{\mathbf{T}}_{rt}, \cdot)$, but this plays little role in our TFP accounting.

9. Again, we stress that, in the accounting framework, efficiency is defined in a static and unconstrained sense.

Wedges and Misallocation of Inputs. As these wedges distort firm-level input choices, they also create measurable differences in marginal products across firms. Appendix A shows that for any input $F \in \{K, L\}$, the firm's optimality condition implies that the marginal revenue product of factor F (MRPF),

$$\text{MRPF}_{nit} = \alpha_{F_n} \frac{\sigma_n - 1}{\sigma_n} \frac{P_{nit} Y_{nit}}{F_{nit}} = \frac{1 + \tau^F_{ni}(\tilde{\mathbf{T}}_{rt}, \cdot)}{1 - \tau^Y_{ni}(\tilde{\mathbf{T}}_{rt}, \cdot)} P^F_{nt}, \tag{5}$$

is proportional to the firm's revenue-to-factor ratio and must equal the wedge-adjusted market price, $\frac{1+\tau^F_{ni}(\tilde{\mathbf{T}}_{rt},\cdot)}{1-\tau^Y_{ni}(\tilde{\mathbf{T}}_{rt},\cdot)} P^F_{nt}$. A higher input wedge $1 + \tau^F_{ni}(\tilde{\mathbf{T}}_{rt}, \cdot)$ increases the effective cost of factor F, discouraging its use and thus elevating MRPF. Conversely, a lower output wedge $\tau^Y_{ni}(\tilde{\mathbf{T}}_{rt}, \cdot)$ raises the effective price of the firm's output, encouraging the use of factor F and consequently lowering MRPF. Therefore, heterogeneity in how wedges respond to climate change can alter the cross-sectional dispersion of MRPF—often termed "misallocation"—as inputs may not flow to the firms that would use them most efficiently. The wedges would thus also change the size of the firm. By writing down firm i's sales share θ_{nit} in n,

$$\theta_{nit} = \frac{P_{nit} Y_{nit}}{\int_0^{J_n} P_{nit} Y_{nit} di} = \frac{B_{nit} A_{nit}^{\sigma_n - 1} \frac{\left(1-\tau^Y_{nit}\right)^{(\sigma_n - 1)}}{\prod_{F \in \{K,L\}} \left(1+\tau^{Fn}_{nit}\right)^{\alpha_{Fn}(\sigma_n - 1)}}}{\int_0^{J_n} B_{nit} A_{nit}^{\sigma_n - 1} \frac{\left(1-\tau^Y_{nit}\right)^{(\sigma_n - 1)}}{\prod_{F \in \{K,L\}} \left(1+\tau^{Fn}_{nit}\right)^{\alpha_{Fn}(\sigma_n - 1)}} di}, \tag{6}$$

we see that, unsurprisingly, a positive input wedge makes the firm inefficiently small and negative output wedge makes the firm inefficiently large. We proceed to explicitly characterize how these wedges lead to the equilibrium (mis-)allocation of factors as follows.

Proposition 1 (Equilibrium (Mis)Allocation.) *In the presence of factor distortions τ^F_{nit} only, the (log) ratio of firm i's distorted and efficient equilibrium allocation of factor, $\frac{F_{nit}}{F^*_{nit}}$,*

$$\log\left(\frac{F_{nit}}{F^*_{nit}}\right) = \underbrace{-\log\left(\frac{1+\tau^F_{nit}}{1+\tau^F_{nt}}\right)}_{\substack{\textit{relative wedge} \\ \textit{effect}}} + \underbrace{\log\left(\frac{\theta_{nit}}{\theta^*_{nit}}\right)}_{\substack{\textit{size} \\ \textit{effect}}} \tag{7}$$

is decreasing in the ratio of firm i's own factor wedge comparing to the aggregate factor wedge , and increasing in the ratio of the firm's sales share θ_{nit} comparing to its efficient counterfactual θ^*_{nit}. Moreover, the efficient allocation of inputs, $\frac{F^*_{nit}}{F_{nt}} = \theta^*_{nit} = \frac{B_{nit} A_{nit}^{\sigma_n - 1}}{\int_0^{J_n} B_{nit} A_{nit}^{\sigma_n - 1} di}$, is entirely determined by firm i's relative preference shifter and physical productivity within the region-sector and aligns with sales share θ^*_{nit}.

Proof. See Appendix A.2. ■

Proposition 1 highlights the two effects through which wedges distorts the equilibrium allocation of factor F. The *relative wedge effect* captures how a higher input wedge on F makes it more expensive firm i pays for factor F relative to the region-sector's average. Firm i is more discouraged from employing factor F and thus ends up with using less of it than under the efficient benchmark. The *size effect* captures how any wedges firm i faces would make the firm inefficiently small, leading to a smaller sales share θ_{nit} compared to efficient level θ^*_{nit} and thus suppresses the

usage of all inputs.

First, they shift the efficient allocation by directing more capital to firms that suffer less heat damage or produce goods with higher demand under hot conditions. Second, they can introduce heterogeneous frictions in the capital market—such as adjustment costs or financing constraints—that distort firms' cost structures and potentially prevent some productive firms from securing an optimal amount of capital.

2.3 Aggregation, TFP Decomposition and Cost of Misallocation

We proceed to perform aggregation in this accounting framework. With a continuum of firms in each region-sector, we adopt the aggregation notion of Krusell and Smith (1998) that the distribution of firm-level fundamentals $\tilde{\mathbf{Z}}_{nit}$ (over i) can be summarized by a finite set of moments and stacked into the aggregate states of the economy $\tilde{\mathbf{X}}_{nt}$. Using a second-order approximation, we show how dispersion in micro wedges maps into aggregate productivity losses:

Proposition 2 (Aggregation and TFP Decomposition.) *Each region-sector n admits an aggregate production function of the form*

$$Y_{nt} = TFP_{nt} K_{nt}^{\alpha_{Kn}} L_{nt}^{\alpha_{Ln}}, \tag{8}$$

where, up to a second-order approximation, the region-sectoral aggregate Total Factor Productivity $TFP_{nt} := TFP_n\left(\tilde{\mathbf{T}}_{rt}, \tilde{\mathbf{X}}_{nt}\right)$ can be decomposed as follows:

$$\begin{aligned}
\log TFP_n(\tilde{\mathbf{T}}_{rt}, \cdot) = {} & \underbrace{\frac{1}{\sigma_n - 1} \log \left[\mathbb{E}_i \left[B_{ni}(\tilde{\mathbf{T}}_{rt}, \cdot) \left(A_{ni}(\tilde{\mathbf{T}}_{rt}, \cdot) \right)^{\sigma_n - 1} \right] \right]}_{\textit{Technology}(\log TFP^E_{nt})} \quad + \quad \frac{1}{\sigma_n - 1} \log J_n \\
& \textit{Misallocation Loss} \left\{ \begin{array}{l}
\underbrace{-\frac{\sigma_n}{2} \operatorname{var}_{\log\left(1-\tau^Y_{ni}\right)}(\tilde{\mathbf{T}}_{rt}, \cdot)}_{\textit{Output Wedge Dispersion}} \underbrace{- \sum_{F \in \{K,L\}} \frac{\alpha_{Fn} + \alpha_{Fn}^2(\sigma_n - 1)}{2} \operatorname{var}_{\log\left(1+\tau^F_{ni}\right)}(\tilde{\mathbf{T}}_{rt}, \cdot)}_{\textit{Factor Wedge Dispersion}} \\
\underbrace{+ \sigma_n \sum_{F \in \{K,L\}} \alpha_{Fn} \operatorname{cov}_{\log\left(1-\tau^Y_{ni}\right), \log\left(1+\tau^F_{ni}\right)} \left(\tilde{\mathbf{T}}_{rt}, \cdot \right)}_{\textit{Output-Factor Mixed Distortion}} \\
\underbrace{- (\sigma_n - 1) \alpha_{Kn} \alpha_{Ln} \operatorname{cov}_{\log\left(1+\tau^K_{ni}\right), \log\left(1+\tau^L_{ni}\right)} \left(\tilde{\mathbf{T}}_{rt}, \cdot \right)}_{\textit{Factor Mixed Distortion}}.
\end{array} \right.
\end{aligned} \tag{9}$$

Proof. See Appendix A.3. ■

Proposition 2 provides a general second-order expression for aggregate TFP in an economy with a continuum of firms. Fixing variety J_n, it decomposes the aggregate TFP into two terms: *technology* and *misallocation loss*. The technology component, $\log \text{TFP}^E_{nt} = \frac{1}{\sigma_n - 1} \log \left[\mathbb{E}_i \left[B_{ni}(\tilde{\mathbf{T}}_{rt}, \cdot) \left(A_{ni}(\tilde{\mathbf{T}}_{rt}, \cdot) \right)^{\sigma_n} \right] \right]$ is a CES aggregation of demand shifter and physical productivity of all firms. This represents the production possibility frontier of the economy. We label this term *technology* in the spirit of Basu and Fernald (2002) and Baqaee and Farhi (2019).

The rest of the terms represent the TFP cost of wedges in the economy, referred to as *misallocation loss*. All the variance and covariance terms are also smooth functions of climate and other aggregate states. They describe how these conditions would alter the distribution of wedges over the cross-section of firms. Dispersion in output wedges $\text{var}_{\log\left(1-\tau_{ni}^{Y}\right)}$ and factor input wedges $\text{var}_{\log\left(1+\tau_{ni}^{F}\right)}$ will both lead to dispersion in the marginal revenue products across firms, creating more misallocation of factors and lowering region-sector TFP. The impact of $\text{var}_{\log\left(1+\tau_{ni}^{F}\right)}$ on TFP are increasing in σ_n and α_{F_n}, as higher product substitutability and larger factor share both imply larger gains of reallocation for a given factor wedge dispersion. Furthermore, the interactions of wedges also impact productivity. All else being equal, more productivity losses occur when (1) firms facing higher tax on output are also those enduring higher input prices ($\text{cov}_{\log\left(1-\tau_{ni}^{Y}\right),\log\left(1+\tau_{ni}^{F}\right)} < 0$), and (2) firms experiencing capital distortions are also more likely to face higher labor distortions ($\text{cov}_{\log\left(1+\tau_{ni}^{K}\right),\log\left(1+\tau_{ni}^{L}\right)} > 0$). These interactions are often referred to as "mixed" distortions.

2.4 Decomposing the Impact of Climate Change on Aggregate TFP

Since all moments in Equation 9 are smooth functions of climate conditions $\tilde{\mathbf{T}}_{rt}$, we can decompose the (first-order) total impact of climate change on TFP via a set of measurable derivatives for each relevant moment. We formalize this in a case when only capital wedges are present.

Benchmark case: only capital wedges are present. We now consider a benchmark case where only capital wedges are present, as is common in the misallocation literature (see, for example, Asker, Collard-Wexler, and De Loecker 2014, David and Venkateswaran 2019, and Sraer and Thesmar 2023). This focus stems from the view that capital, unlike labor, is a more dynamic input that is often financed externally, requires significant adjustment costs, and typically cannot be reallocated on short notice. These features magnify distortions in capital usage—such as through credit frictions or investment irreversibility—and lead to potentially larger and more persistent misallocation relative to labor (Gorodnichenko et al. 2018). Consequently, how and why capital misallocation is affected by climate conditions will be the main focal point throughout the paper.

When the capital wedge is the only source of distortions in the economy within region-sector n, the MRPK of each firm i satisfies that: $\text{MRPK}_{nit} = \alpha_{Kn}\frac{\sigma_n-1}{\sigma_n}\frac{P_{it}Y_{it}}{K_{it}} \propto (1+\tau_{nit}^{K})R_{nt}$. The dispersion of capital wedges is therefore given by the variance of log(MRPK) across firms,

$$\text{var}(\log(1+\tau_{nit})) = \text{var}(mrpk_{nit}) = \text{var}\left(\log\left(\frac{P_{it}Y_{it}}{K_{it}}\right)\right), \tag{10}$$

where we define $mrpk_{nit} = \log(\text{MRPK}_{nit})$. Equation 10 shows that the cross-sectional variance of (log) capital wedges across firms is identical to the dispersion of (log) MRPK, which can be computed via the variance of log sales over capital stock given the common Cobb-Douglas technology within the region-sector-year. We can now formalize how climate conditions affect aggregate TFP via the following Lemma:

Lemma 1 *With only capital wedges, the (first-order) impact of climate conditions on the aggregate TFP of*

region-sector $n = (r, s)$ can be decomposed as:

$$\begin{aligned}\frac{d \log TFP_n(\tilde{\mathbf{T}}_{rt}, \cdot)}{d\tilde{\mathbf{T}}_{rt}} &= \frac{d\ Technology_{nt}}{d\tilde{\mathbf{T}}_{rt}} - \frac{d\ Misallocation\ Loss_{nt}}{d\tilde{\mathbf{T}}_{rt}} \\ &= \frac{1}{\sigma_n - 1} \frac{d \log \mathbb{E}_i \left[B_{ni}(\tilde{\mathbf{T}}_{rt}, \cdot) \left(A_{ni}(\tilde{\mathbf{T}}_{rt}, \cdot) \right)^{\sigma_n - 1} \right]}{d\tilde{\mathbf{T}}_{rt}} \\ &\quad \underbrace{- \frac{\alpha_{Kn} + \alpha_{Kn}^2 (\sigma_n - 1)}{2} \frac{d \operatorname{var}_{mrpk_{ni}}(\tilde{\mathbf{T}}_{rt}, \cdot)}{d\tilde{\mathbf{T}}_{rt}}}_{The\ Misallocation\ Channel},\end{aligned} \tag{11}$$

where $\operatorname{var}_{mrpk_{ni}}(\tilde{\mathbf{T}}_{rt}, \tilde{\mathbf{X}}_{rt}) \equiv \operatorname{var}_{\log(1+\tau_{ni}^K)}(\tilde{\mathbf{T}}_{rt}, \tilde{\mathbf{X}}_{rt})$ denotes a function capturing how n's (log)MRPK dispersion across firms changes with climate and economic conditions.

Lemma 1 shows that the total first-order effect of climate on aggregate TFP can be fully described by changes in (i) *technology* and (ii) *capital misallocation*. The technology channel boils down to the estimation of the (semi-)elasticity of the average firm's demand-adjusted productivity to climate. More importantly to the focus of our paper, measuring the cost of climate-induced misallocation reduces to estimating $\frac{d \operatorname{var}_{mrpk_{ni}}(\tilde{\mathbf{T}}_{rt}, \cdot)}{d\tilde{\mathbf{T}}_{rt}}$—"the misallocation channel." This result also offers practical guidance for the reduced-form approach in Section 4, which focuses on the causal estimation of $\frac{d \operatorname{var}_{mrpk_{ni}}(\tilde{\mathbf{T}}_{rt}, \cdot)}{d\tilde{\mathbf{T}}_{rt}}$.

In theory, the derivatives of our structural objects with respect to climate conditions are globally well-defined and could vary with the long-run evolution of climate and development. However, in practice, they can only be well estimated with respect to the observed equilibrium allocations. We will address this limitation explicitly in Section 4.4 to capture the heterogeneous effect arising from long-term climate conditions and economic development.

3 Data

3.1 Global Firm-level Microdata

We compile a global sample of firm-level microdata from both developed and developing economies that include 30 European countries, China and India, which covers 38.6% of world GDP. The firm-level data for the 30 European countries are sourced from Bureau van Dijk's (BvD) Orbis database, while the data for China and India are obtained from government-conducted surveys, the China National Bureau of Statistics (NBS) Annual Survey of Industrial Firms, and the India Annual Survey of Industries (ASI). These datasets provide comprehensive financial accounting information, including revenue, fixed assets, wage bills, and employment figures. The three datasets are widely utilized in the literature and could be regarded as nationally representative.[10]

10. A significant advantage of using the Orbis database for European countries is that company reporting is regulatory, ensuring comprehensive coverage even for small private firms. The China NBS surveys cover all industrial firms with annual sales exceeding nominal CNY 5 million (approximately USD 0.61 million) from 1998 to 2007, representing over 90.7% of total output. The India ASI includes large plants employing more than 100 workers and a random sample of smaller plants registered under the Indian Factories Act, ensuring representativeness at the state and industry levels.

Table B.1 provides a comprehensive list of countries, year coverage, and data sources for the three datasets. For all datasets, we harmonize the sectoral classifications of all firms into eight major divisions according to the U.S. Standard Industrial Classification (USSIC) code.[11] Regions are defined to be the NUTS 3 regions in Europe, prefectures in China, and districts in India. The size of these regions is close to the size of a county in the US.

Our primary economic variables of interest are the sufficient statistics of firm-level activities that map directly into aggregate TFP at the region-sector-year level, in particular, the variance of marginal revenue product of capital across firms. Thus, for all datasets we use, we restrict ourselves to work with firm-year observations that report data on both revenue and capital stock. We measure revenue $P_{it}Y_{it}$ with the reported operating revenue in both Orbis and China NBS data, and the reported total sales in India ASI. We use the book value of gross fixed assets as a measure of firm-level capital stock K_{it}.[12] For each country, we trim the observations of extreme values of MRPK at 0.1%.

For all reduced-form analysis using region-sector-year level sufficient statistics, we restrict our sample to the region-sector-year pairs with more than 30 firm-year observations of revenue and capital stock data, to minimize the noises in the variance measures and preserve log-normality in the data. To make sure variations in these sufficient statistics are not due to changes in data collection patterns and measurement errors, we also drop the observations after which there are sudden jumps in the number of firms and aggregate sales in the region-sector. The final region-sector sample is an unbalanced sample consisting 124,567 of region-sector-year observations, covering 76,826,956 firm-year observations. For the firm-level analysis in Section 4, we include all firm-year observations in the raw data after trimming the 0.1% extreme values of all firm-level dependent variables and covariates. Below, we provide a brief overview of each of the datasets.

BvD Orbis. The firm-level data for the 30 European countries are drawn from Orbis, a database maintained by Bureau van Dijk (BvD). Orbis originates from administrative records collected at the firm level, primarily by each country's local Chambers of Commerce. A significant advantage of focusing on European countries with Orbis is that company reporting is regulatory, even for small private firms. It covers firms from all sectors and approximately 99 percent of the companies included are private entities.

To organize and clean the Orbis dataset, we follow the approach in Kalemli- Özcan et al. (2024), Gopinath et al. (2017), and Nath (2025). A notable departure from the papers cited earlier lies in our method for expanding MRPK's coverage. We include firms that have complete data on revenue and capital (fixed assets) while allowing for variability in the extent of coverage for other variables such as material costs, wage bills, and employee numbers.[13] Each firm in the Orbis data has its associated USSIC sector code, and its various address information can be matched with a NUTS3 region in Europe. Different countries in Orbis have different years of data coverage,

11. The industries included are agriculture, mining, construction, manufacturing, transportation & utilities, wholesale trade, retail trade, finance, insurance, and real estate(FIRE) and Services. We choose the SIC classification mainly due to its availability in the Orbis Data.

12. The only exception is India ASI, which reports the book value of net fixed assets in a much more consistent manner while the gross values are reported with a major amount of missing values.

13. Nath (2025) keeps the firms with complete revenue and labor data, while Gopinath et al. (2017) use a more restrictive sample that only preserves observations having all production-related information in south European countries.

detailed in Table B.1. We use the sample period of 1998-2018.

China NBS. The annual firm-level data for China is derived from surveys conducted by the National Bureau of Statistics (NBS) in China. These surveys encompass all industrial firms with annual sales exceeding nominal CNY 5 million (approximately USD 0.61 million) from 1998 to 2007. Such firms are commonly referred to as "above-scale" industrial firms.[14] The NBS data includes sectors such as mining, manufacturing, and utilities, with manufacturing constituting more than 90% of the total observations in the dataset. In processing the NBS data, we follow the methodology outlined in Zhang et al. (2018). Each firm in the dataset is categorized using a four-digit Chinese Industry Classification (CIC) code and is harmonized to the USSIC division level. Each firm's reported location can be mapped into a prefecture-level division. We only use the sample period of 1998-2007 due to inconsistent reporting after 2008 as discussed in Brandt, Van Biesebroeck, and Zhang (2014) and Nath (2025).

India ASI. Our data for India is drawn from India's Annual Survey of Industries (ASI). ASI is a census of large plants employing more than 100 workers and a random sample of about one-fifth of smaller plants that are registered under the Indian Factories Act.[15] The sampling procedure assures representativeness at the state and industry levels. Almost all plants included in the ASI data are in the manufacturing sector. We match the plants to the Indian districts following the approach of Somanathan et al. (2021). From 2001 to 2014, ASI also collects whether the plant is AC equipped which we will utilize as a proxy variable for a firm's adaptability. We use the sample period of 1998 to 2018.

3.2 Weather and Forecast Data

Climate. For climate data, we use the land component of the European ReAnalysis, known as ERA5-Land (Sabater 2019), produced by the European Centre for Medium-Range Weather Forecasts (ECMWF). ERA5-Land is a reanalysis dataset that combines historical observations with models to create a consistent time series of various climate variables. A main advantage of ERA5-Land is its enhanced temporal and horizontal resolution. It provides hourly data on surface variables at a spatial resolution of 0.1°longitude $\times$ 0.1°latitude (approximately 9 km), covering the entire world. Such high resolution allows for a clearer depiction of the spatial patterns of surface temperature between neighboring locations.

Our analysis uses variables of air temperature at 2 meters above the land surface. We aggregate daily average temperatures[16] up to the annual level. Specifically, in our main specification, we bin daily temperature every 5°C from -5°C to 30°C. Each temperature bin counts the number

14. Brandt, Van Biesebroeck, and Zhang (2014) shows that when comparing to the 2004 NBS census of industrial firms that covers all industrial plants in China, these above-scale firms in the sample account for over 90.7% of the total output.

15. As noted by Allcott, Collard-Wexler, and O'Connell (2016), large plants in the census scheme are defined as factories with 100 or more workers in all years except 1997-2003 when it included only factories with 200 or more workers. The sampling scheme for smaller registered plants included one-third of factories until 2004 and one-fifth since then.

16. The daily average temperature is the simple geometric average of the maximum and minimum temperatures. The daily maximum temperature is identified by the highest value among the hourly temperatures, and the daily minimum temperature is the lowest recorded value.

of days in a year when the daily average temperature falls within specific temperature ranges. This is calculated for every region in each year.

Figure 1a plots the difference of the number of hot days above 25°C in a year between periods of our sample firm coverage, 1999-2008 and 2009-2018, and the baseline periods, from 1951 to 1980. The dark red color represents an increase of more than 13.2 days in a year with temperatures above 25°C. Figure 1b depicts the daily temperature distributions in baseline periods, sample periods, and the projection year of 2100. The global warming trend reveals that the number of days above 25 has increased, and the number of days below 10 has reduced in each country in the past decades. The temperature distribution shifts rightward when we compare across and within countries, as climates grow warmer.

The use of temperature bins in our analysis better conceptualizes climate. Because climate change represents a long-term shift in weather patterns, the year-to-year variation in the whole temperature distribution offers a more accurate depiction of climate change than merely examining year-to-year variations in mean temperature. A key feature of climate change is the increased frequency of extreme heat events (Oudin Åström et al. 2013; Christidis, Mitchell, and Stott 2023), therefore the increase in the number of extreme hot bins, indicative of a rightward shift in the tail of the weather distribution, captures the idea of global warming more accurately.

Projection and Forecast. We collect global projection data computed by the sixth phase of the Coupled Model Intercomparison Project (CMIP6).[17] We use the SSP3-4.5 experiment in our main analysis, which is based on the SSP3 scenario that involves high mitigation and adaptation challenges, along with the RCP4.5 pathway with a radiative forcing of 4.5 $\mathrm{W/m^2}$ in the year 2100. The SSP3-4.5 scenario represents the intermediate greenhouse gas emissions level with modest mitigation policy and is described as a more likely path (O'Neill et al. 2016).

For weather forecast data, we collect the long-range (seasonal) forecast from ECMWF (Copernicus Climate Change Service and Climate Data Store 2018), which provides information about atmospheric and oceanic conditions up to seven months into the future. The forecast data have a spatial resolution of 1°longitude by 1°latitude.[18] We collect forecast daily maximum and minimum 2m temperature from the first day of each month from January to December with forecasts up to 30 days measured in 724 lead-hours.

3.3 Other Data

Regional GDP. We collect regional-level global GDP data from DOSE (Wenz et al. 2023). We then clean and map global GDP data to our firm and weather datasets using spatial coordinates. This involves aligning different geographical units with administrative divisions like NUTS, prefectures, and districts.

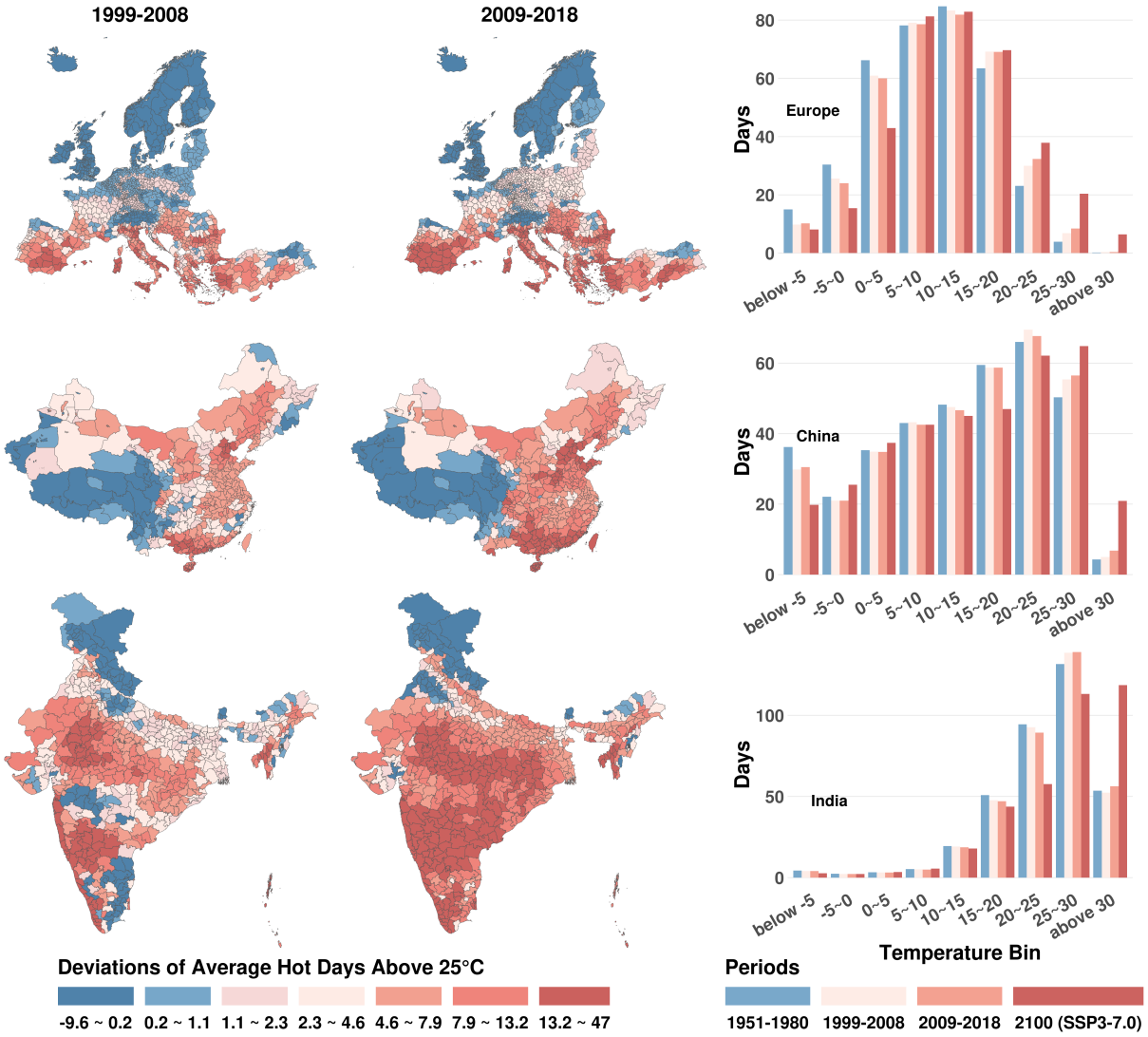
17. We use the GFDL-ESM4 model with a 1-degree nominal horizontal resolution produced by the National Oceanic and Atmospheric Administration, Geophysical Fluid Dynamics Laboratory (NOAA-GFDL).

18. From 1981 to 2016, the forecast values were hindcasts generated with a 25-member ensemble. Starting in 2017, they are forecasts produced monthly with a 51-member ensemble. These ensembles are run on the first day of each month, providing forecasts for up to seven months ahead.

Income Projection Projections of national income per capita are collected from the SSP Database, using the OECD EnvGrowth model (Dellink et al. 2017) hosted by the International Institute for Applied Systems Analysis.

Figure 1: Climates of our sample regions

(a) Number of Hot Days Deviation Relative to 1951-1980 (b) Average Daily Temperature Distribution



Notes: Figure 1a plots the difference of average number of days above 25°C between sample periods and baseline periods. The baseline period is from 1950 to 1980. The sample periods consist of two parts, 1999 to 2008, and 2009 to 2018. We calculate the 10-year average number of days above 25°C and deduct the 30-year baseline average number of days to obtain the difference. Figure 1b plots the average daily temperature distributions for baseline periods 1950-1980, two sample periods, and the projection year of 2100 under the SSP3-7.0 scenario.

4 Estimating the Misallocation Channel of Climate Change

4.1 Mapping to Estimation

We aim to estimate the *total* causal effect of climate shocks on capital misallocation, measured by the dispersion of the marginal revenue product of capital (MRPK). Following Deschênes and

Greenstone (2011) and Carleton et al. (2022), we exploit interannual variation in daily temperature distributions grouped into $5°C$ bins. Specifically, we construct current climate conditions as a vector $\mathbf{T}_{r,t} = \left\{\text{Tbin}_{r,t}^{<-5°\text{C}}, \text{Tbin}_{r,t}^{-5\sim0°\text{C}}, ..., \text{Tbin}_{r,t}^{>30°\text{C}}\right\}$, where each element $\text{Tbin}_{r,t}^{b}$ counts the number of days region r's average temperature falls within bin b (ranging from below $-5°$C to above $30°$C) in year t. This approach leverages detailed daily temperature data and captures nonlinear climate effects with linear representations.

Our baseline panel regression equation is the following:

$$\sigma^2_{mrpk_{(s,r),t}} = \sum_{b \in B/\{5\sim10°\text{C}\}} \lambda^{b}_{\sigma^2_{mrpk}} \times \text{Tbin}^{b}_{r,t} + \boldsymbol{\delta}_{\sigma^2_{mrpk}} \mathbf{X}_{s,r,t} + \alpha_{c(r),t} + \eta_{s,r} + \varepsilon_{r,s,t}, \tag{12}$$

which serves as the empirical counterpart to the first-order approximation of $\text{var}^{mrpk_i}_{(s,r)}(\tilde{\mathbf{T}}_{r,t}, \tilde{\mathbf{X}}_{s,r,t})$ around the region-sector steady states.[19] $\sigma^2_{mrpk_{(s,r),t}}$ measures the variance of (log) MRPK across firms within region-sector (s,r) for year t. We control for region–sector fixed effects $\eta_{s,r}$ and country–year fixed effects $\alpha_{c(r),t}$, which absorb differences in baseline development or long-run climate conditions across region–sector cells as well as any macro-level shocks that could simultaneously affect all regions within the same country and year. With both sets of fixed effects included, the coefficients $\lambda^{b}_{\sigma^2_{mrpk}}$ on the temperature bins are identified from within-region–sector variation in temperature shocks over time, net of any country-year-level aggregate changes. Such conditional variations in climate are presumably as-good-as-random. Standard errors are clustered at the region level to allow for arbitrary within-region correlation of the error term across sectors or over time.[20] Equation (12) estimates the average causal effects in the sample, with heterogeneous effects across regions and sectors analyzed separately in Section 4.4.

The coefficients $\lambda^{b}_{\sigma^2_{mrpk}}$ measure the average causal effect of one additional day in temperature bin b on contemporaneous MRPK dispersion, relative to the baseline bin of 5°C to 10°C range (which is normalized to zero).[21] $\mathbf{X}_{s,r,t}$ is a control vector that includes the log number of firms, average log sales, and average log MRPK. The first two variables control for sample size and business-cycle fluctuations, respectively. By controlling for average (log) MRPK, we aim to show that climate's impact on MRPK *dispersion* is mostly not driven by the similar mechanisms through which climate affects *average* productivity.[22] However, our preferred specification omits these controls since climate shocks also plausibly influence these variables $\left(d\mathbf{X}_{s,r,t}/d\mathbf{T}_{r,t} \neq 0\right)$ and might bias the estimates of $\lambda^{b}_{\sigma^2_{mrpk}} = \mathbb{E}\left[d\sigma^2_{mrpk_{(s,r),t}}/d\mathbf{T}_{r,t} | \alpha_{c(r),t}, \eta_{s,r}\right]$ as the average total effect (conditional

19. We apply a first-order Taylor expansion around the region–sector steady state $\left(\overline{\text{var}^{mrpk_i}_{(s,r)}}, \overline{\tilde{\mathbf{T}}_r}, \overline{\tilde{\mathbf{X}}_{s,r}}\right)$:

$$\begin{aligned}\text{var}^{mrpk_i}_{(s,r)}\left(\tilde{\mathbf{T}}_{r,t}, \tilde{\mathbf{X}}_{s,r,t}\right) &= \overline{\text{var}^{mrpk_i}_{(s,r)}} + \boldsymbol{\lambda}^{s,r}_{\sigma^2_{mrpk}}\left(\tilde{\mathbf{T}}_{r,t} - \overline{\tilde{\mathbf{T}}_r}\right) + \boldsymbol{\delta}^{s,r}_{\sigma^2_{mrpk}}\left(\tilde{\mathbf{X}}_{s,r,t} - \overline{\tilde{\mathbf{X}}_{s,r}}\right) + O\left(\left\|\left(\tilde{\mathbf{T}}_{r,t} - \overline{\tilde{\mathbf{T}}_r}, \tilde{\mathbf{X}}_{s,r,t} - \overline{\tilde{\mathbf{X}}_{s,r}}\right)\right\|^2\right) \\ &\approx \boldsymbol{\lambda}^{s,r}_{\sigma^2_{mrpk}} \tilde{\mathbf{T}}_{r,t} + \boldsymbol{\delta}^{s,r}_{\sigma^2_{mrpk}} \tilde{\mathbf{X}}_{s,r,t} + \eta_{s,r},\end{aligned}$$

where $\eta_{s,r}$ represents time-invariant region–sector effects. For our baseline specification in (4.1), we estimate the average effects in the sample.

20. Throughout the paper, regions are defined as NUTS 3 areas in Europe, provinces in China, and first-level administrative divisions in India.

21. Since all $\text{Tbin}^{b}_{r,t}$ in a year sum up to 365 days, we must omit one temperature bin to avoid perfect collinearity. We choose the 5–10°C bin as the omitted category.

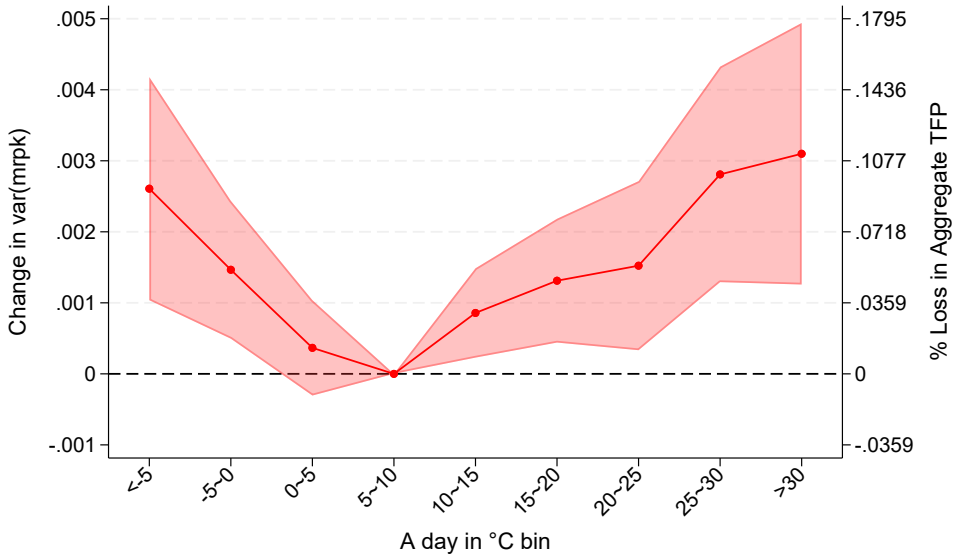
22. Controlling for average MRPK also captures the average financial constraints across firms.

on fixed effects).[23]

4.2 Average Effects of Temperature on Capital Misallocation

The baseline estimates of $\hat{\lambda}^b_{\sigma^2_{mrpk}}$ and the implied TFP losses are reported in columns (1) and (5) of Table 1 and shown in Figure 2. We convert $\hat{\lambda}^b_{\sigma^2_{mrpk}}$ into implied TFP losses using the relationship $-\frac{\alpha_{Kn}+\alpha^2_{Kn}(\sigma_n-1)}{2}\hat{\lambda}^b_{\sigma^2_{mrpk}}$ in Equation (11), adopting the standard parameter values of capital share $\alpha_{Kn} = 0.35$ and elasticity of demand $\sigma_n = 4$ (Redding and Weinstein 2020) for all region-sector n.

Figure 2: Estimated impact of daily temperature shocks on annual MRPK dispersion and implied TFP loss



Notes: This figure shows the aggregate impact linking annual MRPK dispersion and TFP loss to average daily temperatures. The formula for computing TFP loss from misallocation is $-\frac{\alpha_{Kn}+\alpha^2_{Kn}(\sigma_n-1)}{2}\hat{\lambda}^b_{\sigma^2_{mrpk}}$. The estimation is normalized by setting the range of 5°C - 10°C as the reference category. Therefore, each $\lambda^b_{\sigma^2_{mrpk}}$ represents the estimated effect of an additional day in temperature bin b on annual MRPK dispersion or TFP loss, relative to a day with temperatures between 5°C - 10°C. The figure also includes the 90% confidence interval for these estimates where standard errors are clustered at the region level.

The estimated coefficients reveal that MRPK dispersion and the inferred TFP loss from temperature-induced misallocation peak at the most extreme temperatures, both coldest and hottest. This observed U-shape pattern between MRPK dispersion and temperature can also be translated into an inverted U-shape pattern between TFP and temperature, a well known result in the climate econometrics literature (Burke, Hsiang, and Miguel 2015).

Temperature bins above 25°C and below -5°C have economically large effects on MRPK dispersion, statistically significant at the 1% level. Specifically, substituting a day from the moderate 5-10°C range with a day above 30°C increases MRPK dispersion by approximately 0.31 log points. This translates to a 0.11% reduction in annual aggregate TFP due to increased capital misallocation, equivalent to roughly 40% of one day's GDP. At colder extremes, an additional day below -5°C raises MRPK dispersion by about 0.26 log points, corresponding to an annual TFP loss of

23. In practice, including or excluding these controls does not materially affect our estimates.

Table 1: Effects of daily mean temperature bins on MRPK dispersion and TFP loss

	(1) σ^2_{mrpk}	(2) σ^2_{mrpk}	(3) σ^2_{mrpk}	(4) σ^2_{mrpk}	(5) Implied TFP Loss
< -5°C	0.0026***	0.0025***	0.0028***	0.0012	0.0935***
	(0.0010)	(0.0009)	(0.0009)	(0.0023)	(0.0342)
$-5 \sim 0$°C	0.0015**	0.0013**	0.0016***	0.0006	0.0526**
	(0.0006)	(0.0006)	(0.0006)	(0.0013)	(0.0212)
$0 \sim 5$°C	0.0004	0.0002	0.0005	-0.0019**	0.0131
	(0.0004)	(0.0004)	(0.0004)	(0.0009)	(0.0146)
$10 \sim 15$°C	0.0009**	0.0008**	0.0008**	0.0036***	0.0308**
	(0.0004)	(0.0004)	(0.0004)	(0.0010)	(0.0137)
$15 \sim 20$°C	0.0013**	0.0012**	0.0014***	0.0045***	0.0471**
	(0.0005)	(0.0005)	(0.0005)	(0.0013)	(0.0190)
$20 \sim 25$°C	0.0015**	0.0015**	0.0015**	0.0080***	0.0546**
	(0.0007)	(0.0007)	(0.0007)	(0.0020)	(0.0259)
$25 \sim 30$°C	0.0028***	0.0027***	0.0027***	0.0095***	0.1008***
	(0.0009)	(0.0009)	(0.0009)	(0.0021)	(0.0331)
> 30°C	0.0031***	0.0030***	0.0030***	0.0090***	0.1112***
	(0.0011)	(0.0011)	(0.0011)	(0.0021)	(0.0401)
Controls	No	No	Yes	No	No
Region-Sector FE	Yes	Yes	Yes	Yes	Yes
Country-Year FE	Yes	No	Yes	Yes	Yes
Country-Sector-Year FE	No	Yes	No	No	No
1995 VA Weighted	No	No	No	Yes	No
Observations	124,065	123,518	124,065	123,847	124,065
R^2	0.876	0.903	0.878	0.897	0.876

Notes: Standard errors in parentheses. We cluster standard errors at the regional level (NUTS3 level for European countries, prefecture level for China, and district level for India). Dependent variables in columns (1) to (4) represent the variance of log MRPK. Results from estimating Equation 12 are displayed in columns (1) to (4), with controls in column (3) and weighted OLS regression in column (4). Column (5) is the implied TFP loss calculated using the formula, $-\frac{\alpha_{Kn}+\alpha^2_{Kn}(\sigma_n-1)}{2}\hat{\lambda}^b_{\sigma^2_{mrpk}}$, and the regression estimates. Countries included are China, India, and 30 European countries.

$^{*}\ p < 0.10$, $^{**}\ p < 0.05$, $^{***}\ p < 0.01$

0.09%.

Robustness. Table 1 columns (2)-(4) present results with different specifications of fixed effects, inclusions of control variables, and weighting method. We introduce country-sector-year fixed effects instead of country-year fixed effects in column (2). Column (3) adds the set of control variables, including total number of observed firms, average firm-level sales, and average level of MRPK across firms in a region-sector-year (all in logs). Column (4) reports the results of the weighted OLS using the 1995 region-sector value-added as the regression weight. Our results, in particular the "U-shaped" pattern, remain robust under various specifications.

4.3 Technology vs. Misallocation

A natural question is how to interpret the magnitude of climate-induced productivity losses through misallocation relative to the well-documented technology channel.

The technology effect is typically understood in the literature as shifts in the physical productivity frontier of the aggregate economy driven by climate conditions. Our decomposition of aggregate TFP from Equation (11) separately identifies climate's effects on capital misallocation and aggregate technology. Specifically, the technology channel can be expressed as:

$$\frac{d\,\text{Technology}_{nt}}{d\tilde{\mathbf{T}}_{rt}} = \frac{d\log \text{TFP}_n^E(\tilde{\mathbf{T}}_{r,t},\cdot)}{d\tilde{\mathbf{T}}_{r,t}} = \frac{1}{\sigma_n-1}\frac{d\log\left[\mathbb{E}_i \text{TFP}_{ni}(\tilde{\mathbf{T}}_{r,t},\cdot)^{\sigma_n-1}\right]}{d\tilde{\mathbf{T}}_{r,t}}.$$

Here $\text{TFP}_{ni}\left(\tilde{\mathbf{T}}_{r,t},\cdot\right) := B_{ni}\left(\tilde{\mathbf{T}}_{r,t},\cdot\right)^{\frac{1}{\sigma_n-1}} A_{ni}\left(\tilde{\mathbf{T}}_{r,t},\cdot\right)$. This representation makes clear that climate shocks $\tilde{\mathbf{T}}_{r,t}$ shift the CES aggregate of firms' physical productivity, implicitly placing greater weight on higher productivity firms. The magnitude of the technology channel is therefore summarized by the semi-elasticity $\frac{1}{\sigma_n-1}\frac{d}{d\tilde{\mathbf{T}}_{r,t}}\log\left[\mathbb{E}_i\,\text{TFP}_{ni}\left(\tilde{\mathbf{T}}_{r,t},\cdot\right)^{\sigma_n-1}\right]$.

To accurately estimate the "elasticity of the average" rather than the "average elasticity",[24] we employ a Poisson Psuedo Maximum Likelihood (PPML) regression which yields consistent estimates of the "elasticity of the average" as demonstrated in Tyazhelnikov, Zhou, and Shi (2024). Specifically, we impose the following moment conditions:

$$\mathrm{E}_i\left[\tfrac{1}{\sigma_n-1}\widetilde{\text{TFP}}_{nit}^{\sigma_n-1} \mid \tilde{\mathbf{T}}_{rt}, \eta_i, \log(P_{nt}Y_{nt}), \kappa_{c(r)st}\right] = \exp\left[\boldsymbol{\beta}\tilde{\mathbf{T}}_{rt} + \eta_i + \delta\log(P_{nt}Y_{nt}) + \kappa_{c(r)st}\right], \tag{13}$$

24. Note that the elasticity of the average can be viewed as a productivity-share-weighted average of individual firm elasticities, where more productive firms with larger market shares have greater influence on the aggregate response. This contrasts with the "average elasticity" across all firms:

$$\underbrace{\frac{d\log\mathbb{E}_i\left[\text{TFP}_{ni}(\tilde{\mathbf{T}}_{r,t},\cdot)^{\sigma_n-1}\right]}{d\tilde{\mathbf{T}}_{r,t}}}_{\text{Elasticity of the Average}} = \mathbb{E}_i\left[\frac{\text{TFP}_{nit}^{\sigma_n-1}}{\mathbb{E}_i[\text{TFP}_{nit}^{\sigma_n-1}]}\cdot\frac{d\log\text{TFP}_{ni}(\tilde{\mathbf{T}}_{r,t},\cdot)^{\sigma_n-1}}{d\mathbf{T}_{r,t}}\right] \neq \underbrace{\mathbb{E}_i\left[\frac{d\log\text{TFP}_{ni}(\tilde{\mathbf{T}}_{r,t},\cdot)^{\sigma_n-1}}{d\mathbf{T}_{r,t}}\right]}_{\text{Average Elasticity}}.$$

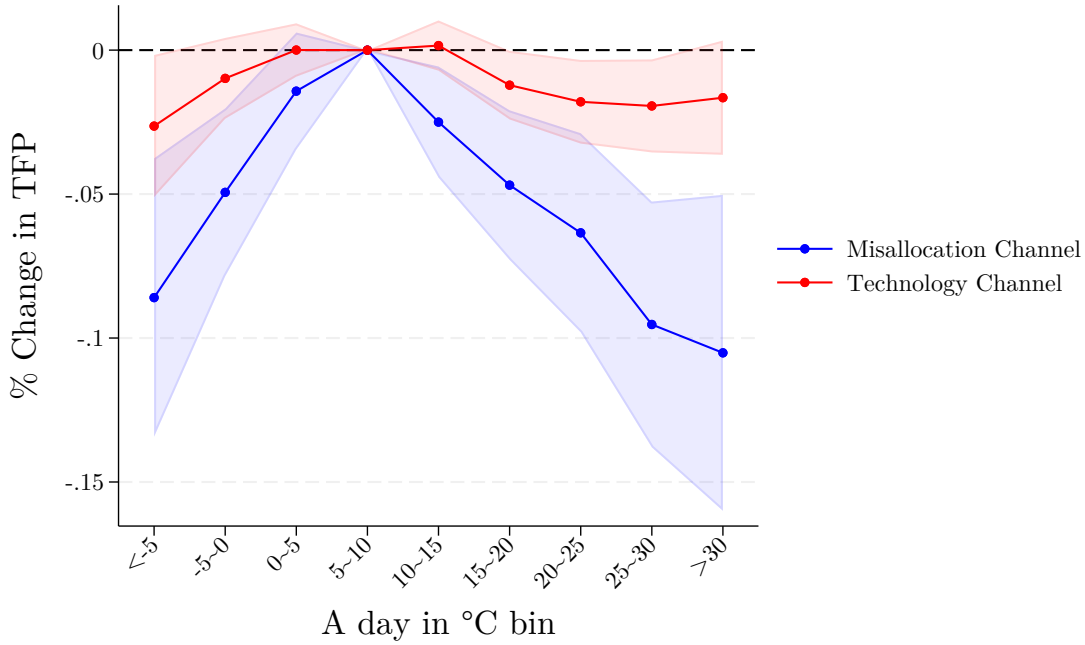
A simple OLS estimation, which assigns equal weight to the observations of all firms, would yield the "average elasticity", rather than the "elasticity of the average." This approach could bias the aggregate estimate downward for heat shocks, as larger, more productive firms are likely more resilient to heat (i.e., $\text{cov}\left(\frac{\text{TFP}_{nit}^{\sigma_n-1}}{\mathbb{E}_i[\text{TFP}_{nit}^{\sigma_n-1}]}, \frac{d\log\text{TFP}_{ni}(\tilde{\mathbf{T}}_{r,t},\cdot)^{\sigma_n-1}}{d\text{Tbin}_{r,t}^{>30C}}\right) > 0$). We draw caution to the practice of using (unweighted) micro-level OLS estimates to infer aggregate impacts.

where we define $\widetilde{\text{TFP}}_{nit} := \frac{(P_{nit}Y_{nit})^{\frac{\sigma_n}{\sigma_n-1}}}{K_{nit}^{\alpha_{Kn}} L_{nit}^{\alpha_{Ln}}}$ as the model-consistent empirical measure of TFP from the data, up to a constant consisting of the aggregate demand and price index of n. In this specification, η_i represents firm fixed effects. The term $\log(P_{nt}Y_{nt})$, along with the country-sector fixed effect $\kappa_{c(r),s,t}$, captures differences between local and national price levels. Estimating this equation by PPML yields a theory-consistent estimate of $\boldsymbol{\beta} = \mathbb{E}\left[\frac{1}{\sigma_n - 1}\frac{d\log \mathbb{E}_i[\text{TFP}_{nit}^{\sigma_n-1}|\cdot]}{d\tilde{\mathbf{T}}_{rt}}\right]$, which is plotted alongside the aggregate TFP impact from the misallocation channel in Figure 3.

We find that while the estimated effect of climate shocks through the technology channel is noticeable, it remains considerably smaller than the effect through the misallocation channel. Specifically, a cold shock of an additional day below -5°C (relative to the 5°C–10°C range) results in an annual aggregate physical productivity loss of about 0.03%, and a heat shock above 25°C or 30°C leads to a loss of approximately 0.02%. The impact of a heat shock on aggregate technology is roughly one-fifth of the corresponding loss through the misallocation channel.

The previous estimates in the literature indicates a sum of the two channels, and we are able to pin down the two channels separately.

Figure 3: Technology vs. Misallocation



Notes: The graphs include 90% confidence intervals, and standard errors are clustered at the regional level. The reference temperature is at 5∼10°C.

4.4 Heterogeneous Effect by Climate and Development from Misallocation Channel

Our benchmark specification in Equation 12 captures the average effect of temperature on capital misallocation. We now estimate the heterogeneous impact of temperature shocks across regions with different long-run climate conditions and levels of economic development. This analysis allows us to interpret our findings in terms of climate rather than merely short-term weather fluctuations.

It is not immediately clear whether a hot day consistently leads to more or less *misallocation* in regions that are already warm or economically thriving. This ambiguity arises from two potentially counteracting factors. For simplicity, consider two types of firms: "heat-loving" versus "heat-averse." On one hand, heat-averse firms in warmer climates may have adapted to high temperatures—by investing in heat-tolerant capital, securing more flexible financing, or adjusting production methods—such that additional heat shocks impose relatively mild disruptions on their marginal products and factor usage. On the other hand, heat-averse businesses in hotter regions might still face disproportionately large *adjustment frictions*—for example, steeper capital-investment costs or financing constraints—once temperatures surpass their adaptation threshold. Limited adaptability (Moscona and Sastry 2023) and the convexity of damage from cumulative heat exposure (Burke, Hsiang, and Miguel 2015) might still sharply widen cross-firm differences in marginal products. Similarly, in higher-income regions, while firms may, on average, possess greater resources for adaptation to heat shocks, these economies often have highly specialized productions and services and exhibit larger dispersion in firm sizes (e.g., Chen 2022; Poschke 2018). Such heterogeneity can magnify responses to climate shocks: some firms manage to shield themselves from heat shocks by making quick adjustments while others cannot, causing greater MRPK divergence and reinforcing the misallocation channel.

To more precisely account for the heterogeneous impact stemming from different long-run climate and development levels across regions, we follow the approach of Carleton et al. (2022) and Nath (2025) by interacting a time-invariant measure of climate (i.e., long-run average temperature) and GDP per capita with each temperature bin. This method allows us to capture how climate and income jointly influence the effects of temperature variations on capital misallocation. The modified regression model is formulated as follows:

$$\begin{aligned}\sigma^2_{mrpk_{s,r,t}} = &\sum_{b\in B_{/(5\sim10^\circ C)}} \lambda^b \times \text{Tbin}^b_{r,t} + \sum_{b\in B_{/(5\sim10^\circ C)}} \lambda^b_{\overline{T}} \times \text{Tbin}^b_{r,t} \times \overline{T}_r \\ &+ \sum_{b\in B_{/(5\sim10^\circ C)}} \lambda^b_{\text{GDP}_{\text{pc}}} \times \text{Tbin}^b_{r,t} \times \ln \overline{\text{GDP}_{\text{pc}}}_r + \boldsymbol{\delta}\tilde{\mathbf{X}}_{s,r,t} + \alpha_{c,t} + \eta_{s,r} + \varepsilon_{s,r,t},\end{aligned} \tag{14}$$

where $\overline{T}_r$ represents the long-run annual average temperature and $\ln \overline{\text{GDP}_{\text{pc}}}_r$ is the log of long-run average GDP per capita in region r.[25] Both long-run temperature and GDP per capita are computed as sample averages from 1997-2018. The coefficients $\lambda^b_{\overline{T}}$ and $\lambda^b_{\text{GDP}_{\text{pc}}}$ quantify how the impact of temperature shocks on MRPK dispersion varies across regions with different income levels and climates.[26]

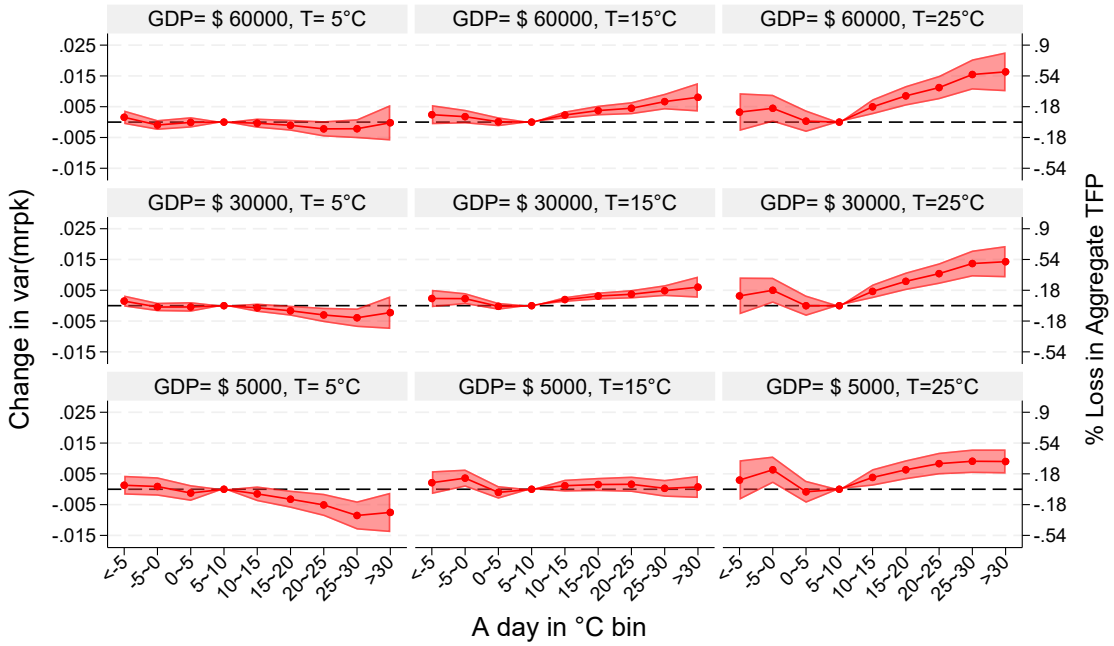
Figure 4 presents the results from estimating Equation 14. We predict the impact of temperature shocks on MRPK dispersion and its equivalent TFP loss across a combination of three levels of income and three levels of long-run climate. The left y-axis indicates the projected effects of temperature shocks on MRPK dispersion, while the right y-axis shows the implied TFP loss sug-

25. The sub-national level (PPP-adjusted) GDP per capita data is from DOSE. It is important to use sub-national level data as countries like India and China admit large income heterogeneity across the districts or prefectures. The GDP per capita data is in 2017 International Dollars.

26. Interacting temperature bins with the region's long-term average temperature allows us to analyze how an additional hot day has differential effects across areas with varying baseline climates. Similarly, by interacting temperature bins with a country's annual per capita income, we evaluate how the same heat shock impacts developed and developing economies differently.

gested by the estimates.

Figure 4: MRPK Dispersion and TFP Loss Across Climates and Income



Notes: The graphs plot the predicted effect of exposure to daily mean temperature bins on MRPK dispersion and TFP loss at varying levels of income and climates. These predicted effects are derived from the interacted panel regression specified in Equation 14. The graphs include 90% confidence intervals, and standard errors are clustered at the regional level. The left y-axis indicates changes in MRPK dispersion, and the right y-axis shows the calculated TFP loss. The reference temperature is at 5∼10°C.

Level Effect: Hotter Regions Suffer More from the Misallocation Channel Figure 4 shows that an extremely hot day (above 30°C) increases MRPK dispersion more in regions with higher baseline temperatures. Among regions with comparable income levels, the adverse effects of heat on misallocation intensify as the regional climate becomes warmer. For instance, in regions with baseline temperatures around 25°C, an additional day above 30°C reduces TFP substantially-by approximately 0.3% to 0.58%-regardless of income levels. In contrast, in colder climates (e.g., $\overline{T}_r \approx 5$°C), heat shocks have minimal or even negative effects on MRPK dispersion, implying smaller TFP losses. Interestingly, cold shocks (below 0°C) also increase misallocation more strongly in hotter regions, though their magnitude is typically smaller than that of extreme heat shock, except in certain hot, low-income contexts (e.g., India, GDP ≈ $5,000, $\overline{T}_r = 25$°C).

The quantitative implications can be best understood by comparing two regions with similar incomes but different climates. Arizona (U.S.) and Norway both have an average per capita income of around $60,000 but vastly different average annual temperatures (14.68°C in Arizona vs. 0.53°C in Norway). According to our estimates, an additional day above 30°C compared to a $5 \sim 10$°C day in Norway *reduces* MRPK dispersion by 0.41 log points, implying a 0.14% *increase* in TFP. In Arizona, the same heat shock *increases* MRPK dispersion by 0.75 log points and lowers TFP by 0.27%. In Section 5, we discuss how these divergent responses can be explained by deviations from the "bliss-point" temperature for production, estimated to be around 13°C.

Income Effect: Richer Economies Suffer More from the Misallocation Channel A second key finding is that wealthier economies incur greater losses through the misallocation channel in response to extreme heat—what we term the *Income Effect*. Figure 4 illustrates that for each fixed long-run temperature (each column), moving from lower to higher income levels amplifies the impact of heat shocks and makes the MRPK response more U-shaped. For instance, the Netherlands and Türkiye both have an average temperature of around $9.9°$C, yet the Netherlands' per capita income ($56,784) is more than double that of Türkiye ($28,150). Our estimates suggest that an additional day above $30°$C causes a 0.03% TFP loss in Türkiye, but 0.11% in the Netherlands—nearly four times higher. To explain the income effect, in Section 6, we show how firm size dispersion rises with economic development, potentially resulting in greater cross-firm MRPK divergence under similar heat shocks.

Overall, the heterogeneous effect shows that the nature of the misallocation channel of climate change may differ substantially from other channels, such as labor productivity (Nath 2025) and mortality risk (Carleton et al. 2022), where richer economies and hotter regions are often found to experience smaller heat-related losses due to long-run adaptation. The *opposite* pattern emerges here: hotter and richer regions face larger TFP losses via misallocation, suggesting that market-based adaptation may do little to curb the efficiency losses across firms.As an economy develops to be more sophisticated in its techniques of production among firms, it might become more vulnerable to climate variations since achieving efficient resource allocations becomes more challenging.

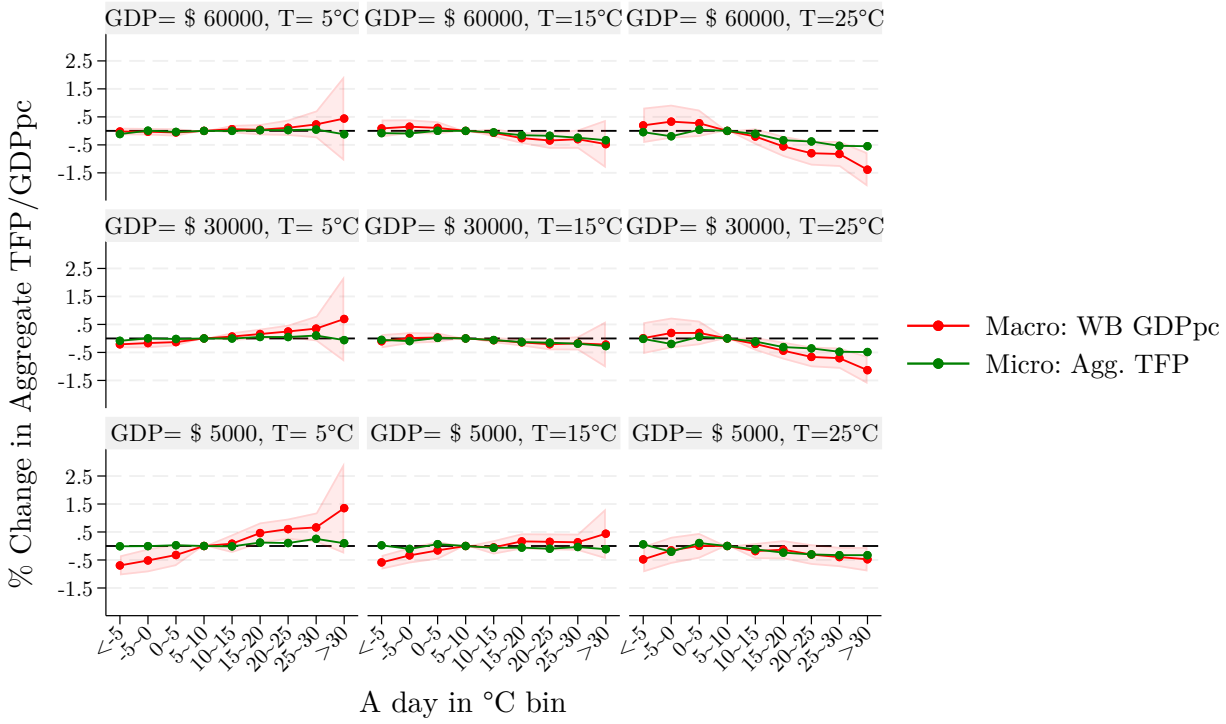
Micro Estimates vs. Macro Estimates We compare our *micro estimates*, derived from firm-level data and aggregation theory, with *macro estimates* obtained from country-level aggregate data. To construct the micro estimates, we first apply the PPML estimator (Equation (13)) incorporating the interaction terms used in Equation (14), capturing heterogeneous effects of climate change through the technology channel. We then combine these estimated technology effects with our misallocation effects to produce a comprehensive micro-based measure of the total climate impact. For the macro estimates, we use annual GDP per capita data from the World Bank (1990-2019) and run a country-level regression analogous to Equation (14), including country and year fixed effects.

We plot both sets of estimates in Figure 5 and find that the micro-based estimates closely track the macro-based estimates, except in two instances: (1) the micro estimates understate the damage of heat shocks (above $30°$C) in regions with per capita GDP over $30,000 and mean temperatures above $25°$C, and (2) overstate the benefits of heat shocks in colder, poorer regions. Both types of regions are infrequent in our dataset and globally. Overall, these findings suggest that our micro estimates capture the same cross-country heterogeneity in temperature sensitivity as the macro estimates, making them suitable for out-of-sample extrapolation.

4.5 Other Robustness Exercises

Appendix D examines whether our baseline relationship between temperature and MRPK dispersion within region–sector–year cells is sensitive to measurement, sample construction, or inference choices. We report six sets of robustness checks.

Figure 5: Aggregate Impact of Climate shocks: Micro vs. Macro Estimates



Notes: The graphs include 90% confidence intervals, and standard errors are clustered at the region level. The reference temperature is at 5∼10°C.

First, we re-estimate the baseline specification separately by broad SIC divisions to verify that the aggregate pattern is not driven by a small subset of industries. Reassuringly, we find that the increase in MRPK dispersion under extreme heat is concentrated in all major divisions such as agriculture, manufacturing, transportation, retail trade and services. Effects are generally small and statistically insignificant in mining, construction, wholesale trade and FIRE.

Second, we replicate the analysis using dispersion in the marginal revenue products of labor and materials (MRPL and MRPM) to test whether temperature generates a broad increase in dispersion across inputs. Unlike MRPK, MRPL dispersion rises slightly under extreme cold and shows little response to heat, while MRPM dispersion is essentially flat across temperature bins. This contrast suggests that temperature affects misallocation primarily through capital returns rather than through a general widening of marginal products. Thus our main analysis only focuses on climate-induced capital misallocation.

Third, we vary how weather enters the regression by using daily maximum-temperature bins, population-weighted average-temperature bins, and a polynomial temperature specification. The estimated relationship remains U-shaped and quantitatively similar. Fourth, we test alternative inference procedures, including two-way clustering and spatial-HAC standard errors, with no material change in conclusions. Fifth, we vary the definitions of regions and sectors and obtain very similar estimates. Finally, we relax the Cobb–Douglas and Hicks-neutral productivity assumptions by allowing for CES production with factor-augmenting technology; the temperature–MRPK dispersion relationship remains robust under these alternative production specifications.

4.6 End-of-the-century Projection of the Misallocation Channel

In this subsection, we use the estimates from Section 4.4 to project how climate-induced misallocation will affect aggregate TFP by the end of the 21st century (2081–2100) for 4,881 regions in 172 countries.[27]

Such projections require detailed region-level daily temperature distributions, average temperature levels, and GDP per capita projections at the end of the century. We use near-surface air temperature forecasts from the sixth phase of the Coupled Model Intercomparison Project (CMIP6) (Copernicus Climate Change Service 2021) under RCP 4.5, a scenario featuring moderate mitigation efforts. To project each region's daily temperature distribution, we calculate the average number of days in each temperature bin (as defined in Section 4.1) and the mean annual temperature for 2081–2100, taking a 20-year average to smooth over short-term climate fluctuations. Following Carleton et al. (2022), we obtain national per capita income projections from the OECD EnvGrowth model (Dellink et al. 2017) under the SSP3 scenario. For the average region in our sample, the mean annual temperature is expected to rise by about $1.78°\mathrm{C}$ between 2000–2014 and 2081–2100, while GDP per capita (in 2017 international dollars) is projected to increase by approximately \$20,748 relative to 2019. Figure C.1 illustrates these projected evolution in income and temperature.

Our objective is to measure how much additional aggregate TFP loss arises from climate-induced misallocation by the end of the 21st century (EOC), compared to baseline conditions near the century's start. To make these mechanisms transparent, we decompose the total effect of climate-induced misallocation into three components:

Notice that any change in region-level TFP can be written as two components:

$$\begin{aligned}\underbrace{\Delta^{\text{Loss}} \ln \text{TFP}_r}_{\text{Total Effect}_r} = \frac{\alpha_{Kn} + \alpha_{Kn}^2(\sigma_n - 1)}{2} \Bigg[& \underbrace{\sum_b \left(\lambda^b + \lambda^b_{\text{GDP}_{pc}} \ln \text{GDP}_{pc,r,\text{base}} + \lambda^b_{\bar{T}} \bar{T}_{r,\text{base}} \right) \times \Delta \text{Tbin}^b_r}_{\text{Shock Effect}_r} \\ & + \underbrace{\sum_b \lambda_{b,\bar{T}} \text{Tbin}^b_{r,\text{base}} \times \Delta T_r}_{\text{Level Effect}_r} \\ & + \underbrace{\sum_b \lambda^b_{\text{GDP}_{pc}} \text{Tbin}^b_{r,\text{base}} \times \Delta \ln \text{GDP}_{pc,r}}_{\text{Income Effect}_r} \Bigg] + \underbrace{\varepsilon_{rt}}_{\text{Residuals}_r},\end{aligned} \tag{15}$$

where Δ denotes the difference between a variable's end-of-century (EOC) value and its baseline value. The *shock effect* refers to the change in TFP losses due to shifts in daily temperature distributions ΔTbin^b_r, conditional on the baseline income and long-run temperature; the *level effect* refers to the change in TFP losses due to the change in long-run temperature ΔT_r; and the *income effect* reflects the cost of the region's increasing misallocation arising from economic development, proxied by $\Delta \ln \text{GDP}_{pc,r}$. To render the results more interpretable, we aggregate each region's TFP

27. For our 32-country sample, regions are defined as in Section 3. For other countries, we use GADM1-level administrative units from the GADM dataset.

losses to the country level using a weighted sum of projected regional GDP shares under SSP3.[28]

Figure 6 displays each country's projected TFP loss from the capital misallocation channel. While most countries experience substantial losses, the magnitudes vary widely. Among the most severely affected are Tanzania, Malaysia, Honduras, and India, where TFP losses exceed 40%. In India, for instance, the number of days above $30°$C is projected to increase from 76.24 to 99.78 by 2100, accompanied by rises in average temperature (from $23.29°$C to $25°$C) and income per capita (from \$6,608.62 to \$14,615.39). Combined, these factors yield a TFP loss of roughly 50.45%. As illustrated in Figure 4, such substantial heat-related damages become more pronounced in already-warm (tropical/subtropical), lower-income countries that simultaneously grow hotter and wealthier.

In contrast, countries like the United States, Argentina, and Spain are projected to lose 20–30%. For example, in the U.S., the TFP loss is about 20.92%. Per capita income is expected to rise from \$62,478 to \$95,801, while average annual temperature increases from $10.07°$C to $12.45°$C, and days above $30°$C grow from 3.97 to 8.94. Meanwhile, countries with milder impacts—such as France, the United Kingdom, Russia, and Canada—see losses below 15%. In the U.K., for instance, the average temperature climbs from $9.15°$C to $10.16°$C, with days above $25°$C increasing from 0.03 to 0.37, and income per capita rising from \$47,362.27 to \$85,615.36. Taken together, these lead to a TFP loss of 8.23%. Although climate change slightly raises average temperatures in temperate, maritime climates, the incidence of extreme heat remains relatively low, moderating the misallocation losses compared to tropical regions.

Finally, by weighting each country's misallocation-induced TFP losses by its projected share of global GDP,[29] we estimate the worldwide cost of climate-induced misallocation to be:

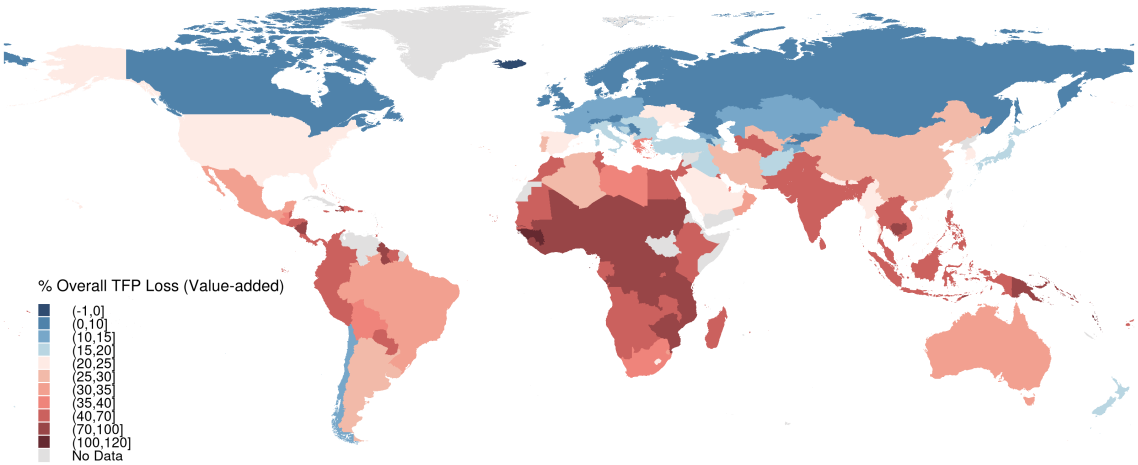
$$\underbrace{\Delta^{\text{Loss}} \ln \text{TFP}}_{\text{Total Effect}=36.73\%} = \underbrace{\text{Shock Effect}}_{2.13\%} + \underbrace{\text{Level Effect}}_{11.34\%} + \underbrace{\text{Income Effect}}_{19.46\%} + \underbrace{\text{Resid.}}_{3.8\%}.$$

Relative to baseline conditions, this translates into a 36.73% decline in aggregate TFP (GDP). Specifically, shifts in the daily temperature distribution (*shock effect*) contribute 2.13%, rising average temperature (*level effect*) accounts for 11.34%, and higher income per capita (*income effect*) explains 19.46%. Figure 7a depicts the projected evolution of misallocation-driven TFP losses from 7.60% in 2030 to 41.62% by 2100, with 90% confidence intervals accounting for parameter uncertainty. Figure 7b further separates these losses into the three components over time, highlighting the dominant roles of the level and income effects.

28. Grid-level SSP3 GDP data from Wang and Sun (2022) provides projected GDP shares.

29. Under this weighting scheme, the resulting TFP losses correspond to a model-implied global TFP loss based on a Cobb-Douglas aggregator of country-level value added. This also serves as a first-order approximation under any constant-returns-to-scale aggregator for global output.

Figure 6: End-of-century Projected TFP Loss Due to the Misallocation Channel

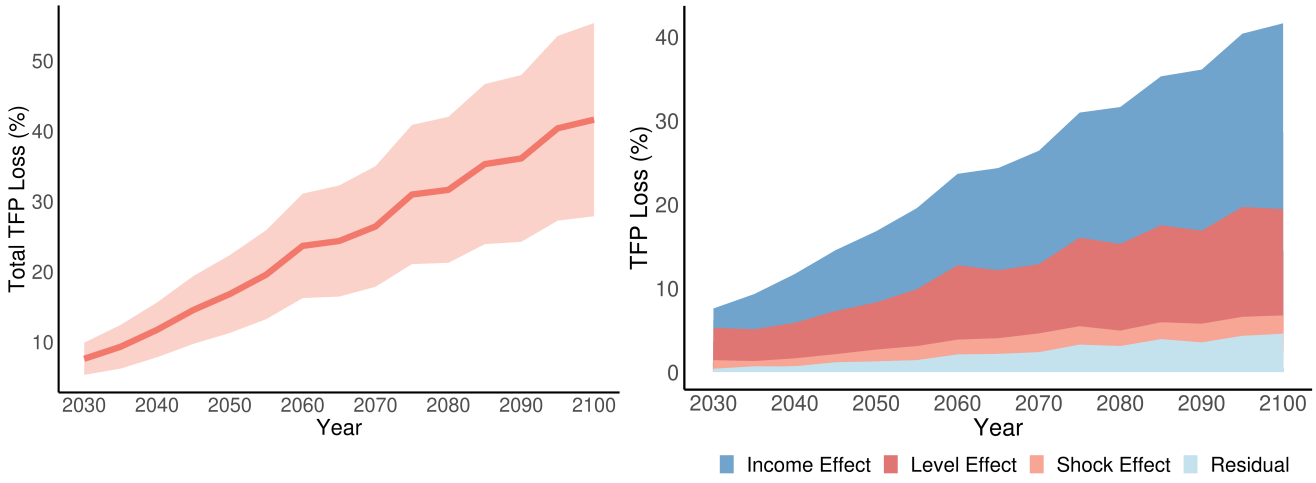


Notes: Figure shows the projected TFP losses from capital misallocation under SSP3-4.5 scenarios. The estimation follows Equation 15 where we estimate the total effect in MRPK dispersion and compute the equivalent value of TFP losses.

Figure 7: Projected Global TFP Loss and Its Decomposition: 2030-2100

(a) Total TFP Loss from the Misallocation Channel

(b) TFP Loss Decomposition



Notes: Figure 7a plots the total TFP loss across years. The dark red line plots the estimates and the shaded area is 90% confidence intervals from the parameter uncertainty. Figure 7b plots the three effects contributing to total TFP loss. All computations are under the SSP3-4.5 scenario and the percentage loss is compared to the baseline level.

These estimates are substantial and comparable to the overall projected impacts reported by Burke, Hsiang, and Miguel (2015) and, more recently, Bilal and Känzig (2024). Much of the total projected effect arises from the sharp increase in the marginal effect of daily temperature shocks, driven by rising temperatures and incomes. As with any century-scale forecast, our projection is subject to various caveats—most notably out-of-sample extrapolation—since income and temperature levels by the end of the century lie well beyond historical experience. However, even if we only adjust the daily temperature distribution while keeping the first-order marginal effect

of temperature shocks at current levels, we still project a 2.14% global TFP loss from misallocation. Overall, these results underscore the quantitative importance of the misallocation channel of climate change, which may serve as a one of the key forces driving up the social cost of carbon.

5 A Firm Dynamics Model of Climate and MRPK Dispersion

We now turn to the question of *why*. Our empirical evidence indicates that both long-run climatic conditions and short-run temperature fluctuations affect capital misallocation. Moreover, the climate-induced misallocation channel is more pronounced in hotter and more economically developed regions. To explain these patterns, we build a tractable general-equilibrium model with risk-averse households and heterogeneous firms, featuring time-to-build capital, pre-existing capital wedges, and costly endogenous adaptation to climate. A novel feature of our framework is that firm-level climate adaptation is fully endogenous: firms choose their effective productivity process by selecting adaptation intensity in response to expected climate conditions and weather risk. This builds on recent advances in modeling endogenous risk-exposure choices in disaggregated economies (Kopytov, Taschereau-Dumouchel, and Xu 2024).

The model's demand and production structure mirrors the structure of our accounting framework and is defined at the region-year level. For expositional clarity, we suppress the region-year notation here and introduce regional heterogeneity later.

5.1 Model Structure

5.1.1 Household

In each region, there is a representative, risk-averse household with King-Plosser-Rebelo preferences. Each period t, it consumes C_t, inelastically supplies a mass N of unskilled labor to production, and elastically supplies skilled labor $\mathcal{R}_t$ to an adaptation sector. Supplying skilled labor for adaptation is costly and scales down the utility from consumption. The household chooses $\{C_t, \mathcal{R}_t\}_{t\geq 0}$ to maximize expected discounted lifetime utility

$$\max_{\{C_t,\mathcal{R}_t\}} \mathbb{E}_0 \sum_{t=0}^{\infty} \left(\frac{1}{1+r}\right)^t \frac{\left(C_t \exp\left(-\mathcal{R}_t\right)\right)^{1-\gamma}}{1-\gamma},$$

where r is the discount rate and $\gamma \geq 1$ governs relative risk aversion. The adaptation sector produces adaptation resources R_t (e.g., air conditioning, building insulation, hazard mitigation services) with a linear technology

$$R_t = \frac{1}{\eta}\mathcal{R}_t.$$

The parameter $\eta > 0$ governs the cost of producing adaptation resources: a larger η means more skilled labor is required per unit of R_t, making adaptation more costly in utility. Typically, we expect more economically developed regions to face a lower adaptation cost η (Carleton et al. 2022).

Households have Dixit-Stiglitz preferences over differentiated goods and consume the bundle $C_t = Y_t = \left(\int_0^1 B_{it}^{\frac{1}{\sigma}} Y_{it}^{\frac{\sigma-1}{\sigma}} di\right)^{\frac{\sigma}{\sigma-1}}$ where $\sigma > 1$ is the elasticity of substitution across varieties i and

B_{it} is a preference shifter. At the end of period t, the household consumes C_t and sets a supply schedule R_{t+1} to meet firms' demand for adaptation resources. At the start of $t+1$, before climate shocks are realized, the predetermined quantity R_{t+1} is supplied and the contracted amount is distributed to each firm. The household owns all the firms in the region, and all profits and revenues from tax-like wedges are rebated lump sum. The period-t budget constraint is therefore

$$C_t = w_t N + w_t^R R_t + \Pi_t + S_t,$$

where w_t is the wage for unskilled labor, w_t^R is the price of adaptation resources, Π_t denotes total firm profits, and S_t denotes lump-sum rebates.

We assume markets are complete with respect to aggregate risk, so firms discount future cash flows using the household's stochastic discount factor (SDF),

$$\Lambda_{t+1} = \frac{1}{1+r}\left(\frac{C_{t+1}}{C_t}\right)^{-\gamma} \exp\left[(\gamma-1)\eta\left(R_{t+1}-R_t\right)\right].$$

The household's optimality conditions imply that the price of adaptation resources satisfies

$$w_{t+1}^R = \eta \frac{\mathbb{E}_t\left[\Lambda_{t+1} C_{t+1}\right]}{\mathbb{E}_t\left[\Lambda_{t+1}\right]}.$$

Thus, w_{t+1}^R increases with the utility-cost parameter η and with the SDF-weighted expectation of next-period consumption.

5.1.2 Firms

Each firm i produces a differentiated variety with Cobb-Douglas technology, $Y_{it} = \tilde{A}_{it} K_{it}^{\tilde{\alpha}_K} N_{it}^{\tilde{\alpha}_N}$, where $\tilde{A}_{it}$ is physical productivity, K_{it} is capital, N_{it} is labor, and $\tilde{\alpha}_K + \tilde{\alpha}_N = 1$. Firms compete monopolistically à la Dixit-Stiglitz. Combining the production function with the demand system implies an equilibrium revenue function of the form

$$P_{it} Y_{it} = Y_t^{\frac{1}{\sigma}} B_{it}^{\frac{1}{\sigma}} \tilde{A}_{it}^{\frac{\sigma-1}{\sigma}} K_{it}^{\alpha_K} N_{it}^{\alpha_N},$$

where $\alpha_F = \left(1 - \frac{1}{\sigma}\right)\tilde{\alpha}_F$ for $F \in \{K, N\}$, and $B_{it}^{\frac{1}{\sigma}} \tilde{A}_{it}^{\frac{\sigma-1}{\sigma}}$ captures the firm's demand-adjusted revenue productivity. Since such market and production structure is identical to Section 2, we know there must also exist an aggregate production function $Y_t = A_t K_t^{\tilde{\alpha}_K} N^{\tilde{\alpha}_N}$ for some aggregate productivity A_t and aggregate capital $K_t = \int_i K_{it}$.

Flexible Inputs and Profits In the beginning of period t, after capital and adaptation decisions are made and all shocks are realized, forms choose labor input from a competitive market to maximize profits: $\Pi_{it} = \max_{N_{it}} Y_t^{\frac{1}{\sigma}} B_{it}^{\frac{1}{\sigma}} \tilde{A}_{it}^{\frac{\sigma-1}{\sigma}} K_{it}^{\alpha_K} N_{it}^{\alpha_N} - W_t N_{it}$. Writing the competitive wage W_t as a function of aggregate output, $W_t = \tilde{\alpha}_N \frac{Y_t}{N}$, we can solve for the optimal labor choice and obtain the profit function:

$$\Pi_{it} = G(A_t K_t^{\tilde{\alpha}_K})^{\theta_A} A_{it} K_{it}^{\alpha} \tag{16}$$

where $G := (1-\alpha_N)N^{\tilde{\alpha}_N}$ and $\theta_A = \frac{1}{\sigma} - \left(\frac{\sigma-1}{\sigma}\right)\frac{\alpha_N}{1-\alpha_N}$ summarizes the a positive aggregate demand effect and a negative wage effect in general equilibrium. We consider an empirical relevant case where $\tilde{\alpha}_N > \frac{1}{\sigma-1}$ such that $\theta_A < 0$. Importantly, we also define $A_{it} = \left(B_{it}^{\frac{1}{\sigma}} \tilde{A}_{it}^{\frac{\sigma-1}{\sigma}}\right)^{\frac{1}{1-\alpha_N}}$ to be the effective productivity (profitability), and $\alpha = \frac{\alpha_K}{1-\alpha_N}$ is the profit curvature of capital.

5.1.3 Productivity Process and Endogenous Adaptation

We assume firm productivity takes the form

$$\log A_{it} \equiv a_{it} = \beta_{it}\big(T_t - T^*\big) + z_{it} + \bar{a}_i,$$

so that productivity depends on the firm's temperature sensitivity β_{it}, the deviation of climate conditions from the bliss-point temperature $(T_t - T^*)$,[30] a transitory idiosyncratic component z_{it}, and a permanent component $\bar{a}_i \sim \mathcal{N}(0, \sigma_{\bar{a}}^2)$. We model the idiosyncratic component as an AR(1) process:

$$z_{i,t+1} = \rho_z z_{it} + \varepsilon_{i,t+1}^z, \qquad \varepsilon_{i,t+1}^z \sim \mathcal{N}(0, \sigma_{\varepsilon^z}^2).$$

The heterogeneous temperature sensitivity is comprised of three components

$$\beta_{it} = \underbrace{\beta_i}_{\text{product sensitivity}} + \underbrace{\xi_{it}}_{\text{random sensitivity}} + \underbrace{\widetilde{\beta}_{it}}_{\text{endogeneous sensitivity}}.$$

The product sensitivity $\beta_i \sim \mathcal{N}\left(\bar{\beta}, \sigma_\beta^2\right)$ captures product- or technology-level exposure (e.g., an ice-cream producer versus a ski resort) and is known to the firm. The random sensitivity $\xi_{it} \sim \mathcal{N}\left(0, \sigma_\xi^2\right)$ captures unpredictable, firm-specific variation in temperature sensitivity (e.g., random disruptions) and the extent of damage scale with climate's deviation from bliss point. Finally, $\widetilde{\beta}_{it}$ is an endogenous state chosen by the firm: improving temperature resilience requires adaptation resources. In particular, increasing $\widetilde{\beta}_{i,t+1}$ costs the firm $R_{it} = \frac{1}{2}H\widetilde{\beta}_{i,t+1}^2$ units of adaptation resources purchased from the household, implying convex adjustment costs-reducing temperature impacts by an additional percentage point becomes progressively more expensive.

5.1.4 Temperature Dynamics and Mid-range Weather Forecasts

We assume local temperature follows a stationary AR(p) process:

$$T_t - \bar{T} = \sum_{\tau=1}^{p} \rho_\tau \left(T_{t-\tau} - \bar{T}\right) + \varepsilon_t^T.$$

In each region, a mid-range weather forecasting center observes a noisy signal about T_t and releases an unbiased one-step-ahead forecast $\mathbb{E}_{t-1}[T_t]$ to households and firms. Agents perceive the forecast error to have conditional variance (forecast uncertainty) $\mathbb{VAR}_{t-1}(T_t)$. We assume per-

30. T^* denotes the bliss-point temperature emphasized in the climate-econometrics literature, typically estimated to lie around $10 - 13°\text{C}$. For example, Burke, Hsiang, and Miguel (2015) estimate $T^* \approx 12°\text{C}$.

ceived forecast uncertainty evolves according to a smoothed ARCH(q) process:

$$\mathbb{VAR}_{t-1}(T_t) = \frac{1}{q}\sum_{\tau=1}^{q}\left(T_{t-\tau} - \mathbb{E}_{t-\tau-1}[T_{t-\tau}]\right)^2.$$

Thus, firms perceive temperature to be more uncertain following periods with larger squared forecast errors (i.e., when recent forecasts have been less accurate).

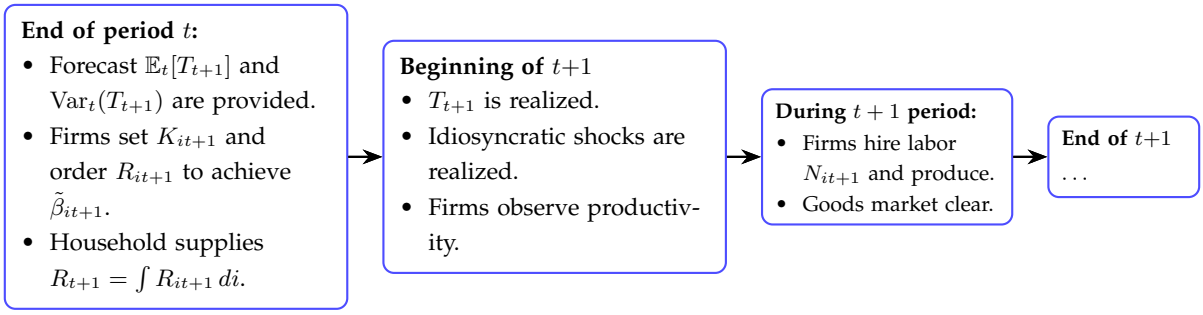
5.1.5 Timing of Events

We briefly summarize the timing of decisions in the model. As shown in Figure 8, at the end of period t, agents observe the forecast $\mathbb{E}_t[T_{t+1}]$ with perceived forecast uncertainty $\mathbb{VAR}_t(T_{t+1})$. Given this information, firms choose next-period capital $K_{i,t+1}$ and adaptation resources $R_{i,t+1}$, which jointly determine adaptation intensity $\widetilde{\beta}_{i,t+1}$. Households supply aggregate adaptation resources,

$$R_{t+1} = \int R_{i,t+1}\, di.$$

At the beginning of period $t+1$, temperature T_{t+1} and all idiosyncratic shocks are realized. Firms then observe realized productivity and choose flexible labor input $N_{i,t+1}$ to produce. During period $t+1$, production takes place and goods markets clear. At the end of period $t+1$, the next forecast is released and the cycle repeats.

Figure 8: Timing of events in the model.



5.1.6 Dynamic Input Investment

Capital and adaptation inputs ordered at period t are installed and put into production at $t+1$.[31] The firm's dynamic problem can be written as the Bellman equation

31. The adaptation investment featured in our model are ex-ante investment. Examples include adjusting crop choices before planting season weather realizes, installing back-up generators, raise equipment or floors in case of flooding etc.

$$V(\mathbf{x}_t, \mathbf{x}_{it}, \mathbf{d}_t, \Gamma_{\text{micro},t}) = \max_{K_{i,t+1},\, \widetilde{\beta}_{i,t+1}} \Bigg\{ G A_t^{\theta_A} K_t^{\theta_K} \underbrace{\exp\Big[\big(\beta_i + \xi_{it} + \widetilde{\beta}_{i,t+1}\big)\big(T_{t+1} - T^*\big) + z_{i,t+1} + \bar{a}_i\Big]}_{\equiv A_{i,t+1}} K_{it}^{\alpha}$$
$$- \left(\frac{1}{2} H \widetilde{\beta}_{i,t+1}^2\right) w_{t+1}^R - K_{i,t+1} - \frac{r+\delta}{1+r} K_{i,t+1}\big(\mathcal{T}_{i,t+1} - 1\big) + (1-\delta) K_{it}$$
$$+ \mathbb{E}_t[\Lambda_{t+1} V(\mathbf{x}_{t+1}, \mathbf{x}_{i,t+1}, \mathbf{d}_{t+1}, \Gamma_{\text{micro},t+1})] \Bigg\}. \tag{17}$$

where

$$\mathbf{x}_t \equiv \Big(\mathbb{E}_t[T_{t+1}],\, \mathbb{VAR}_t(T_{t+1})\Big), \qquad \mathbf{x}_{it} \equiv \Big(K_{it},\, z_{it},\, \bar{a}_i,\, \beta_i,\, \xi_{it},\, \mathcal{T}_{i,t+1}\Big),$$
$$\mathbf{d}_t \equiv \big(A_t,\, K_t,\, R_t\big), \qquad \Gamma_{\text{micro},t} \equiv \text{cross-sectional distribution of firm states/types.}$$

Λ_{t+1} is the stochastic discount factor and δ is the depreciation rate. The term $\mathcal{T}_{i,t+1}$ is the firm-specific capital wedge. Firms choose next-period capital $K_{i,t+1}$ and adaptation intensity $\widetilde{\beta}_{i,t+1}$, paying the adaptation cost $\left(\frac{1}{2} H \widetilde{\beta}_{i,t+1}^2\right) w_{t+1}^R$ and a distorted user cost of capital. We now describe these objects in detail.

Modeling Adaptation Costs Firm i chooses an adaptation intensity $\widetilde{\beta}_{i,t+1}$, which shifts its effective temperature sensitivity in productivity. Achieving $\widetilde{\beta}_{i,t+1}$ requires the firm to hire $\frac{1}{2} H \widetilde{\beta}_{i,t+1}^2$ units of adaptation resources at price w_{t+1}^R. This convex cost structure captures rising marginal costs of adaptation and ensures that optimal policies (and profits) are finite.[32]

Adaptation enters productivity multiplicatively. When $\widetilde{\beta}_{i,t+1}(T_{t+1} - T^*) > 0$, it increases effective TFP by the factor $\exp\{\widetilde{\beta}_{i,t+1}(T_{t+1} - T^*)\}$, so the payoff to a given improvement in adaptation is larger for firms operating at a larger scale. In this sense, adaptation is complementary to firm size: holding $\widetilde{\beta}_{i,t+1}$ fixed, a larger firm obtains a larger absolute gain from the same percentage increase in productivity. Finally, the mapping from adaptation resources to $\widetilde{\beta}_{i,t+1}$ is *non-homothetic*. Because costs are convex in $\widetilde{\beta}_{i,t+1}$ rather than proportional, scaling up the firm does not scale up optimal adaptation one-for-one. As a result, heterogeneity in scale and fundamentals translates into heterogeneity in endogenous adaptation choices.

Frictions in the Capital Market Firms face heterogeneous capital market distortions summarized by the (log) wedge $\tau_{i,t+1} \equiv \log \mathcal{T}_{i,t+1}$:

$$\tau_{i,t+1} = \omega_{\bar{a}} \bar{a}_i + \phi_{i,t+1}^{\tau}, \qquad \omega_{\bar{a}} > 0.$$

The first component captures *size-dependent* distortions: when $\omega_{\bar{a}} > 0$, firms with higher permanent productivity $\bar{a}_i$ (and hence larger scale) face systematically larger wedges, in the spirit of Restuccia and Rogerson (2008). The second component $\phi_{i,t+1}^{\tau}$ captures idiosyncratic distortions and follows an AR(1) process,

$$\phi_{i,t+1}^{\tau} = \rho_{\phi}^{\tau}\, \phi_{i,t}^{\tau} + \varepsilon_{i,t+1}^{\phi^{\tau}}, \qquad \varepsilon_{i,t+1}^{\phi^{\tau}} \sim \mathcal{N}(0, \sigma^2_{\varepsilon^{\phi^{\tau}}}).$$

32. Equivalently, convexity delivers an interior solution for $\widetilde{\beta}$ and rules out unbounded increases in productivity.

A firm with wedge $\mathcal{T}_{i,t+1}$ pays an additional $\mathcal{T}_{i,t+1} - 1$ on the risk-free user cost for each unit of installed capital.

Firm's Optimality Conditions The firm's optimal investment policies follow from the Bellman problem in (17). Optimal capital accumulation satisfies the Euler equation

$$\frac{1}{1+r}(r+\delta)\mathcal{T}_{i,t+1} = \alpha G\, K_{t+1}^{\theta_K} K_{i,t+1}^{\alpha-1}\, \mathbb{E}_t\left[\Lambda_{t+1}\left(A_{t+1}^{\theta_A} e^{a_{i,t+1}}\right)\right] + (1-\delta)\,\mathbb{E}_t\left[\Lambda_{t+1} - \frac{1}{1+r}\right].$$

This condition equates the distorted user cost of installed capital to the expected discounted marginal revenue product of capital plus the expected discounted value of undepreciated capital.

Optimal adaptation satisfies

$$\widetilde{\beta}_{i,t+1} = \frac{G}{w_{t+1}^R H}\, K_{t+1}^{\theta_K} K_{i,t+1}^{\alpha}\, \mathbb{E}_t\left[\Lambda_{t+1} A_{t+1}^{\theta_A} e^{a_{i,t+1}}\left(T_{t+1} - T^*\right)\right].$$

Thus, holding prices fixed, adaptation is increasing in expected scale and in the expected marginal benefit of insulation from temperature realizations—which is larger when the region is expected to be further from the bliss point—and decreasing in the resource cost of adaptation w_{t+1}^R and the curvature parameter H.

The Homogeneous Deterministic Steady State To build intuition, consider a homogeneous deterministic steady state (HDSS) with no firm heterogeneity and no uncertainty.

$$\widetilde{\beta} = \kappa\,(\bar{T} - T^*), \qquad \kappa = \frac{1-\alpha_N}{(1+r)\eta H} > 0.$$

The expression highlights that the HDSS adaptation direction depends on if the firm is in a climate regime warmer than the bliss point ($\bar{T} > T^*$) or colder ($\bar{T} < T^*$). Firms optimally choose $\widetilde{\beta} > 0$ in warm regions and $\widetilde{\beta} < 0$ in cold regions to improve productivity.

5.2 Solving the Model via Risk-adjusted Perturbation

We solve the model in closed form using a risk-adjusted perturbation around the homogeneous deterministic steady state (HDSS) as in David and Venkateswaran (2019). The key difficulty is that firms' Euler equations feature *risk-adjusted* expectations—products of the stochastic discount factor (SDF) and future payoffs—under non-linear temperature exposure and endogeneous heterogeneity. Our approach proceeds in three steps.

Step 1: Risk-adjusted approximation of FOCs. We extend the risk-adjusted approximation in Coeurdacier, Rey, and Winant (2011) beyond log-normal environments by developing a second-order expansion of stochastic variables in conditional moments of shocks (means, variances, and covariances), and then applying it systematically to the firms' optimality conditions. As a simple illustration, the one-period risk-free return is $R_{f,t+1} = \frac{1}{\mathbb{E}_t[\Lambda_{t+1}]}$. Let $\widehat{x}_t \equiv x_t - x^{\text{HDSS}}$ denote deviations from the HDSS and let $\lambda_{t+1} \equiv \log \Lambda_{t+1}$. A second-order expansion delivers the convenient

risk-adjusted representation

$$\widehat{r}_{f,t+1} \equiv \log R_{f,t+1} - \log R_f^{\text{HDSS}} \;=\; - \underbrace{\widehat{\mathbb{E}_t \lambda_{t+1}}}_{\substack{\text{Consumption} \\ \text{Smoothing}}} \; \underbrace{- \frac{1}{2} \mathbb{VAR}_t \left(\widehat{\lambda}_{t+1} \right)}_{\text{Precautionary}}$$

which makes clear that the risk-free rate falls when expected marginal utility growth rises (consumption smoothing) and when uncertainty in the pricing kernel increases (a precautionary-savings effect).

Step 2: Bilinear policy-function approximation. We approximate firms' policy rules for next-period capital and adaptation using an affine–bilinear expansion in (i) firm-level state vectors $\mathbf{x}_{it}$ (e.g., persistent and transitory productivity, wedges, and product exposure) and (ii) aggregate state vectors $\mathbf{x}_t$ (e.g., aggregate productivity, aggregate capital, and temperature moments). For example, for log capital $k_{i,t+1} \equiv \log K_{i,t+1}$,

$$k_{i,t+1} = k^{\text{HDSS}} + \mathbf{G}_i^\top \widehat{\mathbf{x}}_{it} + \mathbf{G}_a^\top \widehat{\mathbf{x}}_t + \underbrace{\widehat{\mathbf{x}}_{it}^\top \mathbf{G}_{ia} \widehat{\mathbf{x}}_t}_{\substack{\text{heterogeneous response to} \\ \text{aggregate shocks and uncertainty}}} + \mathbf{G}_d^\top \widehat{\mathbf{d}}_t + \mathbf{G}_\Gamma^\top \widehat{\mathbf{\Gamma}}_{micro,t},$$

and analogously for $\widetilde{\beta}_{i,t+1}$. The interaction term $\widehat{\mathbf{x}}_{it}^\top \mathbf{G}_{ia} \widehat{\mathbf{x}}_t$ is essential: it captures how a common temperature realization (or a change in forecast uncertainty) loads differently across firms through heterogeneous effective exposure and wedges, generating endogenous dispersion in firm decisions.

Step 3: Aggregation and coefficient identification. We apply the same second-order (affine-bilinear) expansion to the aggregation equations. Because the policy rules are affine-bilinear, aggregates depend on the cross-sectional distribution of $\mathbf{x}_{it}$ only through a finite set of moments, collected in $\mathbf{\Gamma}_{micro,t}$ (in the spirit of Krusell and Smith (1998)). Finally, we substitute the approximated policy rules and aggregation equations into all equilibrium conditions (firms' Euler equations, factor-market clearing, and the household pricing kernel), and solve for the unknown coefficients by matching terms of equal order (constant, linear, and bilinear). This guess-and-verify procedure yields closed-form expressions for both micro policies and macro equilibrium objects, including MRPK dispersion and the resulting aggregate TFP losses.

5.3 Investment and Adaptation in the Cross-section

We now analyze how cross-sectional differences in firms' capital and adaptation responses to climate shocks and climate risk generates dispersion in realized MRPK. We emphasize on the empirically relevant warm-region case in which heat remains productivity-reducing on average despite adaptation.

Definition 1 (A typical warm region.) *The climate is above the bliss point $\bar{T} > T^*$ where firms adapt positively $\tilde{\beta} > 0$, the average firm is heat-sensitive $\bar{\beta} < 0$, and that adaptation is sufficiently costly $\eta H > \frac{(1-\alpha_N)(\bar{T}-T^*)}{(1+r)(-\bar{\beta})}$. Such world implies $\bar{\beta} + \widetilde{\beta} < 0$.*

We now characterize how firms respond to temperature forecasts and risk. Proposition 3 shows that cross-sectional differences in both adaptation and capital investment are driven by the expected productivity and the covariance between firm's profitability and temperature risk.

Proposition 3 (Investment and Adaptation) *Let $\Delta^i x_{it} \equiv x_{it} - \bar{x}_t$ denote firm i's deviation from the time-t cross-sectional mean. The expected profit is increasing in expected productivity but declining in wedges,*

$$\Delta^i \mathbb{E}_t \hat{\pi}_{it+1} \;=\; \Delta^i \mathbb{E}_t \hat{a}_{it+1} - \alpha\, \Delta^i \hat{\tau}_{it+1}.$$

In equilibrium, optimal policy decision satisfies:

(i) ***Adaptation.***

$$\Delta^i \hat{\tilde{\beta}}_{it+1} = \frac{\tilde{\beta}}{1-\alpha}\left[\Delta^i \mathbb{E}_t \hat{\pi}_{it+1} + \Omega\, \mathrm{Cov}_t\left(\hat{a}_{it+1}, \hat{T}_{t+1}\right)\right] \tag{18}$$

(ii) ***Capital.***

$$\Delta^i \hat{k}_{it+1} = -\Delta^i \hat{\tau}_{it+1} + \frac{1}{1-\alpha}\,\Delta^i \mathbb{E}_t \hat{\pi}_{it+1} \;+\; \frac{\bar{\beta}+\tilde{\beta}}{1-\alpha}\,\Theta\,\Delta^i\,\mathrm{Cov}_t\left(\hat{a}_{it+1}, \hat{T}_{t+1}\right). \tag{19}$$

where $\Theta = \left(\frac{\sigma}{\sigma-1} - \tilde{\alpha}_N\right)(\theta_A - \gamma) + 1 < 0$, *and* $\Omega \equiv (\bar{\beta}+\tilde{\beta})\Theta + \frac{1-\alpha}{\bar{T}-T^*} > 0$.

Firms with higher expected productivity $\mathbb{E}_t \hat{a}_{it+1}$ and lower capital wedges $\hat{\tau}_{it+1}$ anticipate a larger profit base, and therefore adapt more and invest more capital. A higher covariance $\mathbb{COV}_t(\hat{a}_{it+1}, \hat{T}_{t+1})$ raises the risk-adjusted return because the firm's productivity are relatively high precisely in hot and high-price states which deliver higher profits. As a result, in the typical warm region, firms whose productivity co-moves more positively with temperature invest and adapt more.

Corollary 1 shows that a firm adapt more instead of investing in capital when the effective user cost of capital and risk-adjusted returns increase. Firms facing larger distortions therefore increase production by adapting production technology instead of investing in more capital. And since that the marginal payoff to adaptation is inherently more state-contingent than the marginal payoff to capital, a firm in a typical warm region whose productivity comoves more positively with temperature tilt further toward adaptation.

Corollary 1 (Within-firm Adaptation-capital Trade-off) *Combining part (i) and (ii) in Proposition 3 yields an expression for how a firm tilts its choices toward adaptation relative to capital:*

$$\frac{\Delta^i \widehat{\tilde{\beta}}_{it+1}}{\widetilde{\beta}} - \Delta^i \hat{k}_{it+1} = \underbrace{\Delta^i \widehat{\tau}_{it+1}}_{\textit{relative price}} + \underbrace{\frac{\widetilde{\beta}}{\bar{T}-T^*}\,\Delta^i \mathbb{COV}_t\left(\hat{a}_{it+1}, \widehat{T}_{t+1}\right)}_{\textit{relative risk/curvature}}.$$

Proposition 3 and Corollary 1 are useful for interpreting equilibrium forces. However, these exact policies are yet to be solved. In particular, both $\Delta^i \mathbb{E}_t \hat{a}_{it+1}$ and $\Delta^i \mathbb{COV}_t\left(\hat{a}_{it+1}, \hat{T}_{t+1}\right)$ are equilibrium objects that depend on firms' choices of $\widetilde{\beta}_{it+1}$ and k_{it+1} through the productivity process and exposure to temperature. We now solve the fixed point problem and express firms'

choices as functions of firm-level primitives and temperature forecast and forecast uncertainty. To ease interpretation, we introduce an endogenous sensitivity index in Definition 2.

Definition 2 (Endogenous Sensitivity index) *Ψ_{it} collects the endogenous component of a firm's effective temperature sensitivity.*

$$\Psi_{it} = \Upsilon \left[\left(\bar{T} - T^* \right) \hat{\beta}_i + \bar{a}_i + \rho_z z_{it} - \alpha \tau_{it+1} \right], \tag{20}$$

where $\Upsilon = \frac{\tilde{\beta}}{1-\alpha-\tilde{\beta}\left(\bar{T}-T^*\right)}$ is the endogenous sensitivity multiplier with $\Upsilon > 0$ in the typical warm region.

The index increases with the firm's persistent and predictable productivity components ($\bar{a}_i$ and $\rho_z z_{it}$), intrinsic temperature exposure $\hat{\beta}_i(\bar{T} - T^*)$ and decreases with the effective user cost of capital (τ_{it+1}). Economically, Ψ_{it+1} summarizes the *aggregate-state-independent* profitability of a firm.

Proposition 4 (Policy Functions.) *(i) **Adaptation.***

$$\Delta^i \hat{\tilde{\beta}}_{it+1} = \Psi_{it+1} + \Upsilon \left(\hat{\beta}_i + \Psi_{it+1} \right) \left(\mathbb{E}_t(\hat{T}_{t+1}) + \Omega \mathbb{VAR}_t \left[\hat{T}_{t+1} \right] \right); \tag{21}$$

*(i) **Capital.***

$$\Delta^i \hat{k}_{it+1} = -\tau_{it+1} + \frac{\Psi_{it+1}}{\tilde{\beta}} + \Upsilon \left(\hat{\beta}_i + \Psi_{it+1} \right) \left(\mathbb{E}_t(\hat{T}_{t+1}) + \left[\left(\bar{\beta} + \tilde{\beta} \right) \Theta + \tilde{\beta} \right] \mathbb{VAR}_t \left[\hat{T}_{t+1} \right] \right). \tag{22}$$

Proposition 4 summarizes the policy functions. Adaptation and capital investment both increase with endogenous sensitivity and the aggregate temperature moments. The effect of expected temperature and forecast uncertainty on adaptation and investment are multiplied by the effective exposure ($\hat{\beta}_i + \Psi_{it+1}$). The effective exposure combines intrinsic product sensitivity with endogenous sensitivity index, and it governs how strongly a firm responds to expected and unexpected weather shocks. Moreover, the expected scale is mapped to adaptation decisions with the *endogenous sensitivity multiplier*,

$$\Upsilon = \frac{\widetilde{\beta}}{1 - \alpha - \widetilde{\beta}(\bar{T} - T^*)} = \frac{\tilde{\beta}}{1-\alpha} \cdot \sum_{r=1}^{\infty} \left(\frac{\tilde{\beta}\left(\bar{T} - T^*\right)}{1-\alpha} \right)^r.$$

which summarizes the fixed-point feedback between scale and adaptation near steady state: an upward shift in the firm's expected profit base raises the marginal value of adaptation; a higher adaptation raises productivity by $(\bar{T} - T^*)$; this additional productivity raises adaptation again; iterating this feedback generates a geometric series with loop gain $\frac{\tilde{\beta}\left(\bar{T}-T^*\right)}{1-\alpha}$.

With perfectly predictable temperatures, policy rules depend only the expected temperature. Higher expected heat raises both adaptation and capital more for firms with greater effective exposure. In a typical warm region, expected warming therefore disproportionately increases investment and adaptation among firms that are already expected to operate at larger scale (high Ψ) or whose products are more temperature exposed (high $\hat{\beta}_i$). Because these firms adjust more strongly, expected heat increases within-region-year dispersion in both adaptation and capital. When temperatures are harder to predict, the forecast uncertainty further widens firms' differences by inducing larger responses among firms with higher effective exposure.

Interestingly, the presence of endogenous adaptation leads to "self-reinforcing" endogenous productivity and risk premia: by raising effective productivity and improving performance in hot states, it lowers risk premia and required returns, which further strengthens incentives to invest and adapt, amplifying cross-sectional differences.

5.3.1 What determines MRPK?

Using the profit function in Equation (16) and the constant markups implied by the Dixit-Stigliz competition, log MRPK can be written (up to constants) as

$$\widehat{mrpk}_{it+1} = \hat{a}_{it+1} - (1-\alpha)\hat{k}_{it+1} + \theta_A \hat{y}_{t+1}. \tag{23}$$

The realized mrpk reflects both ex post productivity surprises, and ex ante optimal choices of capital investment. Holding productivity fixed, higher predetermined capital lowers mrpk. The aggregate term $\theta_A \hat{y}_{t+1}$ is common across firms within a region-year and therefore drops out of cross-sectional comparisons. Substituting the policy functions from Equation (21) and (22) into Equation (23) yields the cross-sectional differences in MRPK.

Proposition 5 (Cross-sectional MRPK differences.) *Comparing to the average firm, the cross-sectional differences in (log) MRPK of firm i can be written as*

$$\Delta^i \widehat{mrpk}_{it+1} = \underbrace{\left(\Delta^i a_{it+1} - \mathbb{E}_t \Delta^i \widehat{a}_{it+1}\right)}_{\textit{Unexpected Productivity}} + \underbrace{\widehat{\tau}_{it+1}}_{\textit{Distortions}} \underbrace{- (\bar{\beta} + \widetilde{\beta})\Theta \left[\widehat{\beta}_i + \Psi_{it+1}\right] \mathbb{VAR}_t \left(\widehat{T}_{t+1}\right)}_{\textit{Temperature Uncertainty}} \tag{24}$$

where the unexpected productivity can be expressed as

$$\Delta^i a_{it+1} - \mathbb{E}_t \Delta^i \widehat{a}_{it+1} = \underbrace{\left[\widehat{\beta}_i + \Psi_{it+1}\right]\left(\widehat{T}_{t+1} - \mathbb{E}_t\left(\widehat{T}_{t+1}\right)\right)}_{\textit{Temperature's Forecast Error}} + \underbrace{\xi_{it+1}\left(T_{t+1} - T^*\right)}_{\textit{Temperature's Random Damage}} + \varepsilon^z_{it+1} \tag{25}$$

Proposition 5 points to three distinct sources of cross-sectional heterogeneity in a firm's realized capital return. Firstly, a positive productivity surprise raises capital return because capital is predetermined, and when realized productivity exceeds its expectation, firms cannot instantaneously adjust capital. And thus the marginal product of capital rises. In a typical warm region, a heat surprise ($\widehat{T}_{t+1} - \mathbb{E}_t\left(\widehat{T}_{t+1}\right) > 0$) is common to all firms but generates heterogeneous productivity shocks through firm-specific effective exposure ($\widehat{\beta}_i + \Psi_{it+1}$). Firms that are better adapted (higher Ψ_{it+1}) or inherently less heat sensitive (higher $\widehat{\beta}_i$) benefit more from the same heat surprise. For example, an ice-cream parlor ($\widehat{\beta}_i > 0$) experiences a more favorable shock than a ski resort ($\widehat{\beta}_i < 0$); and among ice-cream parlors, the more productive and less distorted ones with a higher endogenous sensitivity index gain more. In addition, a transitory firm-specific disruption captured by $\xi_{it+1}\left(T_{t+1} - T^*\right)$ also affect productivity. For example, an unlucky firm hit by a weather-induced plant fire or equipment failure suffers a larger productivity loss than the average firm. Such idiosyncratic shocks are more likely to happen as climate becomes more extreme.

Secondly, a higher capital wedge lowers the level of investment which mechanically raises the capital return. This is the standard misallocation force where the distorted firms are systematically

capital-scarce and therefore have higher marginal products.

Finally, higher temperature uncertainty in a typical warm region lowers realized capital return, especially for firms with greater effective exposure. When a firm's profitability is more aligned with hot states (higher effective exposure), it provides higher payoffs in hot states and therefore commands a more favorable risk premium. They therefore accumulate more capital ex-ante which reduces realized MRPK ex post.

5.3.2 The Equilibrium MRPK Dispersion

This cross-sectional disparity in realized returns leads directly to the equilibrium misallocation of capital. Proposition 6 presents all the forces driving the dispersion.

Proposition 6 (Capital (Mis)Allocation in Equilibrium.) *The equilibrium MRPK dispersion admits the decomposition*

$$\begin{aligned}\sigma^2_{mrpk,t+1} = \quad & \underbrace{\mathbb{VAR}^i(\tau_{it+1})}_{\text{baseline wedge dispersion}} + \underbrace{\sigma^2_{\varepsilon^z}}_{\text{non-climate idiosyncratic productivity}} + \underbrace{\sigma^2_{\xi}\,(T_{t+1}-T^*)^2}_{\text{random climate damages}} \\ & + \underbrace{\mathbb{VAR}^i(\widehat{\beta}_i+\Psi_{i,t+1})\,\left(\widehat{T}_{t+1}-\mathbb{E}_t\left[\widehat{T}_{t+1}\right]-(\bar{\beta}+\widetilde{\beta})\Theta\mathbb{VAR}_t\left(\widehat{T}_{t+1}\right)\right)^2}_{\text{exposure-amplified forecast error \& risk}} \\ & + \underbrace{2\,\mathbb{COV}^i(\tau_{it+1},\widehat{\beta}_i+\Psi_{i,t+1})\,\left(\widehat{T}_{t+1}-\mathbb{E}_t\left[\widehat{T}_{t+1}\right]-(\bar{\beta}+\widetilde{\beta})\Theta\mathbb{VAR}_t\left(\widehat{T}_{t+1}\right)\right)}_{\text{wedge–exposure interaction}},\end{aligned} \tag{26}$$

where

$$\mathbb{VAR}^i(\tau_{it+1}) = \omega^2_{\bar{a}}\sigma^2_{\bar{a}} + \sigma^2_{\phi^\tau}, \tag{27}$$

$$\mathbb{VAR}^i(\widehat{\beta}_i+\Psi_{i,t+1}) = \frac{(1-\alpha)^2\sigma^2_{\hat{\beta}} + \widetilde{\beta}^2\Big((1-\alpha\omega_{\bar{a}})^2\sigma^2_{\bar{a}} + \rho^2_z\sigma^2_z + \alpha^2\sigma^2_{\phi^\tau}\Big)}{\left(1-\alpha-\widetilde{\beta}(\bar{T}-T^*)\right)^2}, \tag{28}$$

$$\mathbb{COV}^i(\tau_{it+1},\widehat{\beta}_i+\Psi_{i,t+1}) = \frac{\widetilde{\beta}}{1-\alpha-\widetilde{\beta}(\bar{T}-T^*)}\left(\omega_{\bar{a}}(1-\alpha\omega_{\bar{a}})\sigma^2_{\bar{a}} - \alpha\sigma^2_{\phi^\tau}\right). \tag{29}$$

The first two terms of Proposition 6 capture baseline dispersion from wedges and non-climate productivity shocks, which would arise even without any temperature risk. The third term captures unpredictable climate damage that happen as temperature moves away from the bliss point. The magnitude of the impact is governed by idiosyncratic sensitivity dispersion σ^2_ξ. Importantly, this channel remains active even if all firms are well-adapted and aggregate temperature perfectly forecasted.

The last two terms capture the impact of an aggregate weather component, governed by both the dispersion of effective exposure and its interaction with firm distortion. The aggregate weather component bundles the realized forecast errors and risk-adjusted temperature uncertainty. The higher the aggregate temperature moments, the higher the capital misallocation of a region-sector in a given year. For two warm regions with the same aggregate temperature moments, their capital misallocation differs through the variance of effective exposure, $\mathbb{VAR}^i\left(\widehat{\beta}_i+\Psi_{i,t+1}\right)$, and its interaction with capital wedges, $\mathbb{COV}^i\left(\tau_{it+1},\widehat{\beta}_i+\Psi_{i,t+1}\right)$.

The variance captures the dispersion of both time-invariant product sensitivity and firm-specific endogenous sensitivity. A region with more dispersed effective exposure of firms, tend to have a higher capital misallocation, even facing the same aggregate temperature moments comparing to another region. The dispersion of endogenous sensitivity across firms also imply that better average adaptation does not necessarily mean smaller misallocation responses. One important factor of the endogenous sensitivity is the steady-state adaptation $\tilde{\beta}$, which rises with lower adaptation costs. For a typical warm region with lower adaptation costs, firms are more incentivized to adapt, which naturally increase the differential adaptation among firms. This further steepen temperature risk into MRPK dispersion. The covariance captures the co-movement between firm wedge and effective exposure. For a region with more distorted firms that offer more temperature exposed products or more adapted endogenously, the higher the misallocation. The two second-order channels highlight that regional differences of capital misallocation are governed not only by cross-region temperature and forecast, but also within-region firm heterogeneity.

6 Reduced form evidence for the model mechanisms

The model developed in the previous section delivers a transparent mapping from temperature realizations and temperature risk into cross-sectional dispersion in realized capital returns. Two mechanisms are central. First, a *level (damage-volatility) channel*: idiosyncratic climate damages scale with the distance of realized temperature from the bliss point, so regions operating in more extreme climates face greater dispersion in realized productivity and hence in MRPK. Second, a *forecast-and-risk channel*: a common temperature surprise and common forecast uncertainty translate into dispersed MRPK because firms differ in *effective exposure* to temperature, which combines intrinsic product sensitivity with endogenous adaptation and scale.

This section provides reduced-form evidence for these channels using variation at both the firm level and the region–sector level.

6.1 Firm-level evidence

6.1.1 Adaptation rises with capital and distortions

A core feature of the model is that adaptation is a *non-homothetic* choice: the payoff to improving temperature resilience scales with the firm's operating scale. At the same time, capital wedges raise the effective user cost of capital and therefore tilt the firm toward adaptation *relative to capital*, holding scale fixed. A convenient way to summarize these forces is the within-firm capital–adaptation trade-off implied by the linearized policy rules:

$$\frac{\Delta^i \widehat{\widetilde{\beta}}_{i,t+1}}{\widetilde{\beta}} = \Delta^i \hat{k}_{i,t+1} + \Delta^i \widehat{\tau}_{i,t+1} + \frac{1}{\bar{T} - T^*} \Delta^i \mathbb{COV}_t \left(\hat{a}_{i,t+1}, \widehat{T}_{t+1} \right), \tag{30}$$

where Δ^i denotes deviations from the average firm within a region-year, $\widetilde{\beta}$ is the steady-state adaptation intensity in that region, and $\widehat{\tau}_{i,t+1}$ is the (log) capital wedge. Equation (30) has two immediate implications for a warm region (where $\widetilde{\beta} > 0$): (i) larger firms (higher $\hat{k}$) choose higher

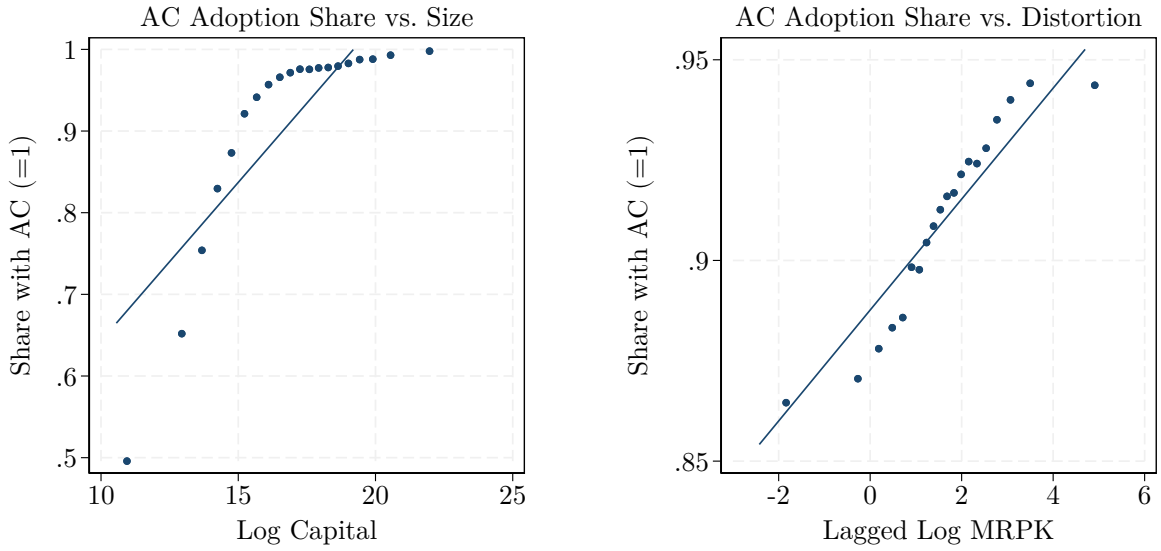
adaptation; and (ii) conditional on scale and common risk conditions, firms facing higher capital wedges tilt toward greater adaptation.

To take this prediction to the data, we need a firm-level proxy for adaptation. While direct measures are rarely available, the Indian Annual Survey of Industries (ASI) reports whether a plant has installed computerized air-conditioning (AC) systems. We therefore proxy adaptation with AC adoption and focus this exercise on the ASI sample years for which the measure is available. We thus estimate the following conditional relationship (and present it as residualized binscatters):

$$\mathbf{1}\{AC_{it} = 1\} = \lambda_1 k_{it} + \lambda_2 mrpk_{i,t-1} + \eta_{r,s,t} + u_{it}, \tag{31}$$

where $\eta_{r,s,t}$ are region–sector–year fixed effects that absorb common temperature realizations, forecast moments, and local prices within the cell. We use lagged (log) MRPK as a proxy for wedges: in the accounting framework, wedge-induced capital scarcity maps into systematically higher MRPK. Consistent with the model, AC adoption is increasing in firm capital (scale) and is also increasing in lagged MRPK conditional on scale (Figure 9, panels (a) and (b)). The latter pattern is exactly the substitution effect emphasized by (30): when capital is effectively more expensive, firms tilt toward adaptation.

Figure 9: AC adoption, capital and wedges



Notes: Figure 9 is constructed using the `binsreg` while controlling for firm and region-sector-year fixed effects.

6.1.2 Heterogeneous MRPK Responses to Heat Shocks due to Endogenous Exposure

The model further implies that heterogeneous adaptation and exposure generate heterogeneous MRPK responses to identical temperature shocks. To test this prediction, the key objective is to identify observables that can be mapped into firms' endogenous effective exposure. In the model, the realized MRPK response to a common temperature surprise is proportional to this effective exposure $\Delta^i \widehat{mrpk}_{i,t} \propto \left(\Delta^i \widehat{\beta}_i + \Delta^i \widehat{\tilde{\beta}}_{it}\right)\left(\widehat{T}_t - \mathbb{E}_{t-1}[\widehat{T}_t]\right)$. Moreover, since $\frac{\Delta^i \widehat{\tilde{\beta}}_{i,t+1}}{\widetilde{\beta}} \propto \Delta^i \hat{k}_{i,t+1} + \Delta^i \widehat{\tau}_{i,t+1}$, conditional on the same $\widehat{\beta}_i$, we can write the following approximate relationship:

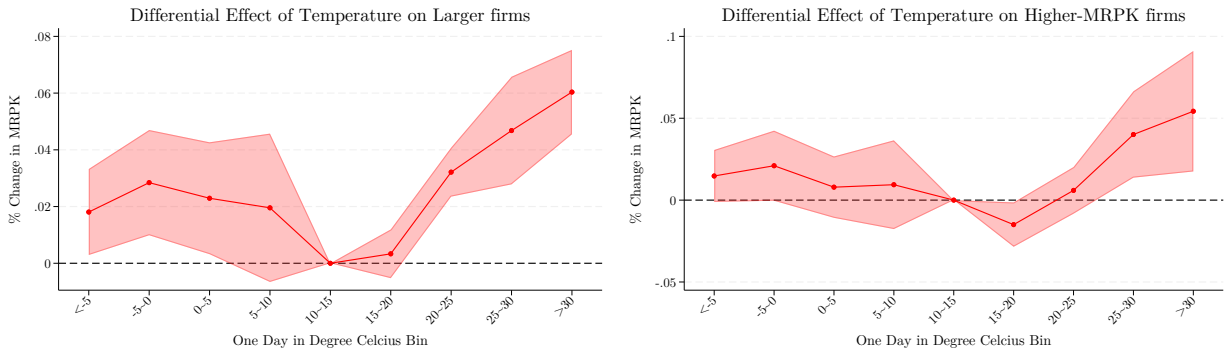
$$\Delta^i \widehat{mrpk}_{i,t} \propto \widetilde{\beta}\left(\Delta^i \hat{k}_{it} + \Delta^i \hat{\tau}_{it}\right)\left(\widehat{T}_t - \mathbb{E}_{t-1}[\widehat{T}_t]\right).$$

To test this implication, we interact temperature shocks with two predetermined firm-level proxies for the endogenous component of effective exposure: (i) *relative capital* (a proxy for scale), and (ii) *relative distortions* (a proxy for wedges). Concretely, we measure scale by lagged log capital and distortions by lagged log MRPK. We then estimate a temperature-bin specification with heterogeneous effects:

$$\begin{aligned} mrpk_{i,t} = &\sum_{b \in B/\{5\text{–}10^\circ\text{C}\}} \lambda_b \, Tbin^b_{r,t} + \sum_{b \in B/\{5\text{–}10^\circ\text{C}\}} \lambda_{b,k} \left(Tbin^b_{r,t} \times \widetilde{k}_{i,t-1} \right) \\ &+ \sum_{b \in B/\{5\text{–}10^\circ\text{C}\}} \lambda_{b,\tau} \left(Tbin^b_{r,t} \times \widetilde{mrpk}_{i,t-1} \right) + \boldsymbol{\delta} \boldsymbol{X}_{it} + \delta_i + \alpha_{s,c(r),t} + \varepsilon_{i,t}, \end{aligned} \tag{32}$$

where $Tbin^b_{r,t}$ counts the number of days in year t that region r experiences daily mean temperature in bin b, δ_i are firm fixed effects, and $\alpha_{s,c(r),t}$ are country–sector–year fixed effects. The variables $\widetilde{k}_{i,t-1}$ and $\widetilde{mrpk}_{i,t-1}$ are (demeaned) measures, so the interaction coefficients capture how firms with higher scale or higher wedges respond differently to the same region-year temperature realization. Using lagged firm variables aligns with the model's timing: capital and adaptation are chosen before temperature is realized, so predetermined capital and wedges are the relevant shifters of effective exposure.

Figure 10: Differential MRPK response to heat shocks interacted with capital and distortions



(a) Heterogeneous Effect with Capital

(b) Heterogeneous Effect with Distortion

The coefficients of interest are $\{\lambda_{b,k}, \lambda_{b,\tau}\}_{b \in B}$. A positive $\lambda_{b,k}$ for hot bins implies that larger firms exhibit a more positive (or less negative) MRPK response to extreme heat than smaller firms, consistent with greater endogenous adaptation/insurance capacity at larger scale. Similarly, a positive $\lambda_{b,\tau}$ for hot bins implies that, conditional on capital, more distorted (higher-lagged-MRPK) firms display a different MRPK response to heat shocks, consistent with wedges tilting firms toward adaptation relative to capital as in (30). Empirically, we find precisely this pattern: conditional on distortions, extreme heat shifts MRPK more for firms with more capital, and conditional on capital, extreme heat shifts MRPK more for more distorted firms (Figure 10).

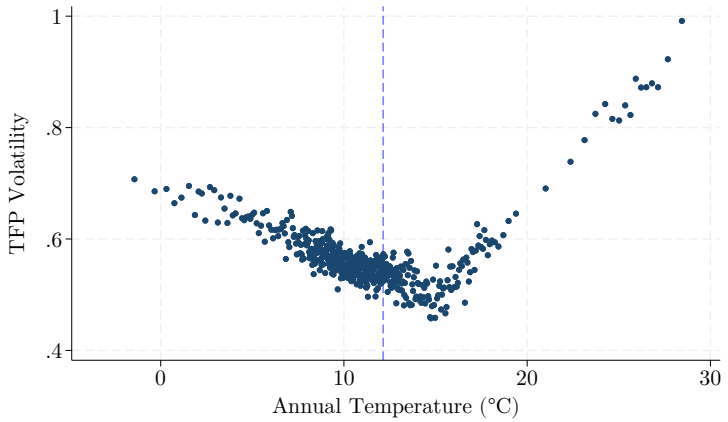
6.2 Region–sector Evidence

The model's equilibrium decomposition of MRPK dispersion implies two reduced-form implications that can be tested at the region–sector level.

6.2.1 Mechanism 1: Climate Extremes Raise Damage Volatility

A direct implication of the random-damage component is a level effect: the same dispersion in firm-specific random damage sensitivities generates larger productivity dispersion when realized temperature is farther from the bliss point T^*, either too hot or too cold. This mechanism predicts that volatility is minimized near T^* and rises as climates become more extreme. As it is difficult to directly measure the dispersion unexpected TFP shocks $(\hat{a}_{nit} - \mathbb{E}_{t-1}[\hat{a}_{nit}])$, due to possible misspecifications of the law of motion of productivity and agents' information set, we adopt the approach of Asker, Collard-Wexler, and De Loecker (2014) and use the variance of 'first-differenced' TFP shocks, $\text{Var}_{(r,s)t}(\hat{a}_{it} - \hat{a}_{it-1})$, as our measure of region-sector-year-level TFP volatility.

Figure 11: TFP volatility and average temperature.



Notes: Figure 11 is constructed using the `binsreg` while controlling for region-sector and country-sector-year fixed effects. The dash line indicates the minimum from a quadratic fit.

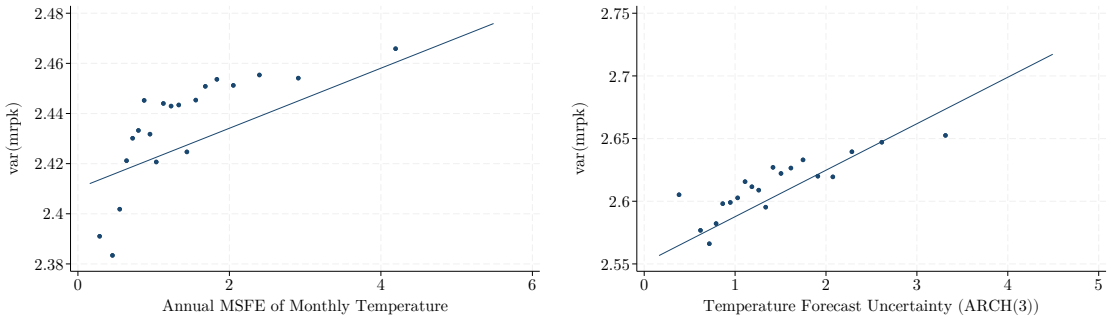
After residualzing with two-way fixed effects, Figure 11 plots TFP volatility against annual average temperature and shows a clear U-shape: volatility is minimized around the empirically relevant bliss-point range (roughly 12–15°C) and increases as temperature moves away from that optimum. This pattern is consistent with the model's level channel: extreme climates increase the volatility of idiosyncratic damages and thereby raise the scope for dispersed investment mistakes and misallocation.

6.2.2 Mechanism 2: Forecast Errors and Forecast Uncertainty Amplify MRPK Dispersion

The second mechanism operates through imperfect predictability. In the model, a common temperature forecast error generates dispersed realized productivity shocks because it is multiplied by heterogeneous effective exposure across firms. In addition, forecast uncertainty affects investment and adaptation ex ante through risk-adjusted returns, inducing dispersion in realized MRPK even holding realized temperature fixed.

We bring this mechanism to the data by combining regional temperature outcomes with mid-range forecast data. Figure 12 shows that, after controlling for panel fixed effects, larger forecast errors (higher annual mean-squared forecast error) lead to larger MRPK dispersion, and that higher forecast uncertainty (constructed from a smoothed ARCH(3)) also lead to to MRPK dispersion. These patterns are consistent with the model's forecast-and-risk channel: when mid-range forecasts are less precise, temperature surprises and uncertainty are translated more strongly into cross-firm dispersion in capital returns.

Figure 12: Forecast Accuracy, uncertainty and Misallocation



(a) Contemporaneous Forecast Accuracy

(b) ARCH(3) Forecast uncertainty

Notes: Figure 12 is constructed using the `binsreg` while controlling for region-sector and country-sector-year fixed effects.

Taken together, the firm-level and region–sector evidence supports the two key mechanisms emphasized by the model: (i) climate extremes raise the volatility of idiosyncratic damages, and (ii) imperfect forecasts and forecast uncertainty amplify dispersion in realized MRPK through heterogeneity in firms' effective exposure and adaptation.

7 Model Estimation and Quantitative Results

7.1 Estimation

This section describes how we bring the model in Section 5 to the data and quantify the contribution of temperature-driven misallocation to aggregate climate damages. We estimate the model parameters jointly using firm panels spanning 1,916 regions in the EU, China, and India. The closed-form solution delivers explicit policy rules and an accounting decomposition of realized MRPK dispersion into (i) wedge-driven dispersion, (ii) idiosyncratic climate damages that scale with distance from the bliss point, and (iii) forecast-error and forecast-uncertainty components that are amplified by heterogeneity in firms' effective exposure. This structure yields a transparent mapping from primitives to observable moments, which we exploit in a Generalized Method of Moments (GMM) estimation of regional adaptation costs and climate-damage parameters.

The need for Joint Estimation Two features of the model make joint estimation essential. First, the temperature bliss point T^* is identified from how temperature affects volatility—TFP volatility and MRPK dispersion—but volatility is itself shaped by endogenous adaptation. Pinning

down T^* therefore requires disciplining adaptation costs, because heterogeneity in adaptation contributes mechanically to measured volatility. Second, the firm-level fundamentals that drive the relevant cross-sectional moments are not directly observed. In the model, realized productivity and MRPK reflect not only permanent and transitory productivity components ($\bar{a}_i, z_{it}$) and wedges (τ_{it}) , but also heterogeneous temperature exposure through intrinsic product sensitivity ($\hat{\beta}_i$) and endogenous adaptation (Ψ_{it}). As a result, identification cannot proceed by simply inverting firm outcomes to recover primitives. Instead, bliss point T^*, product sensitivity $\hat{\beta}_i$ and the regional effective adaptation cost $\eta_r H_r$ governing the strength of Ψ_{it} must be jointly identified together with all micro-fundamentals in a model-consistent way under regional general equilibrium.

7.1.1 Parameterization and Measurement

We split parameters into (i) standard preference and technology parameters that we calibrate externally and impose to be common across regions, and (ii) climate- and region-specific objects that we discipline using moments from the data.

We take one model period to be one year and set the discount factor to $1/(1+r) = 0.96$. We set the CRRA coefficient to $\gamma = 5$, which lies within the median range commonly used in the macro literature (e.g., Mehra and Prescott (1985)). On the production side, we adopt the same demand elasticity as in the accounting exercise and set $\sigma = 4$. We set the Cobb–Douglas factor shares to $\hat{\alpha}_K = 0.35$ and $\hat{\alpha}_N = 0.65$. Under monopolistic competition, these imply revenue exponents $\alpha_F = (1 - 1/\sigma)\hat{\alpha}_F$ for $F \in \{K, N\}$, and hence the profit curvature $\alpha \equiv \frac{\alpha_K}{1-\alpha_N} = 0.51$. These parameters are held fixed across all regions in our baseline. With these parameters, we can map observables to model objects. Consistent with the model's profit function, we measure firm productivity as $a_{it} \equiv py_{it} - \alpha k_{it}$, where py_{it} and k_{it} are log sales and log capital, respectively. Similarly, up to constants common within a region-year (e.g., markups and aggregate price terms), log MRPK can be measured as $mrpk_{it} \equiv py_{it} - k_{it}$, which matches our reduced-form construction and is the sufficient statistic that enters the MRPK-dispersion moments.

As is standard in the literature, we assume the temperature bliss point T^* is common across regions, since it is identified from differential responses of TFP volatility to temperature variation across climates. We also impose that the volatility of random climate damages, σ_ξ^2, is common across regions, because all heterogeneity in product exposure and adaptation is captured by β_i and Ψ_i.[33] For product-level sensitivity, β_i, we assume it is common within each 3-digit USSIC sector.[34] For all other firm-level fundamentals (e.g., $\bar{a}_i$, z_{it}, and wedge components), we allow them to be firm-specific, with their cross-sectional moments varying by region.

Adaptation costs. The key regional object governing endogenous adaptation is the effective cost of adaptation resources, $\eta_r H_r$, which enters the model only through the product $\eta_r H_r$ and therefore cannot be separately identified. To allow adaptation costs to vary systematically with development, we parameterize the inverse cost as a flexible function of long-run income: $\frac{1}{\eta_r H_r} \equiv$

33. We also find limited heterogeneity in the TFP-volatility response to temperature across levels of economic development.

34. To implement this in India and China, we harmonize the NIC-04 and GB-2002 classifications to USSIC at the 3-digit level.

$f\big(\overline{\ln \mathrm{GDP}_r}\big)$, where $f(\cdot)$ is a fourth-order polynomial in $\overline{\ln \mathrm{GDP}_r}$. Under this parameterization, steady-state adaptation intensity in region r can be written as $\widetilde{\beta}_r = \frac{1-\alpha_N}{1+r} f\big(\overline{\ln \mathrm{GDP}_r}\big)\ (\bar{T}_r - T^*)$. Moreover, the endogenous-sensitivity multiplier that appears in the policy rules and in the MRPK dispersion, $\widetilde{\beta}_r/\big(1-\alpha-\widetilde{\beta}_r(\bar{T}_r - T^*)\big)$, admits a convenient local approximation around $\bar{T}_r = T^*$ and $f = f^*$:

$$\frac{\widetilde{\beta}_r}{1-\alpha-\widetilde{\beta}_r(\bar{T}_r - T^*)} = \frac{1-\alpha_N}{(1+r)(1-\alpha)}\Big[\, f^*(\bar{T}_r - T^*) + (\bar{T}_r - T^*)\Big(f(\overline{\ln \mathrm{GDP}_r}) - f^*\Big)\Big] + O\big(\Delta f^3, \Delta \bar{T}_r^3\big), \tag{33}$$

so that, under the cubic specification for $f(\cdot)$, the multiplier becomes a simple polynomial function of long-run temperature and long-run GDP per capita.

Temperature and Forecasts. Lastly, we estimate the temperature process. Following Nath, Ramey, and Klenow (2023), we fit a climate-dependent autoregressive process for annual regional temperature with two-way fixed effects:

$$T_{rt} = \sum_{\tau=1}^{p} \Big(\rho_\tau^0 + \rho_\tau^{\bar{T}}\, \bar{T}_r^{1951\text{–}2018}\Big)\, T_{r,t-\tau} + \chi_r + \chi_t + \varepsilon_{rt}^T, \tag{34}$$

where the persistence coefficients vary flexibly with a region's long-run mean temperature $\bar{T}_r^{1951\text{–}2018}$. We set $p = 6$ as our baseline to capture medium-run temperature persistence while remaining parsimonious in annual data. The fitted values from (34) define the one-step-ahead statistical forecast $\widehat{\mathbb{E}}_{t-1}[T_{rt}]$, and we use the estimated innovations $\widehat{\varepsilon}_{rt}^T \equiv T_{rt} - \widehat{\mathbb{E}}_{t-1}[T_{rt}]$ as our empirical counterpart to the model's annual forecast error $T_{rt} - \mathbb{E}_{t-1}[T_{rt}]$.

To discipline squared forecast errors and hence forecast uncertainty, we use mid-range forecast data from ECMWF as in our reduced-form exercise. Let MSFE_{rt} denote the region-year mean squared error of monthly ECMWF forecasts, aggregated to the annual level. Because the ECMWF product is monthly (rather than year-ahead), we rescale the implied monthly forecast errors to be consistent with the unconditional variance of annual forecast innovations in our sample (1998–2018). Concretely, we map MSFE_{rt} into an annual forecast-error variance by preserving ECMWF's relative improvement over a monthly AR(6) benchmark:

$$\big(T_{rt} - \mathbb{E}_{t-1}T_{rt}\big)^2 = \frac{\mathrm{MSFE}_{rt}}{\frac{1}{12}\sum_{m=1}^{12} \mathbb{VAR}^{1998\text{–}2018}\big(\widehat{\varepsilon}_{rmt}^T\big)}\, \mathbb{VAR}^{1998\text{–}2018}\big(\widehat{\varepsilon}_{rt}^T\big), \tag{35}$$

where $\hat{\varepsilon}_{rmt}^T$ denotes the month-m AR(6) forecast error and $\hat{\varepsilon}_{rt}^T$ denotes the annual AR(6) forecast innovation. This scaling preserves time variation in forecast precision from ECMWF while matching the annual scale of temperature innovations in the estimation sample. Finally, we model perceived temperature uncertainty as a smoothed ARCH(3) process:

$$\mathbb{VAR}_{t-1}(T_{rt}) = \frac{1}{3}\sum_{\tau=1}^{3}\big(T_{r,t-\tau} - \mathbb{E}_{t-\tau-1}T_{r,t-\tau}\big)^2, \tag{36}$$

so that agents perceive temperature to be more volatile following periods with larger recent forecast errors.

7.1.2 Moment Conditions for Model Identification

This section summarizes the moment restrictions used to identify the region-level parameters and firm-level latent components.

(i) Firm-level Moment Conditions For each region, we assume the permanent component of productivity $\overline{a}_i$ and $\overline{mrpk}_i$ for each firm satisfy the standard firm fixed effect moment conditions. Given the presence of heterogeneous sensitivities, we assume the firm-level a_{it} and $mrpk_{it}$, once netted out the temperature-related and permanent components, should satisfy the Yule-Walker conditions implied by their respective AR(1) structure.[35] Lastly, for each region r', the correlated distortion satisfy $\mathbb{E}^i[\bar{a}_i(\overline{mrpk}_i - \omega^a \bar{a}_i)|r(i) = r'] = 0$. Given β_i, Ψ_{it} and T^*, these conditions jointly identifies $\left(\omega^a_r,\ \rho_{z,r},\ \rho_{\phi^\tau,r},\ \{\bar{a}_i\}_i\right)$ for each region r. We can also recover all innovations $\varepsilon^{\phi^\tau}_{it}$, ε^z_{it} and therefore z_{it} and τ_{it} up to some unobserved random damage $\xi_{it}(T_{rt} - T^*)$.

(ii) Product sensitivity β_i. We assume intrinsic product sensitivity is constant within 3-digit category p: $\beta_i = \beta_{q(i)}$, where $q(i)$ maps firm i to its category. Define the MRPK residual after removing region–year general-equilibrium components and endogenous adaptation terms,

$$\widetilde{mrpk}_{i,t+1} \equiv mrpk_{i,t+1} - \theta_A\big(a_{t+1} + \tilde{\alpha}_K k_{t+1}\big) - \big(\tilde{\beta} + \Psi_{i,t+1}\big)(T_{t+1} - \mathbb{E}_t[T_{t+1}]).$$

Then β_p is identified by the orthogonality condition implied by Equation (24), for each category p,

$$\mathbb{E}\Big[\mathbf{1}\{q(i) = p\}\left(\widetilde{mrpk}_{i,t+1} - \beta_p(T_{t+1} - \mathbb{E}_t[T_{t+1}])\right)(T_{t+1} - \mathbb{E}_t[T_{t+1}]) \,\Big|\, \gamma_i, \gamma_{c(r)t}\Big] = 0. \tag{37}$$

Intuitively, after netting out endogenous adaptation and region–year aggregate components, exposure to temperature surprises should operate through intrinsic product sensitivity only, conditional on firm and country–year fixed effects. The regional average product sensitivity can also be recovered by using $\bar{\beta}_r = \mathbb{E}[\hat{\beta}_i | r = r(i)]$.

(iii) Adaptation cost $\eta_r H_r$. To identify regional variation in adaptation costs, we parametrize the inverse cost shifter as $\frac{1}{\eta_r H_r} \equiv f\big(\overline{\ln \mathrm{GDP}_r}\big)$, where $f(\cdot)$ is a third-order polynomial in $\overline{\ln \mathrm{GDP}_r}$. Given this parametrization, Equation (24) implies a set of orthogonality conditions that link temperature forecast errors to cross-firm heterogeneity in exposure and scale. Specifically, we impose the moments

$$\mathbb{E}\Bigg[\underbrace{\Big(mrpk_{it} - \rho_{\phi^\tau}\phi^\tau_{i,t-1} - \big(\widehat{\beta}_i + \Psi_{it}\big)\Big[(T_{rt} - \mathbb{E}_{t-1}T_{rt}) - \Theta\big(\overline{\beta}_i + \tilde{\beta}\big)\mathbb{VAR}_{t-1}T_{rt}\Big]\Big)}_{\text{MRPK residual}}$$
$$\cdot \underbrace{\Big(\overline{\ln \mathrm{GDP}_r}^{\,k} \cdot (\bar{T}_r - T^*) \cdot \Big[(\bar{T}_r - T^*)\widehat{\beta}_i + \bar{a}_i + \rho z_{it} - \alpha\tau_{i,t+1}\Big]\ (T_{rt} - \mathbb{E}_{t-1}T_{rt})\Big)}_{\text{instruments for adaptation-cost shifter}} \,|\, \gamma_i, \gamma_{rt}\Bigg] = 0, \tag{38}$$

$\forall\, k \in \{0, 1, 2, 3, 4\}$. Intuitively, after netting out the wedge dynamics and the common aggregate temperature component, the remaining cross-firm variation in MRPK responses to temperature

35. These moment conditions are also conditional on region-year fixed effects.

surprises should be orthogonal to functions of regional income interacted with the model-implied drivers of endogenous adaptation, within-firm and within-region-year. These moments discipline the coefficients of $f(\overline{\ln \mathrm{GDP}_r})$, and therefore identify $\frac{1}{\eta_r H_r}$ across regions.

(iv) Bliss point T^* and random-damage dispersion σ_ξ^2. The model implies that the bliss point T^* and the dispersion of idiosyncratic climate damages σ_ξ^2 can be jointly identified from region–sector–year variation in (i) TFP-growth volatility and (ii) MRPK dispersion. As in Equation (26), after netting out heterogeneous exposure and the components driven by forecast errors and aggregate uncertainty (captured by some $\mathrm{VolCorrection}_{rst}$ and $\mathrm{MisCorrection}_{rst}$), the remaining temperature dependence is governed by the quadratic damage term $\sigma_\xi^2(T_{rt}-T^*)^2$. Define the residual volatility and residual MRPK dispersion, $\widetilde{V}_{rst}^{\Delta a} \equiv \mathbb{VAR}_{rst}^{i}(a_{it}-a_{i,t-1}) - \mathrm{VolCorrection}_{rst}$, and $\widetilde{V}_{rst}^{mrpk} \equiv \mathbb{VAR}_{rst}^{i}\left(mrpk_{it}\right) - \mathrm{MisCorrection}_{rst}$. Because $a_{it}-a_{i,t-1}$ loads on the idiosyncratic damage realizations in both t and $t-1$, the model predicts $\widetilde{V}_{rst}^{\Delta a}$ scales with $(T_{rt}-T^*)^2+(T_{r,t-1}-T^*)^2$, while $\widetilde{V}_{rst}^{mrpk}$ scales with $(T_{rt}-T^*)^2$. We therefore impose the following model-consistent moment conditions:

$$\mathbb{E}\Big[\Big(\widetilde{V}_{rst}^{\Delta a} - \sigma_\xi^2\big[(T_{rt}-T^*)^2+(T_{r,t-1}-T^*)^2\big]\Big)\,(T_{rt}^2+T_{r,t-1}^2)\;\Big|\;\gamma_{rs},\gamma_{ct}\Big]=0, \tag{39}$$

$$\mathbb{E}\Big[\Big(\widetilde{V}_{rst}^{\Delta a} - \sigma_\xi^2\big[(T_{rt}-T^*)^2+(T_{r,t-1}-T^*)^2\big]\Big)\,(T_{rt}+T_{r,t-1})\;\Big|\;\gamma_{rs},\gamma_{ct}\Big]=0, \tag{40}$$

$$\mathbb{E}\Big[\Big(\widetilde{V}_{rst}^{mrpk} - \sigma_\xi^2(T_{rt}-T^*)^2\Big)\,(T_{rt}-T^*)^2\;\Big|\;\gamma_{rs},\gamma_{ct}\Big]=0. \tag{41}$$

Intuitively, once we purge the components of volatility and dispersion accounted for by heterogeneous exposure to temperature shocks and risk, the remaining cross-sectional volatility in productivity growth and dispersion in MRPK should be explained by random climate damages that rise with the squared distance from the bliss point. The first two moments use time-series variation in temperature levels to locate T^* (via how volatility co-moves with temperature), while the third moment disciplines the scale of the quadratic term and helps pin down σ_ξ^2.

Taken together, these moments jointly identify the common parameters $\{T^*, \sigma_\xi^2\}$, as well as the region-specific objects $\{\bar{\beta}_r,\ (\eta_r H_r)^{-1},\ \sigma_{\hat{\beta},r}^2,\ \sigma_{\tilde{a},r}^2,\ \sigma_{\varepsilon^z,r}^2,\ \sigma_{\varepsilon^{\phi^\tau},r}^2,\ \rho_{\phi^\tau,r},\ \rho_{z,r},\ \omega_{a,r}\}_r$.

7.1.3 Implementation via a Fixed-Point Algorithm

We implement the estimator using a transparent fixed-point algorithm that circumvents the computational burden of solving the full joint GMM problem in one step. The algorithm iterates between (i) inverting the model to recover firm-level latent objects and region-level moments given a current parameter guess, and (ii) updating the parameters using the moment conditions described above.

1. **Initialization.** Start from an initial guess for regional adaptation costs and intrinsic product sensitivities, e.g. $\frac{1}{\eta_r H_r} = 0$ and $\beta_i = 0$, together with an initial guess for the common parameters $\{T^*, \sigma_\xi^2\}$. Given these values, compute the implied steady-state adaptation $\{\widetilde{\beta}_r\}_r$ and the corresponding regional sensitivity multipliers. This step enables model inversion:

we recover firm-level fundamentals and construct all region–sector moments needed for the subsequent updates.

2. **Update the bliss point and random-damage dispersion $\{T^*, \sigma_\xi^2\}$.** Using the objects recovered in Step 1, construct the region–sector–year correction terms $\text{VolCorrection}_{rst}$ and $\text{MisCorrection}_{rst}$. We then implement the moment conditions in Equations (39)–(41) via simple two-way fixed-effects regressions to update $\{T^*, \sigma_\xi^2\}$.

3. **Update intrinsic product sensitivity $\{\beta_i\}$.** Given the updated T^*, recompute the endogenous exposure component Ψ_{it} and form the residualized return $\widetilde{mrpk}_{it}$ that nets out the region–year general-equilibrium terms and endogenous adaptation. We then estimate the moment condition in Equation (37) using a high-dimensional fixed-effects specification that allows for 3-digit-category-specific slopes, which updates $\beta_i = \beta_{q(i)}$ for all firms.

4. **Update regional adaptation costs $\{(\eta_r H_r)^{-1}\}_r$.** Under the fourth-order polynomial specification of $\frac{1}{\eta_r H_r} \equiv f\left(\overline{\ln \text{GDP}_r}\right)$, using the updated $\{\beta_i\}$, we first net out the intrinsic temperature-shock component from $mrpk_{it}$. We then estimate the moment conditions in Equation (38) by projecting the relevant MRPK residual on $\left(\bar{T}_r - T^*\right)\left[\left(\bar{T}_r - T^*\right)\widehat{\beta}_i + \bar{a}_i + \rho z_{it} - \alpha\tau_{i,t+1}\right]\left(T_t - \mathbb{E}_{t-1}[T_t]\right)$ interacted with a polynomial in $\overline{\ln \text{GDP}_r}$. This yields an updated estimate of $f(\overline{\ln \text{GDP}_r})$ and hence $(\eta_r H_r)^{-1}$.[36]

5. **Iterate to convergence.** Update the parameter guesses and repeat Steps 1–4 until $\max\left\{\|\Delta\beta\|_i, \left\|\Delta(\eta H)^{-1}\right\|_r, |\Delta T^*|, |\Delta\sigma_\xi^2|\right\}$ falls below a pre-specified tolerance, ensuring convergence of both firm-level latent objects and region-level moments.

While we do not impose a formal uniqueness proof, in practice the fixed-point iteration converges quickly (typically in fewer than 20 iterations) and is robust to a wide range of reasonable initial guesses. Intuitively, temperature-related terms discipline a specific subset of equilibrium wedges and exposure objects, while the remaining components of firm dynamics are primarily pinned down by standard cross-sectional and time-series moments, which stabilizes the overall mapping from moments to parameters.

7.1.4 Estimation Results

We briefly summarize the estimation results. Table 2 reports the common parameters and the coefficients governing the regional adaptation-cost shifter $f(\cdot)$. For region-specific moments and implied parameters, we report the cross-region distribution (p5, p50, p95) in Table 3.

The model-consistent temperature bliss point remains close to its reduced-form counterpart, at roughly 11°C. We also identify substantial dispersion in idiosyncratic (random) climate damages, with $\sigma_\xi^2 \simeq 0.0046$, implying that even conditional on the same (predictable) temperature realization, firms can experience materially different productivity impacts.

Regions' average intrinsic exposure $\bar{\beta}_r$ is tightly centered around zero and slightly negative: the 5th percentile is -0.0074, the median is essentially zero, and the 95th percentile is 0.006. This

36. For the small set of regions (less than 2% of observations) in which the fitted $f(\cdot)$ implies negative values, we set $(\eta_r H_r)^{-1} = 0$.

Table 2: Estimated and calibrated parameters

Parameter	Description	Value
Panel A. Common estimated parameters		
T^*	Temperature bliss point	11.03 °C
σ_ξ^2	Dispersion of random climate sensitivity	0.0046
Panel B. Adaptation-cost shifter coefficients		
c_0	$\frac{1}{\eta_r H_r} = f(\overline{\ln \mathrm{GDP}_r})$	6.9462
c_1	$= c_0 + c_1 g_r + c_2 g_r^2 + c_3 g_r^3 + c_5 g_r^4$	−3.1359
c_2		0.5255
c_3		−0.0387
c_4		0.0011
Panel C. Calibrated parameters		
$\tilde{\alpha}_K$	Capital share	0.35
r	Interest rate	0.042
γ	CRRA risk aversion	5
σ	Elasticity of substitution	4

Table 3: Distribution of region-specific estimates (p5/p50/p95)

Region-specific object	p5	p50	p95
$\bar{\beta}_r$	−.0074	-0.218×10^{-6}	0.006
$(\eta_r H_r)^{-1}$	0.0006	0.0013	0.0063
$\sigma^2_{\hat{\beta},r}$	0.0001	0.0003	0.0007
$\sigma^2_{\bar{a},r}$	0.6516	1.5601	3.3667
$\sigma^2_{\varepsilon^z,r}$	0.0925	0.1946	0.3019
$\sigma^2_{\varepsilon^{\phi^\tau},r}$	0.0327	0.1386	0.4110
$\rho_{z,r}$	0.6401	0.7723	0.9086
$\rho_{\phi^\tau,r}$	0.6310	0.8103	0.9388
$\omega_{a,r}$	0.4713	0.9671	1.1840

pattern suggests that, absent of endogenous adaptation, most regions exhibit a weakly negative response to temperature surprises, while a non-trivial right tail of regions responds positively. Consistent with this interpretation, a sizeable share of regions in our sample have average temperatures below the bliss point.

At the product level, intrinsic sensitivities vary meaningfully across 3-digit categories, spanning roughly -0.11 to 0.09. Within a region, however, dispersion in intrinsic exposure is comparatively modest: $\sigma^2_{\hat{\beta},r}$ ranges from 10^{-4} to 7×10^{-4} (p5–p95). This stands in sharp contrast to the much larger dispersion in random climate damages captured by σ^2_ξ, highlighting that a substantial share of climate-induced heterogeneity operates through unpredictable firm-level disruptions rather than through persistent cross-product differences in exposure.

All regions exhibit positive adaptation responses. The inverse effective adaptation cost $(\eta_r H_r)^{-1}$ has a median of 0.0013 and spans 0.0006 to 0.0063 (p5–p95), implying nearly an order-of-magnitude variation in adaptation capacity across regions. Under the estimated income-based shifter $f(\overline{\ln \text{GDP}_r})$, adaptation is cheaper in higher-income regions on average, which translates into stronger predicted endogenous adaptation—especially in climates farther from the bliss point, where the marginal value of adaptation is higher.

Turning to region-specific parameters governing firm dynamics, we find large dispersion in permanent productivity and substantial idiosyncratic volatility. Permanent productivity dispersion $\sigma^2_{\bar{a},r}$ is sizable (p5 $= 0.65$, p50 $= 1.56$, p95 $= 3.37$), and both transitory productivity and wedge components are highly persistent, with $\rho_{z,r}$ and $\rho_{\phi^\tau,r}$ typically between 0.6 and 0.95. Innovation variances in transitory productivity and idiosyncratic wedges are also economically large, indicating that both long-run heterogeneity and short-run shocks contribute meaningfully to within-region dispersion.

Finally, correlated distortions are strong. The size-dependent wedge coefficient $\omega_{a,r}$ is close to one at the median, implying that a 1% increase in permanent productivity (and hence scale) is associated with roughly a 1% higher effective user cost of capital. This magnitude is consistent with size-dependent distortion mechanisms recently estimated in Ayerst, Nguyen, and Restuccia (2024).

7.2 Quantitative Results

With the model estimated for regions spanning the EU, China, and India, we now quantify the aggregate importance of the misallocation channel. We use the estimated region-level moments to (i) measure the global productivity cost of climate-induced misallocation in an average year, (ii) track how this cost evolves from 1981–2019 as global warming unfolds and (iii) revisit the classic geography-development relationship by comparing the model-implied misallocation losses to cross-country productivity gaps in the macro data.

7.2.1 The Global Cost of Climate-Induced Misallocation

We first measure the total cost of climate-driven misallocation in our framework. We define the *global cost of climate-induced misallocation* as the aggregate TFP (or output) loss when comparing the observed economy to a counterfactual in which all within-region dispersion in climate sensitivi-

ties is eliminated. Operationally, for each region-year we shut down the three within-region dispersion objects that generate climate-driven MRPK dispersion: $\sigma_\xi^2 = 0$, $\mathbb{VAR}^i_{rt}(\hat{\beta}_i + \Psi_{it}) = 0$ and $\mathbb{COV}^i_{rt}\left(\tau_{it+1}, \widehat{\beta}_i + \Psi_{i,t+1}\right) = 0$. All other region-level fundamentals are held fixed. Intuitively, this counterfactual removes the within-region heterogeneity in (effective) temperature exposure and idiosyncratic climate damages, as well as its interaction with wedges, thereby isolating the allocative-efficiency losses that operate through dispersion in MRPK.

Global implementation. To implement this exercise at the global level, we pair our micro estimates with gridded climate data (ERA5) and seasonal forecast data (ECMWF) for all countries worldwide. We partition the globe into roughly 4,894 regions. For China, India, and EU countries, we adopt the same regional definitions used in our empirical analysis; for all other countries, we use GADM level-1 partitions.

For regions in our estimation sample, we use the estimated firm-level moments directly. For regions outside the sample, we extrapolate these moments using long-run GDP per capita, leveraging the fact that firm-level dispersion moments covary systematically with development.[37] We also impute regional adaptation costs using the estimated mapping $\eta_r H_r = f(\bar{T}_r, \overline{\ln \mathrm{GDP}}_r)$.

Aggregation. We aggregate the world economy using a Cobb–Douglas output index across countries and regions. Let

$$\log Y_t^{\mathrm{Global}} = \sum_c \omega_{ct} \log Y_{ct}, \qquad \log Y_{ct} = \sum_{r \in R(c)} \omega_{rt}^c \log Y_{rt},$$

where ω_{ct} is country c's global output share and ω_{rt}^c is region r's share of country c's output. This implies

$$\log \mathrm{TFP}_t^{\mathrm{Global}} = \sum_r \omega_{rt} \log \mathrm{TFP}_{rt}, \qquad \omega_{rt} \equiv \omega_{ct}\omega_{rt}^c.$$

Sufficient-statistics decomposition. Under this aggregation, the global misallocation cost implied by the model can be written as a weighted average of three sufficient statistics: (i) squared deviations from the optimal (bliss) temperature $(T_{rt} - T^*)^2$; (ii) forecast errors and forecast uncertainty, amplified by within-region dispersion in effective exposure; and (iii) the interaction between wedges and exposure. Define the relevant temperature innovation (forecast error net of the risk adjustment) as:

37. For parameters governing climate sensitivity, we extrapolate using both long-run GDP per capita and long-run climate.

$$\underbrace{\overline{\Delta^{T,\text{Mis}} \log \text{TFP}_t^{\text{Global}}}}_{\approx -12.5\%} = -\frac{\tilde{\alpha}_K + \tilde{\alpha}_K^2(\sigma-1)}{2}\Bigg[\underbrace{\sigma_\xi^2\Big(\overline{\sum_r \omega_{rt}(T_{rt}-T^*)^2}\Big)}_{\substack{\text{Random Climate Damage}\\ \approx -10.38\%}}$$
$$+\underbrace{\Big(\overline{\sum_r \omega_{rt}\mathbb{VAR}^i_{rt}(\hat{\beta}_i+\Psi_{it})\cdot\Big(T_{rt}-\mathbb{E}_{t-1}[T_{rt}]-(\bar{\beta}_r+\widetilde{\beta}_r)\Theta\mathbb{VAR}_{t-1}[T_{r,t}]\Big)^2}\Big)}_{\substack{\text{Exposure-amplified Forecast Error \& Risk}\\ \approx -2.11\%}}$$
$$+\underbrace{\Big(2\overline{\sum_r \omega_{rt}\mathbb{COV}^i_{rt}(\tau_{it},\hat{\beta}_i+\Psi_{it})\cdot\Big(T_{rt}-\mathbb{E}_{t-1}[T_{rt}]-(\bar{\beta}_r+\widetilde{\beta}_r)\Theta\mathbb{VAR}_{t-1}[T_{r,t}]\Big)}\Big)}_{\substack{\text{Wedge–exposure Interaction}\\ \approx -0.01\%}}\Bigg]. \tag{42}$$

Here $\overline{(\cdot)}$ denotes the time average over 1981–2019. Averaging these output-weighted sufficient statistics over 1981–2019, we find that climate-induced misallocation lowers global TFP by about 12.5% in an average year. Of this total, 10.38% arises from the *random climate damage* channel (persistent displacement from the bliss point, which magnifies heterogeneous and unpredictable firm-level disruptions), while 2.11% comes from forecast errors and climate uncertainty amplified by dispersion in effective exposure. The wedge–exposure interaction, while heterogeneous in the cross-section of regions, is quantitatively negligible in the global aggregate (about 0.01%).

The quantitative message is clear: most climate-induced misallocation reflects persistent deviations of regional climates from the optimal temperature—which magnify heterogeneous, unpredictable firm-level disruptions—rather than short-run forecast errors or forecast uncertainty. In other words, long-run climate displacement dominates weather predictability as a driver of global allocative inefficiency in our estimates.

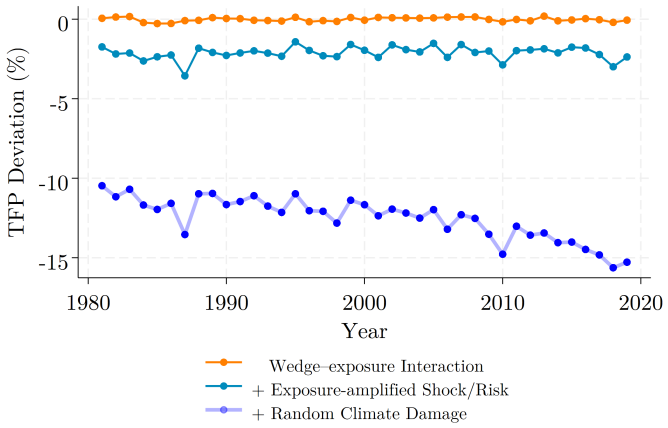
The Changing Cost with Global Warming. We next quantify how the global misallocation cost evolves over time, feeding the observed paths of regional temperatures and ECMWF forecasts into (42) from $t_0 = 1981$ to $t_1 = 2019$. Figure 13a plots the implied evolution of the three components. Over this period, climate-induced misallocation becomes more costly, lowering global TFP by an additional

$$\Delta^{T,\text{Mis}}_{t_1,t_0} \log \text{TFP}^{\text{Global}} \approx -4.81\%.$$

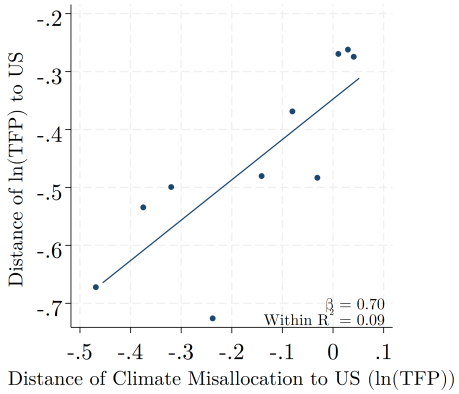
The dominant driver is again the level/random-damage channel: warming pushes many already-warm, high-output regions further away from T^*, more than it brings cooler regions closer, mechanically raising disruption-driven volatility and worsening allocative efficiency. The exposure-amplified forecast/risk component and the wedge–exposure interaction contribute little to the aggregate time trend.

Figure 13: The Cost of Climate-Induced Misallocation and Cross-country Development

(a) The Changing Cost of Climate-Induced Misallocation



(b) Cross-country TFP Dispersion: Model vs. Data



7.2.2 Climate and Productivity Differences Across Countries: Macro Data vs. Model Estimates

We next use our framework to revisit a central question in development economics: what explains large cross-country productivity gaps? Geography and climate have long been emphasized in comparative development (Montesquieu 1748; Sachs and Warner 1997; Gallup, Sachs, and Mellinger 1999; Nordhaus 2006; Dell, Jones, and Olken 2012), but the mechanisms linking climate to aggregate productivity remain debated. Here we focus on one mechanism—the misallocation channel—and ask how much of the observed cross-country TFP dispersion can be explained with the model-implied climate-misallocation losses.

We match our model-generated country-year misallocation costs to country-level TFP from the Penn World Table (PWT) 10.01 (Feenstra, Inklaar, and Timmer 2015). For each country-year, we compare the measured TFP gap relative to the United States, $\ln \mathrm{TFP}_{c,t} - \ln \mathrm{TFP}_{\mathrm{US},t}$, to the model-predicted climate-misallocation gap relative to the United States, $\Delta^{T,\mathrm{Mis}} \log \mathrm{TFP}_{c,t} - \Delta^{T,\mathrm{Mis}} \log \mathrm{TFP}_{\mathrm{US},t}$. The U.S. is a natural benchmark as a productivity frontier, and it is also close to the estimated temperature optimum ($T^* \approx 11.03°\mathrm{C}$), implying comparatively low climate-induced misallocation.

Figure 13b reports a binned scatter plot of macro TFP gaps against model-implied misallocation gaps, with both variables demeaned by year fixed effects to remove common global trends. The fitted relationship has a slope of about 0.7: when a country's predicted TFP distance to the U.S. due to climate misallocation rises by 1%, its measured TFP distance rises by about 0.7% on average. The corresponding R^2 of 0.094 implies that roughly 9% of observed cross-country TFP differences can be accounted for by climate through the misallocation channel. Notably, the model object is constructed solely from micro estimates combined with granular temperature and forecast data, yet it aligns well with the macro evidence.

8 Conclusion

This paper provides the first causal estimates of the misallocation effect from temperature shocks using firm-level microdata from 32 countries. On average, an additional hot day with > 30°C of temperature increases MRPK dispersion by 0.31 log points and contributes to a 0.11 % decline in annual aggregate TFP. Intriguingly, the detrimental impact of extreme heat on capital misallocation is more severe in regions with hotter climates and higher incomes, highlighting a significant productivity cost of climate change coupled with a limited capacity for market-based adaptation. A novel firm dynamics model of endogenous adaptation rationalizes these pattern and reveals the quantitative important of random climate damages on TFP volatility and undermining the allocative efficiency investment. Climate-induced misallocation explains 9% of cross-country aggregate productivity differences.

References

Acharya, Viral V, Abhishek Bhardwaj, and Tuomas Tomunen. 2023. *Do Firms Mitigate Climate Impact on Employment? Evidence from US Heat Shocks.* Working Paper, Working Paper Series 31967. National Bureau of Economic Research.

Addoum, Jawad M, David T Ng, and Ariel Ortiz-Bobea. 2020. "Temperature shocks and establishment sales." *The Review of Financial Studies* 33 (3): 1331–1366.

Allcott, Hunt, Allan Collard-Wexler, and Stephen D O'Connell. 2016. "How do electricity shortages affect industry? Evidence from India." *American Economic Review.*

Asker, John, Allan Collard-Wexler, and Jan De Loecker. 2014. "Dynamic Inputs and Resource (Mis)Allocation." *Journal of Political Economy* 122 (5): 1013–1063.

Ayerst, Stephen, Duc M Nguyen, and Diego Restuccia. 2024. *The micro and macro productivity of nations.* Technical report. National Bureau of Economic Research.

Bakkensen, Laura A, and Lint Barrage. 2021. "Going Underwater? Flood Risk Belief Heterogeneity and Coastal Home Price Dynamics." *The Review of Financial Studies* 35 (8): 3666–3709.

Baqaee, David Rezza, and Emmanuel Farhi. 2019. "The Macroeconomic Impact of Microeconomic Shocks: Beyond Hulten's Theorem." *Econometrica* 87 (4): 1155–1203.

Basu, Susanto, and John G. Fernald. 2002. "Aggregate productivity and aggregate technology." *European Economic Review* 46 (6): 963–991.

Bau, Natalie, and Adrien Matray. 2023. "Misallocation and Capital Market Integration: Evidence From India." *Econometrica* 91 (1): 67–106.

Bilal, Adrien, and Diego R Känzig. 2024. *The Macroeconomic Impact of Climate Change: Global vs. Local Temperature.* Technical report. National Bureau of Economic Research.

Bils, Mark, Peter J. Klenow, and Cian Ruane. 2021. "Misallocation or Mismeasurement?" *Journal of Monetary Economics* 124:S39–S56.

Brandt, Loren, Johannes Van Biesebroeck, and Yifan Zhang. 2014. "Challenges of working with the Chinese NBS firm-level data." *China Economic Review.*

Burke, Marshall, Solomon M. Hsiang, and Edward Miguel. 2015. "Global non-linear effect of temperature on economic production." *Nature* 527 (7577): 235–239.

Caggese, Andrea, Andrea Chiavari, Sampreet Goraya, and Carolina Villegas-Sanchez. 2023. "Climate Change, Firms, and the Aggregate Productivity." Working Paper.

Carleton, Tamma, Amir Jina, Michael Delgado, Michael Greenstone, Trevor Houser, Solomon Hsiang, Andrew Hultgren, et al. 2022. "Valuing the Global Mortality Consequences of Climate Change Accounting for Adaptation Costs and Benefits." *The Quarterly Journal of Economics* 137 (4): 2037–2105.

Casey, Gregory, Stephie Fried, and Matthew Gibson. 2022. "Understanding Climate Damages: Consumption versus Investment." Federal Reserve Bank of San Francisco Working Paper 2022-21.

Chen, Zhang. 2022. "Economic Growth and the Rise of Large Firms."

Christidis, Nikolaos, Dann Mitchell, and Peter A. Stott. 2023. "Rapidly increasing likelihood of exceeding 50°C in parts of the Mediterranean and the Middle East due to human influence." *npj Climate and Atmospheric Science* 6, no. 1 (May 26, 2023): 45.

Coeurdacier, Nicolas, Helene Rey, and Pablo Winant. 2011. "The risky steady state." *American Economic Review* 101 (3): 398–401.

Copernicus Climate Change Service. 2021. *CMIP6 climate projections.* Copernicus Climate Change Service (C3S) Climate Data Store (CDS).

Copernicus Climate Change Service and Climate Data Store. 2018. *Seasonal forecast daily and subdaily data on single levels.*

Cruz, José-Luis, and Esteban Rossi-Hansberg. 2023. *The Economic Geography of Global Warming.*

David, Joel M., Hugo A. Hopenhayn, and Venky Venkateswaran. 2016. "INFORMATION, MISALLOCATION, AND AGGREGATE PRODUCTIVITY." *The Quarterly Journal of Economics* 131 (2): 943–1006. Accessed November 27, 2023.

David, Joel M., and Venky Venkateswaran. 2019. "The Sources of Capital Misallocation." *American Economic Review* 109 (7): 2531–67.

David, Joel M., and David Zeke. 2021. *Risk-Taking, Capital Allocation and Optimal Monetary Policy.* Federal Reserve Bank of Chicago.

Dell, Melissa, Benjamin F Jones, and Benjamin A Olken. 2012. "Temperature Shocks and Economic Growth: Evidence from the Last Half Century." *American Economic Journal: Macroeconomics* 4 (3): 66–95.

Dellink, Rob, Jean Chateau, Elisa Lanzi, and Bertrand Magné. 2017. "Long-term economic growth projections in the Shared Socioeconomic Pathways." *Global Environmental Change.*

Deschênes, Olivier, and Michael Greenstone. 2011. "Climate Change, Mortality, and Adaptation: Evidence from Annual Fluctuations in Weather in the US." *American Economic Journal: Applied Economics* 3 (4): 152–185.

Dundas, Steven J., and Roger H. von Haefen. 2020. "The Effects of Weather on Recreational Fishing Demand and Adaptation: Implications for a Changing Climate." *Journal of the Association of Environmental and Resource Economists* 7 (2): 209–242.

Erda, Tarikua. 2024. "Disasters, Capital, and Productivity." In *2024 APPAM Fall Research Conference, APPAM.*

Fan, Jingting. 2024. "Talent, Geography, and Offshore R
amp;D." *The Review of Economic Studies* (April): rdae044. ISSN: 0034-6527.

Feenstra, Robert C, Robert Inklaar, and Marcel P Timmer. 2015. "The next generation of the Penn World Table." *American economic review* 105 (10): 3150–3182.

Gallup, John Luke, Jeffrey D. Sachs, and Andrew D. Mellinger. 1999. "Geography and Economic Development." *International Regional Science Review* 22 (2): 179–232.

Ginglinger, Edith, and Quentin Moreau. 2023. "Climate risk and capital structure." *Management Science* 69 (12): 7492–7516.

Gopinath, Gita, Sebnem Kalemli-Ozcan, Loukas Karabarbounis, and Carolina Villegas-Sanchez. 2017. "Capital Allocation and Productivity in South Europe." *Quarterly Journal of Economics* 132 (4).

Gorodnichenko, Yuriy, Debora Revoltella, Jan Svejnar, and Christoph T Weiss. 2018. *Resource misallocation in European firms: The role of constraints, firm characteristics and managerial decisions.* Technical report. National Bureau of Economic Research.

Hsieh, Chang-Tai, and Peter J. Klenow. 2009. "Misallocation and Manufacturing TFP in China and India." *Quarterly Journal of Economics* 124 (4): 1403–1448.

Kalemli- Özcan, Şebnem, Bent E. Sørensen, Carolina Villegas-Sanchez, Vadym Volosovych, and Sevcan Yeşiltaş. 2024. "How to Construct Nationally Representative Firm-Level Data from the Orbis Global Database: New Facts on SMEs and Aggregate Implications for Industry Concentration." *American Economic Journal: Macroeconomics* 16, no. 2 (April): 353–74.

Kopytov, Alexandr, Mathieu Taschereau-Dumouchel, and Zebang Xu. 2024. "The Origin of Risk." *Available at SSRN.*

Krusell, Per, and Anthony A. Smith Jr. 1998. "Income and Wealth Heterogeneity in the Macroeconomy." *Journal of Political Economy* 106 (5): 867–896.

Lemoine, Derek. 2018. *Estimating the Consequences of Climate Change from Variation in Weather.* Working Paper, Working Paper Series 25008. National Bureau of Economic Research.

Mehra, Rajnish, and Edward C Prescott. 1985. "The equity premium: A puzzle." *Journal of monetary Economics* 15 (2): 145–161.

Montesquieu, Baron de, Charles de Secondat. 1748. *The Spirit of Laws.* Printed for T. Evans.

Moscona, Jacob, and Karthik A Sastry. 2023. "Does directed innovation mitigate climate damage? evidence from us agriculture." *The Quarterly Journal of Economics* 138 (2): 637–701.

Nath, Ishan. 2025. "Climate change, the food problem, and the challenge of adaptation through sectoral reallocation." *Journal of Political Economy.*

Nath, Ishan, Valerie Ramey, and Peter Klenow. 2023. "How Much Will Global Warming Cool Global Growth?"

Nordhaus, William D. 1992. "An optimal transition path for controlling greenhouse gases." *Science* 258 (5086): 1315–1319.

———. 2006. "Geography and Macroeconomics: New Data and New Findings." *Proceedings of the National Academy of Sciences* 103 (10): 3510–3517.

O'Neill, B. C., C. Tebaldi, D. P. van Vuuren, V. Eyring, P. Friedlingstein, G. Hurtt, R. Knutti, et al. 2016. "The Scenario Model Intercomparison Project (ScenarioMIP) for CMIP6." *Geosci. Model Dev.*

Oudin Åström, Daniel, Bertil Forsberg, Kristie L. Ebi, and Joacim Rocklöv. 2013. "Attributing mortality from extreme temperatures to climate change in Stockholm, Sweden." *Nature Climate Change* 3, no. 12 (December 1, 2013): 1050–1054.

Piao, Shilong, Philippe Ciais, Yao Huang, Zehao Shen, Shushi Peng, Junsheng Li, Liping Zhou, Hongyan Liu, Yuecun Ma, Yihui Ding, et al. 2010. "The impacts of climate change on water resources and agriculture in China." *Nature.*

Ponticelli, Jacopo, Qiping Xu, and Stefan Zeume. 2023. *Temperature and Local Industry Concentration.* Technical report w31533. National Bureau of Economic Research.

Poschke, Markus. 2018. "The Firm Size Distribution across Countries and Skill-Biased Change in Entrepreneurial Technology." *American Economic Journal: Macroeconomics* 10 (3): 1–41.

Redding, Stephen J, and David E Weinstein. 2020. "Measuring aggregate price indices with taste shocks: Theory and evidence for CES preferences." *The Quarterly Journal of Economics* 135 (1): 503–560.

Restuccia, Diego, and Richard Rogerson. 2008. "Policy distortions and aggregate productivity with heterogeneous establishments." *Review of Economic dynamics* 11 (4): 707–720.

Rode, Ashwin, Rachel E Baker, Tamma Carleton, Anthony D'Agostino, Michael Delgado, Timothy Foreman, Diana R Gergel, Michael Greenstone, Trevor Houser, Solomon Hsiang, et al. 2022. "Labor disutility in a warmer world: The impact of climate change on the global workforce."

Rudik, I., G. Lyn, W. Tan, and A. Ortiz-Bobea. 2021. *The Economic Effects of Climate Change in Dynamic Spatial Equilibrium.*

Sabater, Joaquin Muñoz. 2019. *ERA5-Land monthly averaged data from 1950 to present.* Copernicus Climate Change Service (C3S) Climate Data Store (CDS).

Sachs, Jeffrey D., and Andrew M. Warner. 1997. "Sources of Slow Growth in African Economies." *Journal of African Economies* 6 (3): 335–376.

Somanathan, E., Rohini Somanathan, Anant Sudarshan, and Meenu Tewari. 2021. "The Impact of Temperature on Productivity and Labor Supply: Evidence from Indian Manufacturing" [in en]. *Journal of Political Economy* 129 (6). Accessed November 27, 2023.

Sraer, David, and David Thesmar. 2023. "How to Use Natural Experiments to Estimate Misallocation." *American Economic Review* 113 (4): 906–38.

Tarsia, Romano. 2023. "Heterogeneous effects of weather shocks on firm economic performance." *Available at SSRN 4672552.*

Tyazhelnikov, Vladimir, Xinbei Zhou, and Xuetao Shi. 2024. *PPML, Gravity, and Heterogeneous Trade Elasticities.* Technical report.

Wang, Tingting, and Fubao Sun. 2022. "Global gridded GDP data set consistent with the shared socioeconomic pathways." *Scientific Data.*

Wenz, Leonie, Robert Devon Carr, Noah Kögel, Maximilian Kotz, and Matthias Kalkuhl. 2023. "DOSE – Global data set of reported sub-national economic output." *Scientific Data* 10 (1): 425.

Zhang, Peng, Olivier Deschenes, Kyle C Meng, and Junjie Zhang. 2018. "Temperature effects on productivity and factor reallocation: Evidence from a half million Chinese manufacturing plants." *Journal of Environmental Economics and Management* 88:1–17.

Zivin, Joshua Graff, and Matthew Neidell. 2014. "Temperature and the Allocation of Time: Implications for Climate Change." *Journal of Labor Economics* 32 (1): 1–26.

Online Appendix

A Additional Derivations for Section 2

This appendix provides the derivation of the expressions and propositions featured in Section 2.

A.1 Equilibrium Allocations in Distorted Equilibrium

In this appendix, we solve the firm's profit maximization problem in Equation 4 and derive Equation 5.

Subject to the inverse demand and wedges, each firm i in region-sector n engages in monopolistic competition and optimally chooses its quantity of inputs and price to maximize profits

$$\max_{P_{nit},K_{nit},L_{nit}} \left(1-\tau^Y_{nit}\right) P_{nit} \underbrace{A_{nit}K^{\alpha_{Kn}}_{nit}L^{\alpha_{Ln}}_{nit}}_{Y_{nit}} - \left(1+\tau^K_{nit}\right) R_{nt}K_{nit} - \left(1+\tau^L_{nit}\right) W_{nt}L_{nit}$$
$$\text{subject to : } Y_{nit} = B_{nit}Y_{nt}\left[\frac{P_{nit}}{P_{nt}}\right]^{-\sigma_n}.$$

After substituting the demand curve $P_{nit}Y_{nit} = P_{nt}Y^{\frac{1}{\sigma_n}}_{nt}B^{\frac{1}{\sigma_n}}_{nit}Y^{\frac{\sigma_n-1}{\sigma_n}}_{nit}$ into the objective function, we derive the first-order condition with respect to any factor input F_{nit} used (where F_{nit} can be either K_{nit} or L_{nit})

$$MRPF_{nit} = \frac{\partial P_{nit}Y_{nit}}{\partial F_{nit}} = \alpha_{F_n}\frac{\sigma_n-1}{\sigma_n}\frac{P_{nit}Y_{nit}}{F_{nit}} = \frac{1+\tau^F_{ni}(\tilde{\mathbf{T}}_{rt},\cdot)}{1-\tau^Y_{ni}(\tilde{\mathbf{T}}_{rt},\cdot)}P^F_{nt},$$

where P^F_{nt} denotes the factor price, specifically W_{nt} for labor and R_{nt} for capital. $\frac{\sigma_n-1}{\sigma_n}$ is the optimal CES markup. This is Equation 5 in the main text.

Equation 5 can be rearranged to yield the following:

$$K_{nit} = \alpha_{K_n}(1-\tau^Y_{ni}(\tilde{\mathbf{T}}_{rt},\cdot))\frac{\sigma_n-1}{\sigma_n}\frac{P_{nit}Y_{nit}}{(1+\tau^K_{ni}(\tilde{\mathbf{T}}_{rt},\cdot))P^K_{nt}}$$
$$L_{nit} = \alpha_{L_n}(1-\tau^Y_{ni}(\tilde{\mathbf{T}}_{rt},\cdot))\frac{\sigma_n-1}{\sigma_n}\frac{P_{nit}Y_{nit}}{(1+\tau^L_{ni}(\tilde{\mathbf{T}}_{rt},\cdot))P^L_{nt}}$$

Plugging the labor and capital first order conditions into the expression for production yields a relationship between output Y_{nit} and sale $P_{nit}Y_{nit}$

$$\begin{aligned} Y_{nit} &= A_{nit}K^{\alpha_{Kn}}_{nit}L^{\alpha_{Ln}}_{nit} \\ &= A_{nit}\alpha^{\alpha_{Kn}}_{K_n}\alpha^{\alpha_{Ln}}_{L_n}(1-\tau^Y_{ni}(\tilde{\mathbf{T}}_{rt},\cdot))\frac{\sigma_n-1}{\sigma_n}P_{nit}Y_{nit}\left[\frac{1}{(1+\tau^K_{ni}(\tilde{\mathbf{T}}_{rt},\cdot))P^K_{nt}}\right]^{\alpha_{Kn}}\left[\frac{1}{(1+\tau^L_{ni}(\tilde{\mathbf{T}}_{rt},\cdot))P^L_{nt}}\right]^{\alpha_{Ln}} \end{aligned} \tag{43}$$

Using demand curve once again solves for sales $P_{nit}Y_{nit}$

$$
\begin{aligned}
P_{nit}Y_{nit} &= P_{nt}Y_{nt}^{\frac{1}{\sigma_n}}B_{nit}^{\frac{1}{\sigma_n}}Y_{nit}^{\frac{\sigma_n-1}{\sigma_n}} \\
&= P_{nt}Y_{nt}^{\frac{1}{\sigma_n}}B_{nit}^{\frac{1}{\sigma_n}}\left\{A_{nit}\alpha_{K_n}^{\alpha_{K_n}}\alpha_{L_n}^{\alpha_{L_n}}(1-\tau_{ni}^{Y}(\tilde{\mathbf{T}}_{rt},\cdot))\frac{\sigma_n-1}{\sigma_n}P_{nit}Y_{nit}\left[\frac{1}{(1+\tau_{ni}^{K}(\tilde{\mathbf{T}}_{rt},\cdot))P_{nt}^{K}}\right]^{\alpha_{Kn}}\left[\frac{1}{(1+\tau_{ni}^{L}(\tilde{\mathbf{T}}_{rt},\cdot))P_{nt}^{L}}\right]^{\alpha_{Ln}}\right\}^{\frac{\sigma_n-1}{\sigma_n}} \\
(P_{nit}Y_{nit})^{\frac{1}{\sigma_n}} &= P_{nt}Y_{nt}^{\frac{1}{\sigma_n}}B_{nit}^{\frac{1}{\sigma_n}}\left\{A_{nit}\alpha_{K_n}^{\alpha_{K_n}}\alpha_{L_n}^{\alpha_{L_n}}(1-\tau_{ni}^{Y}(\tilde{\mathbf{T}}_{rt},\cdot))\frac{\sigma_n-1}{\sigma_n}\left[\frac{1}{(1+\tau_{ni}^{K}(\tilde{\mathbf{T}}_{rt},\cdot))P_{nt}^{K}}\right]^{\alpha_{Kn}}\left[\frac{1}{(1+\tau_{ni}^{L}(\tilde{\mathbf{T}}_{rt},\cdot))P_{nt}^{L}}\right]^{\alpha_{Ln}}\right\}^{\frac{\sigma_n-1}{\sigma_n}} \\
P_{nit}Y_{nit} &= P_{nt}^{\sigma_n}Y_{nt}B_{nit}\left\{A_{nit}\alpha_{K_n}^{\alpha_{K_n}}\alpha_{L_n}^{\alpha_{L_n}}(1-\tau_{ni}^{Y}(\tilde{\mathbf{T}}_{rt},\cdot))\frac{\sigma_n-1}{\sigma_n}\left[\frac{1}{(1+\tau_{ni}^{K}(\tilde{\mathbf{T}}_{rt},\cdot))P_{nt}^{K}}\right]^{\alpha_{Kn}}\left[\frac{1}{(1+\tau_{ni}^{L}(\tilde{\mathbf{T}}_{rt},\cdot))P_{nt}^{L}}\right]^{\alpha_{Ln}}\right\}^{\sigma_n-1}
\end{aligned}
\tag{44}
$$

We aggregate sales across all firms and obtain

$$
\begin{aligned}
\int_i P_{nit}Y_{nit} &= \int_i P_{nt}^{\sigma_n}Y_{nt}B_{nit}\left\{A_{nit}\alpha_{K_n}^{\alpha_{K_n}}\alpha_{L_n}^{\alpha_{L_n}}(1-\tau_{ni}^{Y}(\tilde{\mathbf{T}}_{rt},\cdot))\frac{\sigma_n-1}{\sigma_n}\left[\frac{1}{(1+\tau_{ni}^{K}(\tilde{\mathbf{T}}_{rt},\cdot))P_{nt}^{K}}\right]^{\alpha_{Kn}}\left[\frac{1}{(1+\tau_{ni}^{L}(\tilde{\mathbf{T}}_{rt},\cdot))P_{nt}^{L}}\right]^{\alpha_{Ln}}\right\}^{\sigma_n-1} \\
&= P_{nt}^{\sigma_n}Y_{nt}\left(\alpha_{K_n}^{\alpha_{K_n}}\alpha_{L_n}^{\alpha_{L_n}}\frac{\sigma_n-1}{\sigma_n}\left(P_{nt}^{K}\right)^{-\alpha_{K_n}}\left(P_{nt}^{L}\right)^{-\alpha_{L_n}}\right)^{\sigma_n-1}\int_i B_{nit}\left\{A_{nit}(1-\tau_{ni}^{Y}(\tilde{\mathbf{T}}_{rt},\cdot))\left[\frac{1}{(1+\tau_{ni}^{K}(\tilde{\mathbf{T}}_{rt},\cdot))}\right]^{\alpha_{Kn}}\left[\frac{1}{(1+\tau_{ni}^{L}(\tilde{\mathbf{T}}_{rt},\cdot))}\right]^{\alpha_{Ln}}\right\}^{\sigma_n-1}
\end{aligned}
\tag{45}
$$

Then the sales share of firm i in region-sector n, θ_{nit} can be expressed in closed form of the fundamentals and parameters as

$$
\begin{aligned}
\theta_{nit} &= \frac{P_{nit}Y_{nit}}{\int_i P_{nit}Y_{nit}} \\
&= \frac{B_{nit}\left\{A_{nit}(1-\tau_{ni}^{Y}(\tilde{\mathbf{T}}_{rt},\cdot))\left[\frac{1}{(1+\tau_{ni}^{K}(\tilde{\mathbf{T}}_{rt},\cdot))}\right]^{\alpha_{Kn}}\left[\frac{1}{(1+\tau_{ni}^{L}(\tilde{\mathbf{T}}_{rt},\cdot))}\right]^{\alpha_{Ln}}\right\}^{\sigma_n-1}}{\int_i B_{nit}\left\{A_{nit}(1-\tau_{ni}^{Y}(\tilde{\mathbf{T}}_{rt},\cdot))\left[\frac{1}{(1+\tau_{ni}^{K}(\tilde{\mathbf{T}}_{rt},\cdot))}\right]^{\alpha_{Kn}}\left[\frac{1}{(1+\tau_{ni}^{L}(\tilde{\mathbf{T}}_{rt},\cdot))}\right]^{\alpha_{Ln}}\right\}^{\sigma_n-1}},
\end{aligned}
$$

which is Equation 6 in the paper.

A.2 Proof of Proposition 1

Proposition 1. Equilibrium (Mis)Allocation. The (log) ratio of firm i's distorted and efficient equilibrium allocation of factor, $\frac{F_{nit}}{F_{nit}^*}$,

$$
\log(\frac{F_{nit}}{F_{nit}^*}) = -\underbrace{\log(\frac{1+\tau_{nit}^{F}}{1+\tau_{nt}^{F}})}_{\substack{\text{relative wedge}\\ \text{effect}}} + \underbrace{\log(\frac{\theta_{nit}}{\theta_{nit}^*})}_{\substack{\text{size}\\ \text{effect}}}
$$

is decreasing in the ratio of firm i's own factor wedge comparing to the aggregate factor wedge $1+\tau_{nt}^{F} \equiv \left(\int_0^{J_n}\frac{1}{(1+\tau_{nit}^{F})}\theta_{nit}di\right)^{-1}$, and increasing in the ratio of the firm's sales share θ_{nit} comparing to its efficient counterfactual θ_{nit}^*. Moreover, the efficient allocation of inputs, $\frac{F_{nit}^*}{F_{nt}} = \theta_{nit}^* = \frac{B_{nit}A_{nit}^{\sigma_n-1}}{\int_0^{J_n}B_{nit}A_{nit}^{\sigma_n-1}di}$, is entirely determined by firm i's relative preference shifter and physical productivity within the region-sector and aligns with sales share θ_{nit}^*.

Proof. We first re-write the expression for output Y_{nit} in Equation 43 by plugging in for P_{nit}

$$\begin{aligned}
Y_{nit} &= A_{nit} K_{nit}^{\alpha_{Kn}} L_{nit}^{\alpha_{Ln}} \\
&= A_{nit} \alpha_{K_n}^{\alpha_{Kn}} \alpha_{L_n}^{\alpha_{Ln}} (1-\tau_{ni}^{Y}(\tilde{\mathbf{T}}_{rt},\cdot)) \frac{\sigma_n - 1}{\sigma_n} \underbrace{P_{nit}}_{\left(\frac{Y_{nit}}{B_{nit}Y_{nt}}\right)^{-\frac{1}{\sigma_n}} P_{nt}} Y_{nit} \left[\frac{1}{(1+\tau_{ni}^{K}(\tilde{\mathbf{T}}_{rt},\cdot))P_{nt}^{K}}\right]^{\alpha_{Kn}} \left[\frac{1}{(1+\tau_{ni}^{L}(\tilde{\mathbf{T}}_{rt},\cdot))P_{nt}^{L}}\right]^{\alpha_{Ln}} \\
Y_{nit}^{\frac{1}{\sigma_n}} &= A_{nit} \alpha_{K_n}^{\alpha_{Kn}} \alpha_{L_n}^{\alpha_{Ln}} (1-\tau_{ni}^{Y}(\tilde{\mathbf{T}}_{rt},\cdot)) \frac{\sigma_n - 1}{\sigma_n} P_{nt} \left(B_{nit} Y_{nt}\right)^{\frac{1}{\sigma_n}} \left[\frac{1}{(1+\tau_{ni}^{K}(\tilde{\mathbf{T}}_{rt},\cdot))P_{nt}^{K}}\right]^{\alpha_{Kn}} \left[\frac{1}{(1+\tau_{ni}^{L}(\tilde{\mathbf{T}}_{rt},\cdot))P_{nt}^{L}}\right]^{\alpha_{Ln}} \\
Y_{nit} &= B_{nit} Y_{nt} \left\{ A_{nit} \alpha_{K_n}^{\alpha_{Kn}} \alpha_{L_n}^{\alpha_{Ln}} (1-\tau_{ni}^{Y}(\tilde{\mathbf{T}}_{rt},\cdot)) \frac{\sigma_n - 1}{\sigma_n} P_{nt} \left[\frac{1}{(1+\tau_{ni}^{K}(\tilde{\mathbf{T}}_{rt},\cdot))P_{nt}^{K}}\right]^{\alpha_{Kn}} \left[\frac{1}{(1+\tau_{ni}^{L}(\tilde{\mathbf{T}}_{rt},\cdot))P_{nt}^{L}}\right]^{\alpha_{Ln}} \right\}^{\sigma_n}
\end{aligned} \tag{46}$$

Next we solve for factor allocation K_{nit} and L_{nit} and express them to be a function of the wedges, aggregate variables, prices and parameters. Plugging Equation 46 back to the first-order conditions of capital and labor, and rearranging terms in the FOCs to connect to sales share θ_{nit} yields

$$\begin{aligned}
F_{nit} = Z_{nt} \frac{(1-\tau_{ni}^{Y}(\tilde{\mathbf{T}}_{rt},\cdot))}{(1+\tau_{ni}^{F}(\tilde{\mathbf{T}}_{rt},\cdot))} \theta_{nit} \int_i B_{nit} \left\{ A_{nit}(1-\tau_{ni}^{Y}(\tilde{\mathbf{T}}_{rt},\cdot)) \left[\frac{1}{(1+\tau_{ni}^{K}(\tilde{\mathbf{T}}_{rt},\cdot))}\right]^{\alpha_{Kn}} \left[\frac{1}{(1+\tau_{ni}^{L}(\tilde{\mathbf{T}}_{rt},\cdot))}\right]^{\alpha_{Ln}} \right\}^{\sigma_n - 1} di \\
F \in (K, L),
\end{aligned} \tag{47}$$

where $Z_{nt} = \alpha_{K_n} \left[\frac{\sigma_n - 1}{\sigma_n} P_{nt}\right]^{\sigma_n} Y_{nt} \frac{1}{P_{nt}^{K}} \left[\left(\frac{\alpha_{Kn}}{P_{nt}^{K}}\right)^{\alpha_{Kn}} \left(\frac{\alpha_{Ln}}{P_{nt}^{L}}\right)^{\alpha_{Ln}}\right]^{\sigma_n - 1}$.

Aggregate across firms:

$$\begin{aligned}
F_{nt} &= \int_i F_{nit} di \\
&= Z_{nt} \int_i B_{nit} \left\{ A_{nit}(1-\tau_{ni}^{Y}(\tilde{\mathbf{T}}_{rt},\cdot)) \left[\frac{1}{(1+\tau_{ni}^{K}(\tilde{\mathbf{T}}_{rt},\cdot))}\right]^{\alpha_{Kn}} \left[\frac{1}{(1+\tau_{ni}^{L}(\tilde{\mathbf{T}}_{rt},\cdot))}\right]^{\alpha_{Ln}} \right\}^{\sigma_n - 1} di \\
&\cdot \int_i \frac{(1-\tau_{ni}^{Y}(\tilde{\mathbf{T}}_{rt},\cdot))}{(1+\tau_{ni}^{F}(\tilde{\mathbf{T}}_{rt},\cdot))} \theta_{nit} di
\end{aligned}$$

The ratio between firm and region allocation $\frac{F_{nit}}{F_{nt}}$ is

$$\frac{F_{nit}}{F_{nt}} = \frac{\frac{(1-\tau_{ni}^{Y}(\tilde{\mathbf{T}}_{rt},\cdot))}{(1+\tau_{ni}^{F}(\tilde{\mathbf{T}}_{rt},\cdot))} \theta_{nit}}{\int_i \frac{(1-\tau_{ni}^{Y}(\tilde{\mathbf{T}}_{rt},\cdot))}{(1+\tau_{ni}^{F}(\tilde{\mathbf{T}}_{rt},\cdot))} \theta_{nit} di}$$

We can evaluate the expression at the efficient equilibrium where all distortions are eliminated and obtain

$$\frac{F_{nit}^{*}}{F_{nt}^{*}} = \frac{\theta_{nit}^{*}}{\underbrace{\theta_{nt}^{*}}_{=1}} = \theta_{nit}^{*}$$

Finally, combining this with Equation (A.2) yields

$$\frac{F_{nit}/F_{nt}}{F_{nit}^{*}/F_{nt}^{*}} = \frac{F_{nit}}{F_{nit}^{*}} = \frac{\frac{(1-\tau_{ni}^{Y}(\tilde{\mathbf{T}}_{rt},\cdot))}{(1+\tau_{ni}^{F}(\tilde{\mathbf{T}}_{rt},\cdot))}}{\int_i \frac{(1-\tau_{ni}^{Y}(\tilde{\mathbf{T}}_{rt},\cdot))}{(1+\tau_{ni}^{F}(\tilde{\mathbf{T}}_{rt},\cdot))} \theta_{nit} di} \frac{\theta_{nit}}{\theta_{nit}^{*}},$$

where the aggregate factor is exogenously given and $K_{nt} = K^*_{nt}$. Taking log yields a more intuitive expression

$$\log \frac{F_{nit}}{F^*_{nit}} = \log \frac{\frac{(1-\tau^Y_{ni}(\tilde{\mathbf{T}}_{rt},\cdot))}{(1+\tau^F_{ni}(\tilde{\mathbf{T}}_{rt},\cdot))}}{\int_i \frac{(1-\tau^Y_{ni}(\tilde{\mathbf{T}}_{rt},\cdot))}{(1+\tau^F_{ni}(\tilde{\mathbf{T}}_{rt},\cdot))}\theta_{nit}di} + \log \frac{\theta_{nit}}{\theta^*_{nit}} = \log \frac{\frac{(1-\tau^Y_{ni}(\tilde{\mathbf{T}}_{rt},\cdot))}{(1+\tau^F_{ni}(\tilde{\mathbf{T}}_{rt},\cdot))}}{(1+\tau^F_{nt})} + \log \frac{\theta_{nit}}{\theta^*_{nit}}.$$

When factor-F distortions $(1+\tau^F_{nit})$ are the only sources of distortions present, we arrive at the exact expression as in (7) in Proposition 1.

■

A.3 Proof of Proposition 2

Proposition 2. Aggregation and TFP Decomposition. Each region–sector n admits an aggregate production function of the form

$$Y_{nt} = \text{TFP}_{nt} K_{nt}^{\alpha_{Kn}} L_{nt}^{\alpha_{Ln}},$$

where, under a second-order approximation, region–sectoral aggregate total factor productivity $\text{TFP}_{nt} := \text{TFP}_n\left(\tilde{\mathbf{T}}_{rt}, \tilde{\mathbf{X}}_{nt}\right)$ can be decomposed as follows:

$$\begin{aligned}
\log \text{TFP}_n(\tilde{\mathbf{T}}_{rt},\cdot) = {} & \underbrace{\frac{1}{\sigma_n - 1}\log\left[\mathbb{E}_i\left[B_{ni}(\tilde{\mathbf{T}}_{rt},\cdot)\left(A_{ni}(\tilde{\mathbf{T}}_{rt},\cdot)\right)^{\sigma_n-1}\right]\right]}_{\text{Technology}(\log \text{TFP}^E_n)} + \frac{1}{\sigma_n-1}\log J_n \\
& \underbrace{-\frac{\sigma_n}{2}\,\text{var}_{\log\left(1-\tau^Y_{ni}\right)}(\tilde{\mathbf{T}}_{rt},\cdot)}_{\text{Output Wedge Dispersion}} \\
& \underbrace{-\sum_{F\in\{K,L\}}\frac{\alpha_{Fn}+\alpha^2_{Fn}(\sigma_n-1)}{2}\,\text{var}_{\log\left(1+\tau^F_{ni}\right)}(\tilde{\mathbf{T}}_{rt},\cdot)}_{\text{Factor Wedge Dispersion}} \\
& \underbrace{+\sigma_n\sum_{F\in\{K,L\}}\alpha_{Fn}\,\text{cov}_{\log\left(1-\tau^Y_{ni}\right),\log\left(1+\tau^F_{ni}\right)}\left(\tilde{\mathbf{T}}_{rt},\cdot\right)}_{\text{Output-Factor Mixed Distortion}} \\
& \underbrace{-(\sigma_n-1)\alpha_{Kn}\alpha_{Ln}\,\text{cov}_{\log\left(1+\tau^K_{ni}\right),\log\left(1+\tau^L_{ni}\right)}\left(\tilde{\mathbf{T}}_{rt},\cdot\right)}_{\text{Factor Mixed Distortion}}
\end{aligned} \tag{48}$$

Proof. Note that $P_{nt} = 1$. Rearranging Equation 47 yields

$$\left(\frac{\alpha_{L_n}}{W_{nt}}\right)^{\alpha_{L_n}(\sigma_n-1)} = \frac{1}{\left(\frac{\sigma_n-1}{\sigma_n}\right)^{\sigma_n-1}\left(\frac{\alpha_{Kn}}{R_{nt}}\right)^{\alpha_{Kn}(\sigma_n-1)} I_{nt}},$$

where $I_{nt} = \int_i B_{nit}\left\{A_{nit}(1-\tau^Y_{ni}(\tilde{\mathbf{T}}_{rt},\cdot))\left[\frac{1}{(1+\tau^K_{ni}(\tilde{\mathbf{T}}_{rt},\cdot))}\right]^{\alpha_{Kn}}\left[\frac{1}{(1+\tau^L_{ni}(\tilde{\mathbf{T}}_{rt},\cdot))}\right]^{\alpha_{Ln}}\right\}^{\sigma_n-1}$. Plugging Equa-

tion A.3 to aggregate capital yields

$$K_{nt} = Y_{nt}\frac{\alpha_{K_n}}{R_{nt}}\left[\frac{\sigma_n-1}{\sigma_n}\right]^{\sigma_n}\left[\left(\frac{\alpha_{K_n}}{R_{nt}}\right)^{\alpha_{Kn}}\left(\frac{\alpha_{L_n}}{W_{nt}}\right)^{\alpha_{Ln}}\right]^{\sigma_n-1}J_{nt}$$
$$\frac{K_{nt}}{Y_{nt}} = \left(\frac{\alpha_{K_n}}{R_{nt}}\right)\frac{\sigma_n-1}{\sigma_n}\frac{J_{nt}}{I_{nt}},$$

where $J_{nt} = \int_i \left[(1-\tau^Y_{ni}(\tilde{\mathbf{T}}_{rt},\cdot))\right]^{\sigma_n} B_{nit}\frac{1}{(1+\tau^K_{ni}(\tilde{\mathbf{T}}_{rt},\cdot))}\left\{A_{nit}\left[\frac{1}{(1+\tau^K_{ni}(\tilde{\mathbf{T}}_{rt},\cdot))}\right]^{\alpha_{Kn}}\left[\frac{1}{(1+\tau^L_{ni}(\tilde{\mathbf{T}}_{rt},\cdot))}\right]^{\alpha_{Ln}}\right\}^{\sigma_n-1}$.
Taking logs yield

$$\log\frac{Y_{nt}}{K_{nt}} = \log I_{nt} - \log J_{nt} - \log\left(\frac{\sigma_n-1}{\sigma_n}\right)\frac{\alpha_{K_n}}{R_{nt}}.$$

Using Equation A.3 once again to obtain aggregate labor

$$L_{nt} = Y_{nt}\left(\frac{\sigma_n-1}{\sigma_n}\right)^{\frac{-\alpha_{K_n}}{1-\alpha_{K_n}}}\left(\frac{\alpha_{K_n}}{R_{nt}}\right)^{-\frac{\alpha_{K_n}}{1-\alpha_{K_n}}}Q_{nt}I_{nt}^{-1-\frac{1}{\alpha_{L_n}(\sigma_n-1)}},$$

where $Q_{nt} = \int_i \left[(1-\tau^Y_{ni}(\tilde{\mathbf{T}}_{rt},\cdot))\right]^{\sigma_n} B_{nit}\frac{1}{(1+\tau^L_{ni}(\tilde{\mathbf{T}}_{rt},\cdot))}\left\{A_{nit}\left[\frac{1}{(1+\tau^K_{ni}(\tilde{\mathbf{T}}_{rt},\cdot))}\right]^{\alpha_{Kn}}\left[\frac{1}{(1+\tau^L_{ni}(\tilde{\mathbf{T}}_{rt},\cdot))}\right]^{\alpha_{Ln}}\right\}^{\sigma_n-1}$.
Taking logs yield

$$\log\frac{Y_{nt}}{L_{nt}} = \left(1+\frac{1}{\alpha_{L_n}(\sigma_n-1)}\right)\log I_{nt} - \log Q_{nt} + \frac{\alpha_{K_n}}{1-\alpha_{K_n}}\log\frac{\sigma_n-1}{\sigma_n}\frac{\alpha_{K_n}}{R_{nt}}.$$

This allows to find aggregate TFP in the distorted economy:

$$\begin{aligned}\text{TFP}_{nt} &:= \frac{Y_{nt}}{K_{nt}^{\alpha_{Kn}}L_{nt}^{\alpha_{Ln}}}\\ \log TFP_{nt} &= \alpha_{K_n}\log\frac{Y_{nt}}{K_{nt}} + \alpha_{L_n}\log\frac{Y_{nt}}{L_{nt}}\\ &= \frac{\sigma_n}{\sigma_n-1}\log I_{nt} - \alpha_{K_n}\log J_{nt} - \alpha_{L_n}\log Q_{nt}\end{aligned}$$

where

$$\log I_{nt} = \log\int_i B_{nit}\left\{A_{nit}(1-\tau^Y_{ni}(\tilde{\mathbf{T}}_{rt},\cdot))\left[\frac{1}{(1+\tau^K_{ni}(\tilde{\mathbf{T}}_{rt},\cdot))}\right]^{\alpha_{Kn}}\left[\frac{1}{(1+\tau^L_{ni}(\tilde{\mathbf{T}}_{rt},\cdot))}\right]^{\alpha_{Ln}}\right\}^{\sigma_n-1}$$
$$\log J_{nt} = \log\int_i \left[(1-\tau^Y_{ni}(\tilde{\mathbf{T}}_{rt},\cdot))\right]^{\sigma_n} B_{nit}\frac{1}{(1+\tau^K_{ni}(\tilde{\mathbf{T}}_{rt},\cdot))}\left\{A_{nit}\left[\frac{1}{(1+\tau^K_{ni}(\tilde{\mathbf{T}}_{rt},\cdot))}\right]^{\alpha_{Kn}}\left[\frac{1}{(1+\tau^L_{ni}(\tilde{\mathbf{T}}_{rt},\cdot))}\right]^{\alpha_{Ln}}\right\}^{\sigma_n-1}$$
$$\log Q_{nt} = \log\int_i \left[(1-\tau^Y_{ni}(\tilde{\mathbf{T}}_{rt},\cdot))\right]^{\sigma_n} B_{nit}\frac{1}{(1+\tau^L_{ni}(\tilde{\mathbf{T}}_{rt},\cdot))}\left\{A_{nit}\left[\frac{1}{(1+\tau^K_{ni}(\tilde{\mathbf{T}}_{rt},\cdot))}\right]^{\alpha_{Kn}}\left[\frac{1}{(1+\tau^L_{ni}(\tilde{\mathbf{T}}_{rt},\cdot))}\right]^{\alpha_{Ln}}\right\}^{\sigma_n-1}$$

We use the following second-order approximation. Let x_i be any firm-level term and normalize the measure so that $\int di = 1$ (so $\int \cdot\, di = \mathbb{E}[\cdot]$). Define

$$\mu \equiv \mathbb{E}[x_i], \qquad \tilde{x}_i \equiv x_i - \mu, \qquad \mathbb{E}[\tilde{x}_i] = 0.$$

Then

$$\ln\left(\int e^{x_i}\,di\right) = \ln\left(\int e^{\mu+\tilde{x}_i}\,di\right) = \mu + \ln\left(\int e^{\tilde{x}_i}\,di\right).$$

A second-order expansion of $e^{\tilde{x}_i}$ around zero implies

$$\int e^{\tilde{x}_i}\, di \approx \int \left(1 + \tilde{x}_i + \frac{1}{2}\tilde{x}_i^2\right) di = 1 + \frac{1}{2}\mathbb{E}[\tilde{x}_i^2] = 1 + \frac{1}{2}\mathbb{VAR}(x_i).$$

Next, apply the second-order expansion of $\ln(1+u)$:

$$\ln(1+u) = u - \frac{u^2}{2} + O(u^3), \qquad u = \frac{1}{2}\mathbb{VAR}(x_i),$$

to obtain

$$\ln\left(\int e^{\tilde{x}_i}\, di\right) = \ln\left(1 + \frac{1}{2}\mathbb{VAR}(x_i)\right) = \frac{1}{2}\mathbb{VAR}(x_i) - \frac{1}{8}\mathbb{VAR}(x_i)^2 + O\big(\mathbb{VAR}(x_i)^3\big)\,.$$

Combining terms yields

$$\ln\left(\int e^{x_i}\, di\right) = \mathbb{E}[x_i] + \frac{1}{2}\mathbb{VAR}(x_i) - \frac{1}{8}\mathbb{VAR}(x_i)^2 + O\big(\mathbb{VAR}(x_i)^3\big)\,.$$

Writing $x_i = \mu + \varepsilon z_i$ with $\mathbb{E}[z_i] = 0$ and $\mathbb{VAR}(z_i) = 1$ implies $\mathbb{VAR}(x_i) = \varepsilon^2$, so $\mathbb{VAR}(x_i)^2 = O(\varepsilon^4)$. Hence, under a second-order approximation,

$$\ln\left(\int e^{x_i}\, di\right) = \mathbb{E}[x_i] + \frac{1}{2}\mathbb{VAR}(x_i) + O(\varepsilon^4),$$

For a multivariate case when x_i is a sum of logs, $x_i = \log A_i + \log B_i + \log C_i$, this implies

$$\begin{aligned}\ln\left(\int e^{\log A_i + \log B_i + \log C_i}\, di\right) \approx\ & \mathbb{E}[\log A_i] + \mathbb{E}[\log B_i] + \mathbb{E}[\log C_i] \\ & + \frac{1}{2}\mathbb{VAR}(\log A_i) + \frac{1}{2}\mathbb{VAR}(\log B_i) + \frac{1}{2}\mathbb{VAR}(\log C_i) \\ & + \mathbb{COV}(\log A_i, \log B_i) + \mathbb{COV}(\log A_i, \log C_i) + \mathbb{COV}(\log B_i, \log C_i).\end{aligned}$$

We apply this second-order approximation to all the $\log I_{nt}, \log J_{nt}, \log Q_{nt}$ to obtain

$$\begin{aligned}\log \mathrm{TFP}_n(\tilde{\mathbf{T}}_{rt}, \cdot) =\ & \underbrace{\frac{1}{\sigma_n - 1}\log \mathbb{E}_i\left[B_{ni}(\tilde{\mathbf{T}}_{rt}, \cdot)\left(A_{ni}(\tilde{\mathbf{T}}_{rt}, \cdot)\right)^{\sigma_n - 1}\right]}_{\text{Technology}(\log \mathrm{TFP}_n^E)} - \underbrace{\frac{\sigma_n}{2}\operatorname{var}_{\log\left(1-\tau_{ni}^Y\right)}(\tilde{\mathbf{T}}_{rt}, \cdot)}_{\text{Output Wedge Dispersion}} \\ & \underbrace{- \sum_{F \in \{K,L\}} \frac{\alpha_{Fn} + \alpha_{Fn}^2(\sigma_n - 1)}{2} \operatorname{var}_{\log\left(1+\tau_{ni}^F\right)}(\tilde{\mathbf{T}}_{rt}, \cdot)}_{\text{Factor Wedge Dispersion}} \\ & \underbrace{+ \sigma_n \sum_{F \in \{K,L\}} \alpha_{Fn} \operatorname{cov}_{\log\left(1-\tau_{ni}^Y\right), \log\left(1+\tau_{ni}^F\right)}\left(\tilde{\mathbf{T}}_{rt}, \cdot\right)}_{\text{Output-Factor Mixed Distortion}} \\ & \underbrace{- (\sigma_n - 1)\alpha_{Kn}\alpha_{Ln} \operatorname{cov}_{\log\left(1+\tau_{ni}^K\right), \log\left(1+\tau_{ni}^L\right)}\left(\tilde{\mathbf{T}}_{rt}, \cdot\right)}_{\text{Factor Mixed Distortion}}\end{aligned} \tag{49}$$

which is the Equation 9 in the text.

■

B Data Sources and Variable Construction

This appendix provides details on data sources and variable constructions.

B.1 Orbis Data

Our data of firms from the European countries comes from the Orbis historical Disk Product. We use the sample period 1995-2018 for our analysis. We detail the cleaning process below.

Sample Cleaning. Following the procedure of Kalemli- Özcan et al. (2024), we link multiple vintages of Orbis products over time and link the firm's descriptive information with its financial information via the unique BVD firm identifier (BVDID). We then apply the following standard cleaning procedure:

1. We restrict our analysis to firms that satisfy the following criteria: the country they reside in from their latest address matches with their ISO codes in their BVDID identifier. For example, if the firm's ISO-2 code in BVDID is FR while its latest address is in Spain, then we exclude this firm from our sample.

2. For some firms that lack address information but have other identifiers such as postcodes, we manually map the postcodes to NUTS3 for each country.

3. We harmonize each firm's fiscal year with the calendar year based on the closing date: if the closing date is on or after July 1st, we use the current year as the calendar year; otherwise, we use the previous year.

4. Firms may report multiple sales figures from different sources (like local registries, annual reports, etc.) for consolidated or unconsolidated accounts. Following Fan (2024), we use the unconsolidated accounts to avoid double-counting that can occur with consolidated accounts.

5. We only keep firms with non-missing and positive sales (`operating_revenue_turnover`) and fixed assets (`fixed_assets`).

6. We calculate firm-level MRPK_{it} for firm i in year t as $\log \text{MRPK}_{it} = \log(\alpha_{Kn} \frac{\sigma_n - 1}{\sigma_n} \frac{P_{it} Y_{it}}{K_{it}})$ where $P_{it} Y_{it}$ is measured with sales and K_{it} is measured with fixed assets.

7. We winsorize the observations of MRPK_{it}, fixed assets, or sales at the top and bottom 0.1% of the distribution in the entire panel for each country. This is to prevent outliers from affecting the variance calculation and estimation.

B.2 China NBS Data

The annual firm-level data for China is derived from surveys conducted by the National Bureau of Statistics (NBS) in China. We only use the sample period of 1998-2007 due to inconsistent reporting after 2008 as discussed in Brandt, Van Biesebroeck, and Zhang (2014) and Nath (2025).

Sample Cleaning. To process the NBS data, we follow the methodology outlined in Zhang et al. (2018). We measure sales using the variable "产品销售收入" (product sales revenue) and capital using the variable "固定资产合计" (total fixed assets). Each firm in the dataset is categorized using a four-digit Chinese Industry Classification (CIC) code and is harmonized to the USSIC division level. Each firm's reported location can be mapped into a prefecture-level division. The rest of the cleaning follows the same procedure as items 5-7 in Appendix B.1.

B.3 India ASI Data

Our data for India are drawn from India's Annual Survey of Industries (ASI). We use the sample period of 1998 to 2018.

Sample Cleaning. We match the plants to the Indian districts following the approach of Somanathan et al. (2021) and harmonize the industries first to the NIC-04 classification, and then to the SIC division level. We measure sales using the gross sale value of all products and capital using an average of the opening and closing gross book value of total capital, as in Bils, Klenow, and Ruane (2021). The rest of the cleaning follows the same procedure as items 5-7 in Appendix B.1.

B.4 Additional Descriptive Statistics

The table below lists out the countries, year coverage, number of regions in each country, and the total number of firm-year pair observations in the final sample we used for the empirical analysis.

Table B.1: Descriptive Table of Dataset by Country

Dataset	Country	Coverage	Number of Regions	Number of Firm-Year Obs
NBS China Industrial	China	1998-2007	325	2069100
India ASI	India	1998-2017	267	473646
	Austria	2004-2018	34	185029
	Belgium	1998-2018	44	781322
	Bulgaria	1998-2018	28	1439871
	Switzerland	2003-2018	3	1701
	Cyprus	2005-2018	1	17356
	Czech Republic	1998-2018	14	1425901
	Germany	1998-2018	346	765981
	Denmark	1999-2018	11	392015
	Estonia	1998-2018	5	791340
	Greece	1998-2018	44	342636
	Spain	1998-2018	52	12210663
	Finland	1998-2018	19	1909080
	France	1998-2018	96	15151185
	Croatia	1998-2018	21	1202515
BvD Orbis	Hungary	2004-2018	20	3095326
	Ireland	2000-2018	8	115344
	Italy	1998-2018	107	12083926
	Lithuania	1998-2018	10	129442
	Luxembourg	1998-2018	1	74287
	Latvia	2010-2018	6	533640
	Malta	2000-2018	1	21249
	Netherlands	1998-2018	36	201182
	Norway	1998-2018	12	2462277
	Poland	1998-2018	73	1207428
	Portugal	1998-2018	24	3882515
	Romania	1998-2018	42	4636047
	Sweden	1998-2018	21	3934403
	Slovenia	1998-2018	12	744495
	Slovakia	1998-2018	8	1008353
	United Kingdom	1998-2018	178	3537701

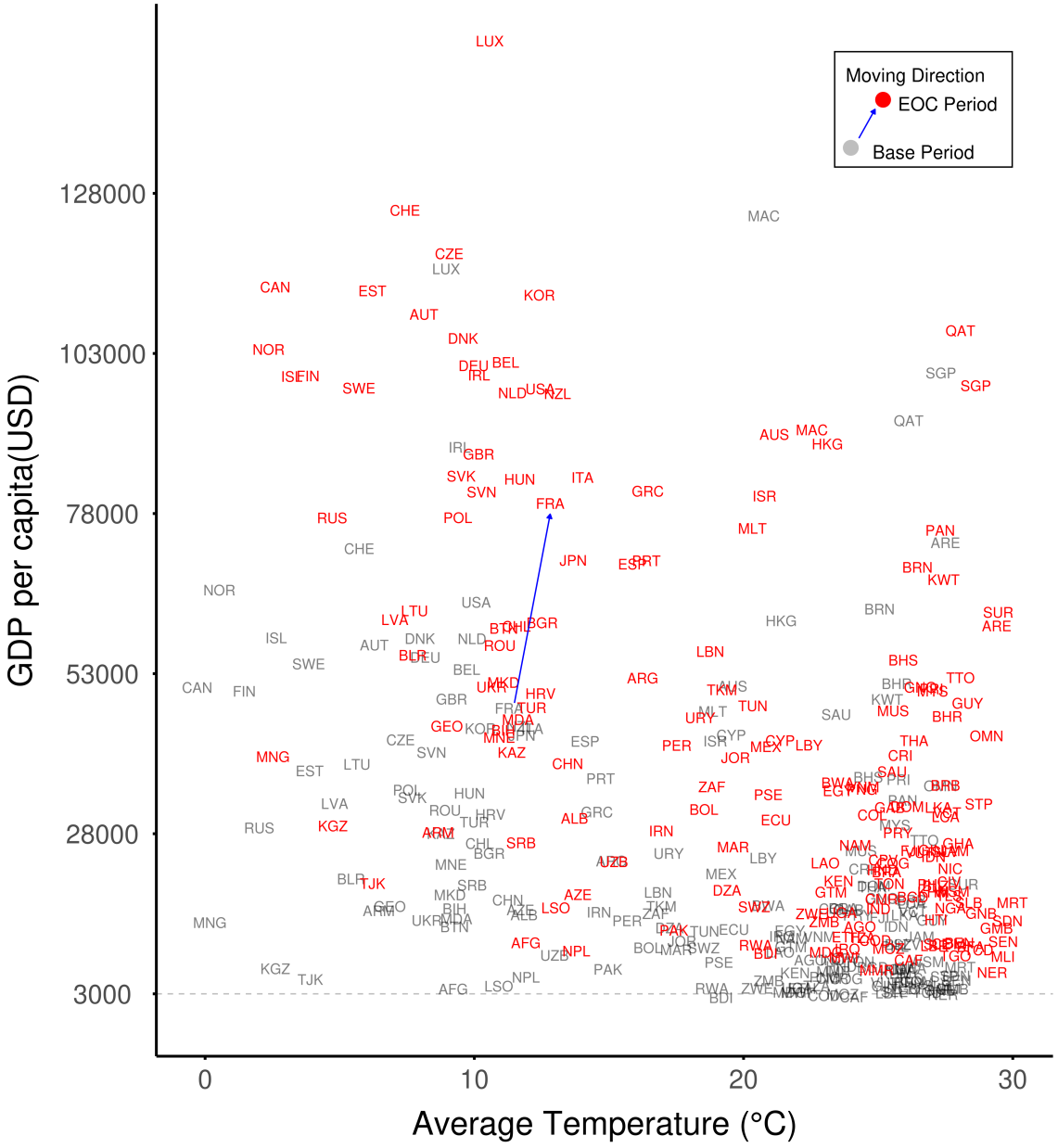
C Additional Figures for Section 4

This appendix provides additional results and figures to complement the main analysis in Section 4.

C.1 Projected Evolution of Income and Temperature under SSP3-4.5

The figure illustrates the projected evolution of income and average temperature from the 2000-2014 baseline to the end of the century (2081-2100) under the SSP3-4.5 scenarios. Among the 172 countries, All 172 countries show a rightward shift (indicating an increase in temperature), and 96% of them also show an upward shift (indicating an increase in per-capita income). In the baseline period, average temperatures are below 5°C in 11 countries, between 5-15°C in 49 countries, between 15-25°C in 62 countries, and above 25°C in 50 countries. Baseline per capita income is below $5000 in 41 countries, between $5000-$30000 in 83 countries, between $30000-$60000 in 38 countries and above $60000 in 10 countries. The blue arrow exemplifies the joint evolution of income and temperature.

Figure C.1: Joint Evolution of Income and Average Temperature from Base Period to End of Century (under SSP3-4.5)



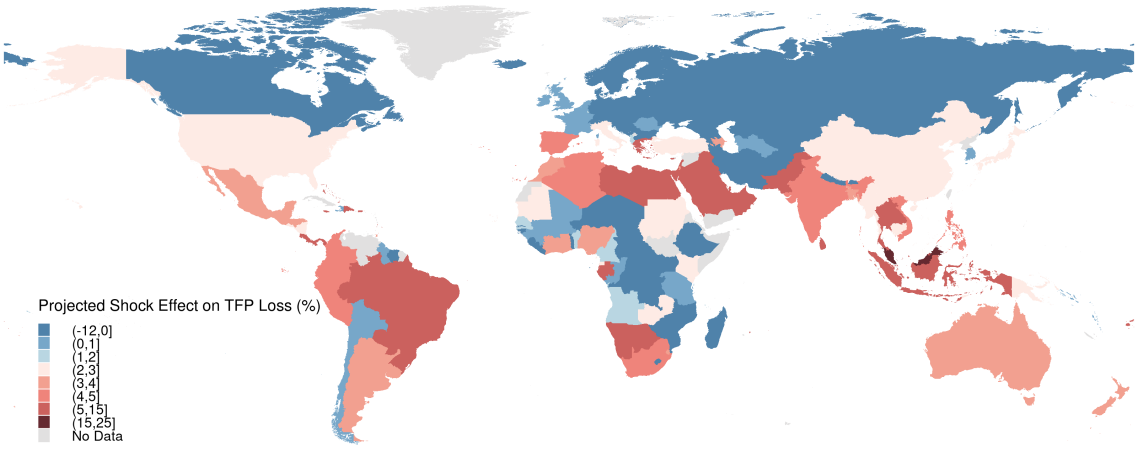
Notes: Grey texts represent the baseline period from 2000 to 2014, and the red texts represent the end of the century (2081 - 2100). End-of-century projection comes from SSP3-4.5 projection. The graph shows the joint evolution of income per capita and average temperature for each country.

C.2 Projection Components

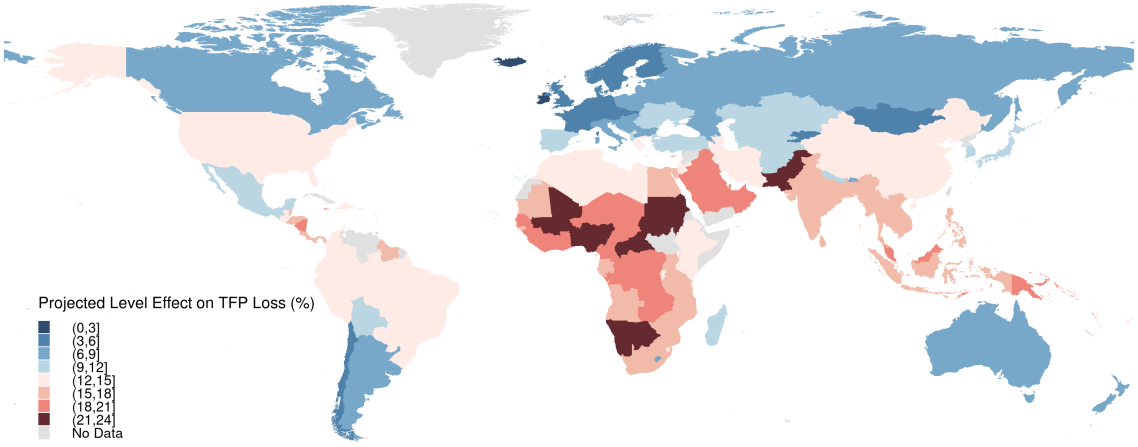
The graph shows a breakdown of the three effects contributing to the total projected TFP loss under SSP3-4.5 scenarios in Section 4.6.

Figure C.2: Three Effects Contribution to Projected TFP Loss (SSP3-4.5)

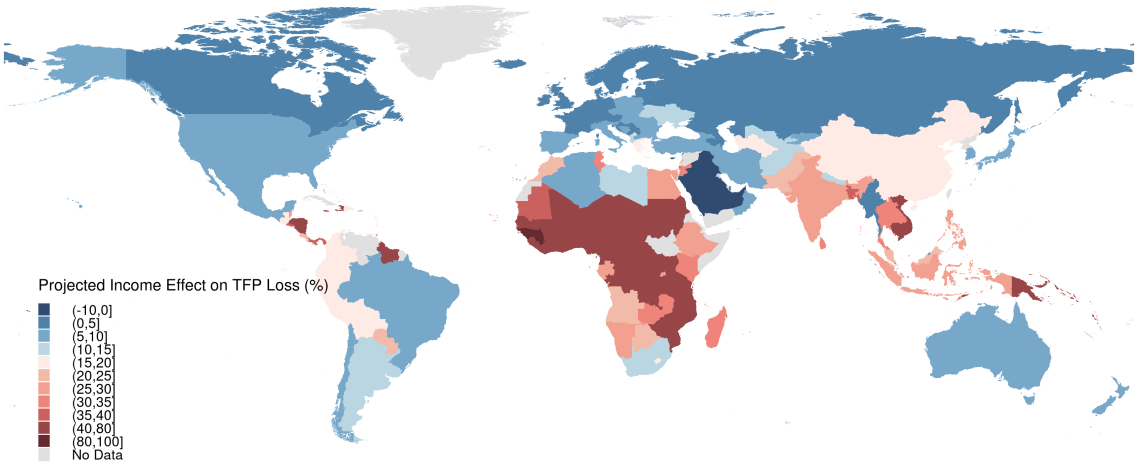
(a) Shock Effects Projection



(b) Level Effects Projection



(c) Income Effects Projection



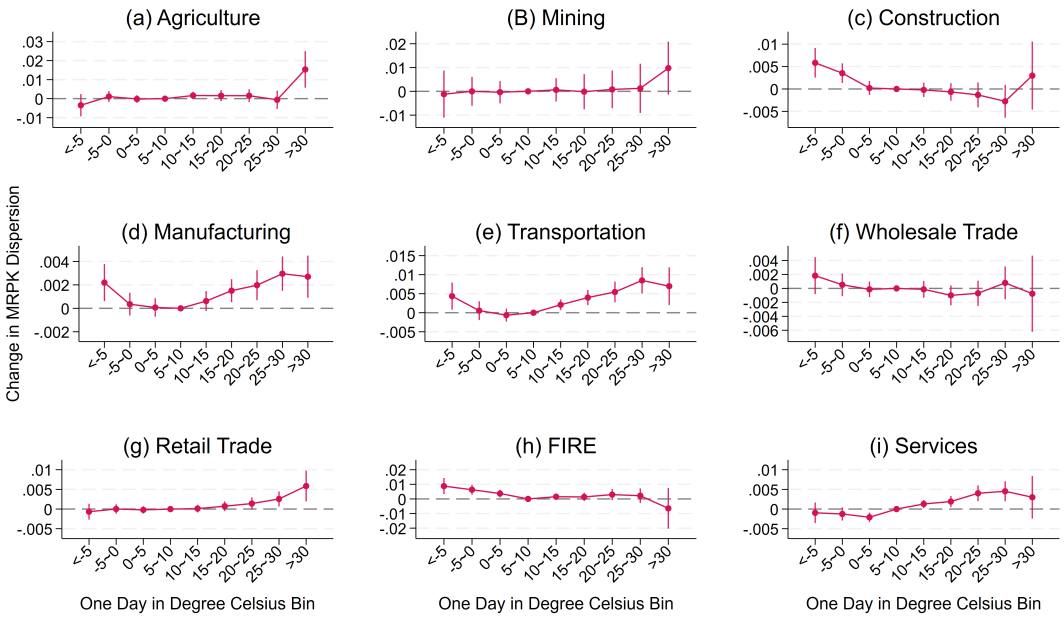
D Robustness for the Empirical Results in Section 4

In this appendix, we display a battery of robustness exercises to replicate Figure 1 and 3 in the paper under alternative specifications and discuss its sectoral heterogeneity.

D.1 Sectoral Results

This section reports the average effects of daily temperature shocks on regional MRPK dispersion across SIC divisions. We find that extreme heat (above $25/30°C$) significantly increases MRPK dispersion in agriculture, manufacturing, transportation, services, and retail trade, whereas the effects are modest in mining, construction, wholesale trade, and FIRE.

Figure D.3: Estimated impact of daily temperature shocks on annual MRPK dispersion by SIC Divisions



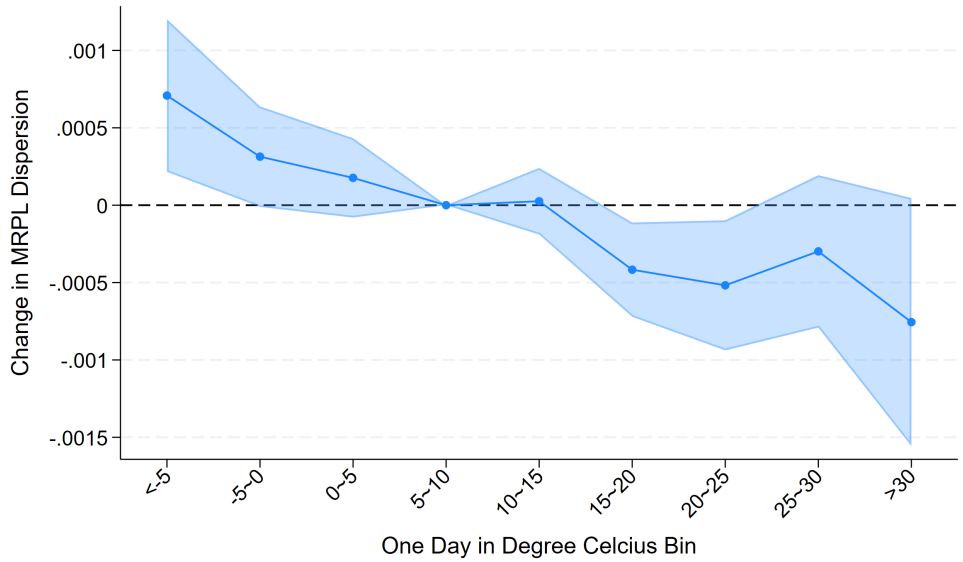
D.2 Temperature's Impact on other marginal product dispersions

We find insignificant effect of heat shocks on the MRPL and MRPM dispersion.

D.2.1 MRPL Dispersion

Extreme cold leads to a slight increase in MRPL dispersion, while extreme heat leads to a decrease in MRPL dispersion at 15-20 °C and 20-25 °C , and insignificant effect at hotter than 25 °C .

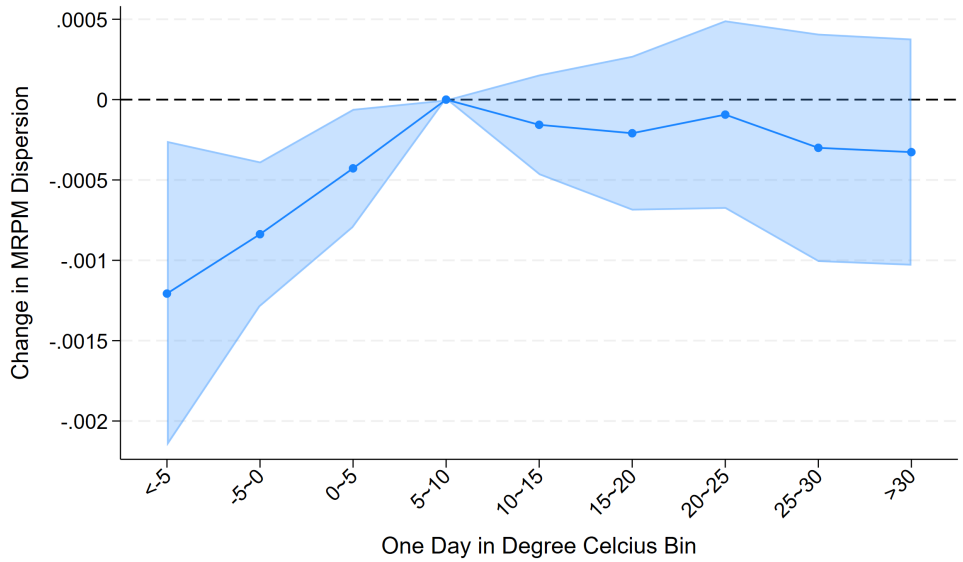
Figure D.4: Estimated impact of daily temperature shocks on annual MRPL dispersion



D.2.2 MRPM Dispersion

Extreme cold leads to a decrease in MRPM. Hot temperatures lead to insignificant impact on MRPM dispersion.

Figure D.5: Estimated impact of daily temperature shocks on annual MRPM dispersion

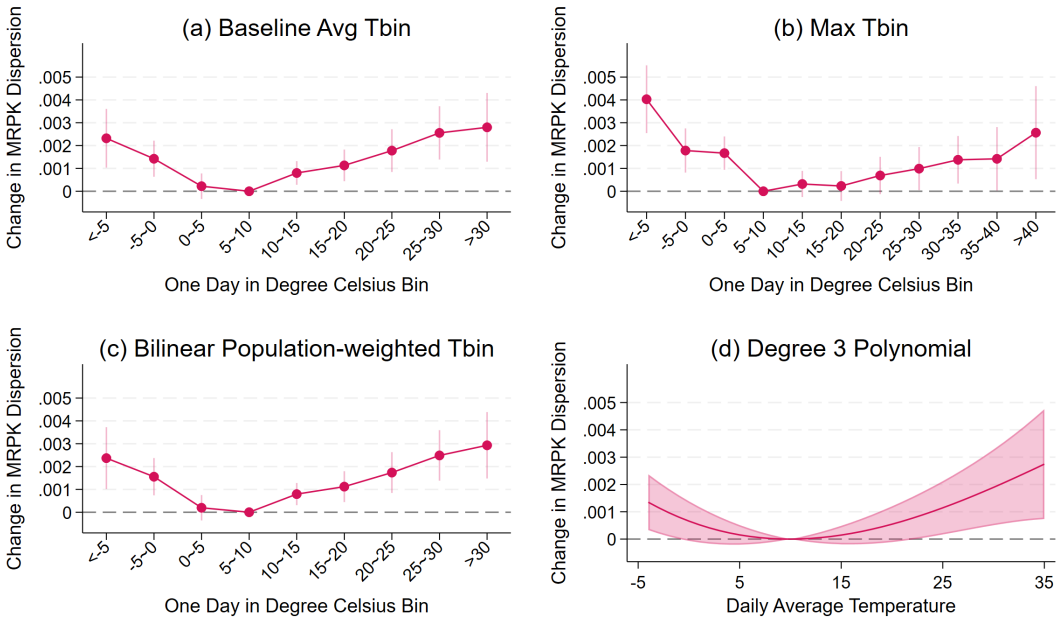


D.3 Other weather variables and weather variable weighting

Panel (a) is the baseline results as in the main text. Panel (b) uses the maximum temperature to calculate temperature bins, as you'd imagine that daily maximum temperature is higher than average maximum temperature, we have more temperature bins at higher than 30, 35 and 40, and we use a different sets of temperature bins to cover the new weather distribution. Panel (c) uses

the population weighted average temperature bins. Panel (d) uses a third polynomial average temperature.

Figure D.6: Robustness with Alternative Weather Variables



Notes:

D.4 Alternative Standard Error clustering

Figure **??** reports alternative standard-error specifications: clustering by region, two-way clustering by region and year, and two-way clustering by region and country–year. Figure D.8 shows robustness to spatial HAC standard errors. Our results remain statistically significant even when allowing for spatial correlation up to a cutoff distance of 1,000 km.

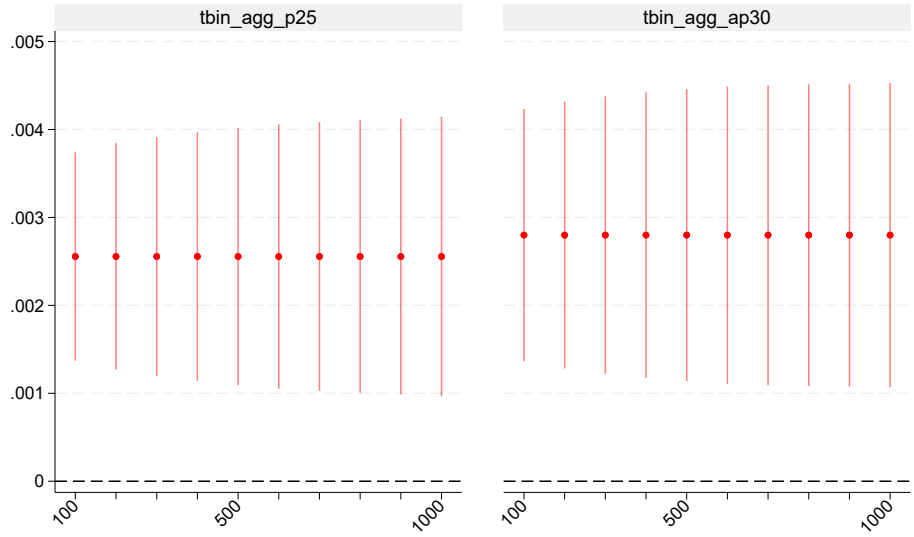
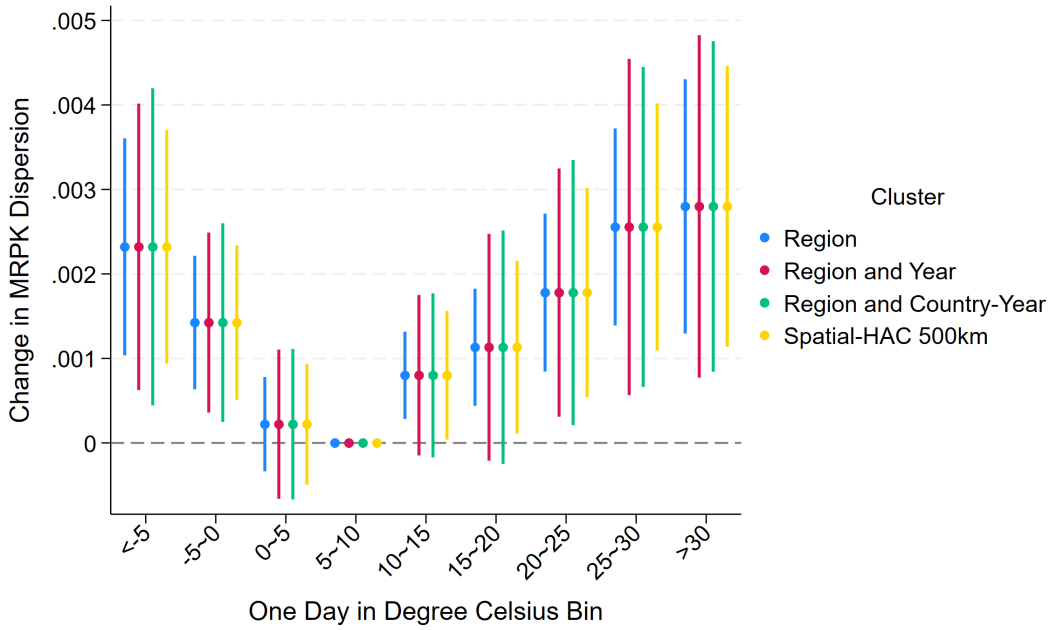


Figure D.8: Robustness with Alternative Distance Cutoffs under Spatail HAC

Figure D.7: Robustness with Alternative Standard Error clustering



D.5 Use different sigma alpha values to calculate TFP losses

sigma, elasticity of substitution, in the main text it's four right now alpha, labor share, in the main text calculation it's 0.35 should try a different combination of values and plot all on the same graph so people can see if there's differences

D.6 Alternative Region-Sector Definitions

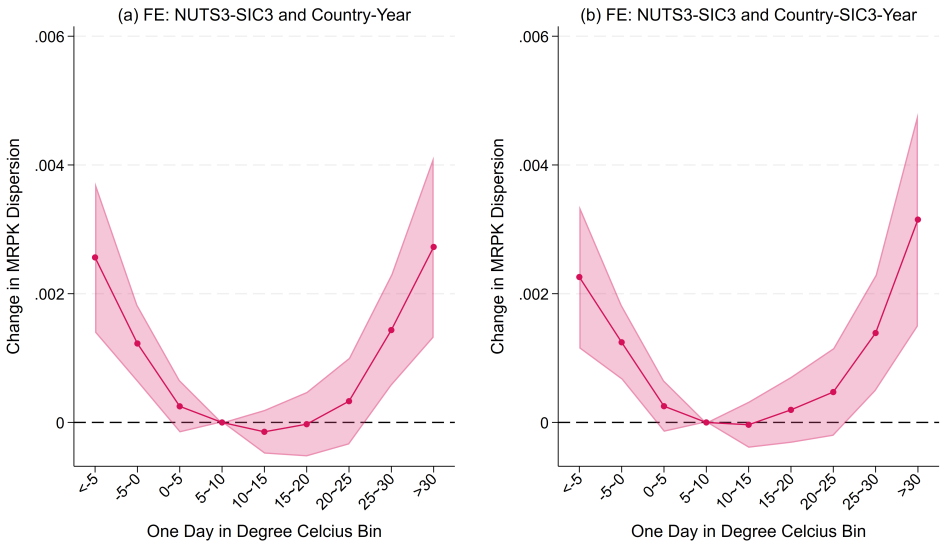
NUTS3–SIC2. We redefine the region–sector unit as NUTS 3 $\times$ SIC 2 (two-digit). We recompute $\mathrm{Var}(\mathrm{MRPK})$ under this alternative definition and re-estimate the main specifications. The results are quantitatively very similar to the baseline.

Figure D.9: Results Using NUTS3–SIC2 as the Region–Sector Unit, Under Alternative Fixed Effects



NUTS3–SIC3 . For European countries, we additionally redefine the region–sector unit as NUTS3 $\times$ SIC3. We then recompute the variance of MRPK and re-estimate the main specifications under this alternative definition.

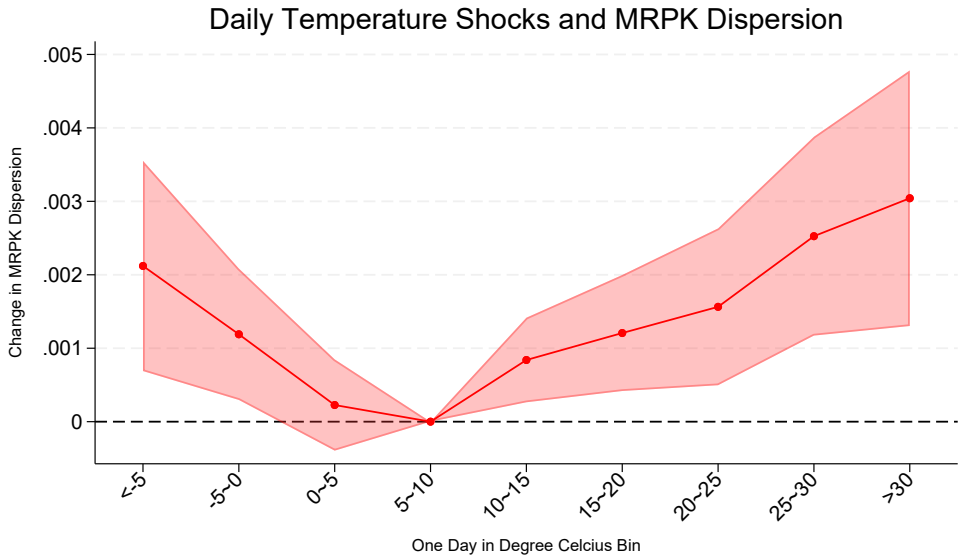
Figure D.10: Results Using NUTS3–SIC3 as the Region–Sector Unit, Under Alternative Fixed Effects



D.7 Alternative Winsorization

We winsorize the MRPK at the 3% level before computing the variance at the region-sector-year level and re-estimate the baseline specifications. The results are very similar to the main findings.

Figure D.11: Estimated Effects of Daily Temperature Shocks on Annual MRPK Dispersion: 3% Winsorized MRPK



D.8 Different production specification

We now explore other possible methods to identify and estimate var $(mrpk_{nit})$. Specifically, we incorporate a more general specification, the CES production function and allow for factor-augmenting productivity.

D.8.1 CES with neutral factor augmenting productivity

We start with a basic two-input CES production function

$$Y_{it} = A_{it}\left[\gamma K_{it}^{\frac{\sigma-1}{\sigma}} + (1-\gamma)B_{it}L_{it}^{\frac{\sigma-1}{\sigma}}\right]_{it}^{\frac{\sigma}{\sigma-1}},$$

where A_{it} is the factor-neutral productivity and σ is the elasticity of substitution between capital and labor. Assume that the hicks-neutral productivity is heterogeneous across firms with firm-specific temperature sensitivity with the following form $A_{it} = \tilde{A}_{it}e^{a_{it}T_{rt}}$, and that labor-augmenting productivity has firm-specific component $\tilde{B}_{it}$ and common temperature sensitivity within region sector in the following form $B_{it} = \tilde{B}_{it}e^{b_{nt}T_{rt}}$. When $\sigma \to 1$, the production becomes Cobb-Douglas. Subject to the inverse demand and capital wedges, each firm i engages in monopolistic competition and optimally chooses its quantity of inputs and price to maximize

profits:

$$\max_{K_{it},L_{it}} A_{it}\left[\gamma K_{it}^{\frac{\sigma-1}{\sigma}}+(1-\gamma)B_{it}L_{it}^{\frac{\sigma-1}{\sigma}}\right]^{\frac{\sigma}{\sigma-1}}-wL_{it}-(1+\tau_{it}^{k})rK_{it}$$

$$\text{subject to}\quad Y_{it}=Y_t(\frac{P_t}{P_{it}})^{\sigma_n},$$

where σ_n is the elasticity of demand.

The two FOCs are

$$P_t Y_t^{\frac{1}{\sigma_n}}\frac{\sigma_n-1}{\sigma_n}Y_{it}^{-\frac{1}{\sigma_n}}Y_{it}^{\frac{1}{\sigma}}A_{it}^{\frac{\sigma-1}{\sigma}}\gamma K_{it}^{-\frac{1}{\sigma}}=(1+\tau_{it}^{k})r$$
$$P_t Y_t^{\frac{1}{\sigma_n}}\frac{\sigma_n-1}{\sigma_n}Y_{it}^{-\frac{1}{\sigma_n}}Y_{it}^{\frac{1}{\sigma}}(1-\gamma)A_{it}^{\frac{\sigma-1}{\sigma}}(B_{it}L_{it})^{\frac{-1}{\sigma}}B_{it}=w$$

The log ratios of the two FOC give us

$$\log\left(\frac{\gamma}{1-\gamma}\frac{K_{it}^{-\frac{1}{\sigma}}}{B_{it}^{\frac{\sigma-1}{\sigma}}L_{it}^{\frac{-1}{\sigma}}}\right)=\log\frac{(1+\tau_{it}^{k})r}{w}$$

We rearrange terms to move $\log\frac{L_{it}}{K_{it}}$ to one side

$$\begin{aligned}\frac{1}{\sigma}\log\frac{L_{it}}{K_{it}}&=\log(1+\tau_{it}^{k})+\frac{\sigma-1}{\sigma}\log B_{it}+\log r-\log w-\log\frac{\gamma}{1-\gamma}\\&=\log(1+\tau_{it}^{k})+\frac{\sigma-1}{\sigma}\log\tilde{B}_{it}+\frac{\sigma-1}{\sigma}b_{nt}T_{rt}+\log r-\log w-\log\frac{\gamma}{1-\gamma}\end{aligned}$$

Within a narrowly-defined region-sector, we assume rental prices and wages are the same. Therefore when we calculate the variance of MRPK within a region-sector, the constants won't affect the value of the variance.

$$\frac{1}{\sigma^2}var(\log\frac{L_{it}}{K_{it}})=var(\log(1+\tau_{it}^{k}))+(\frac{\sigma-1}{\sigma})^2var(\log\tilde{B}_{it})+2\frac{\sigma-1}{\sigma^2}cov(\log(1+\tau_{it}^{k}),\log\tilde{B}_{it})$$

We further assume that firm-specific productivity is orthogonal to temperature so that $\frac{dvar(\log\tilde{B}_{it})}{dT}=0$. And $\frac{dcov(\log(1+\tau_{it}^{k}),\log\tilde{B}_{it})}{dT}=0$ holds true if $cov(\log(1+\tau_{it}^{k})T_{rt}-\log(1+\tau_{it}^{k})T_{r0},\log\tilde{B}_{it})=0$. Eventually, the effect of temperature on region-sector dispersion is

$$\frac{dvar(\log(1+\tau_{it}^{k}))}{dT}=\frac{1}{\sigma^2}\frac{dvar(\log\frac{L_{it}}{K_{it}})}{dT}.$$

The dispersion of log MRPK is then computed via the variance of log number of employees (or costs of employees) over capital stock within a region-sector-year.

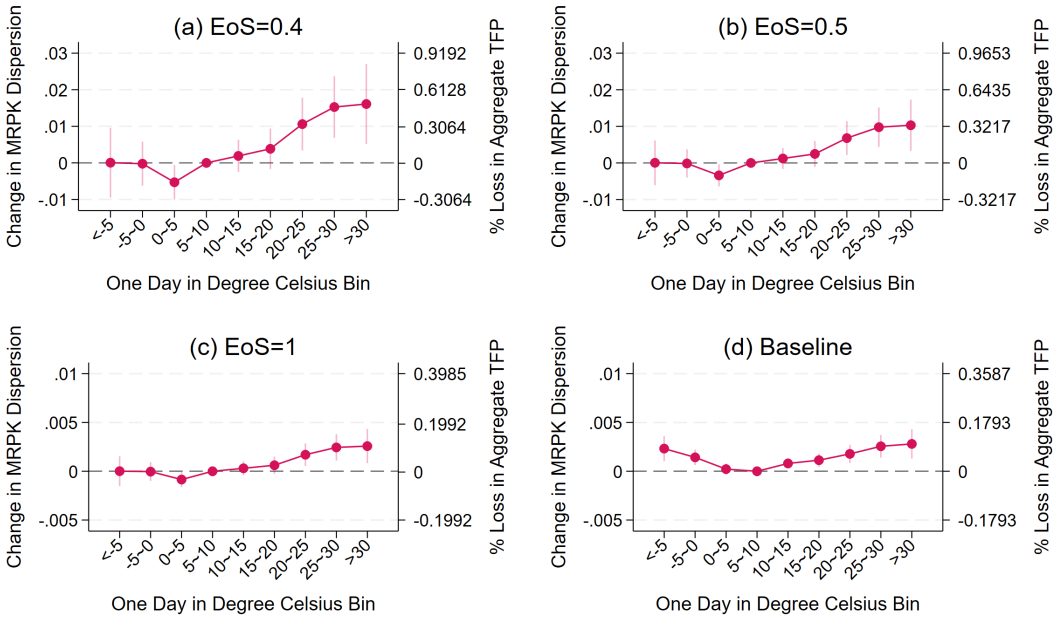
TFP losses. Following Baqaee and Farhi (2019), under a CES production function over capital and labor, the associated TFP loss implied by changes in MRPK dispersion is

$$\left[\frac{(\sigma_n-1)\alpha_K^2+\alpha_K^2+EoS\cdot\alpha_K(1-\alpha_K)}{2}\right]\hat{\lambda}^{b}_{\sigma^2_{mrpk}},$$

where $EoS \equiv \sigma$ denotes the elasticity of substitution between capital and labor.

Regression Results. The estimation results are shown in Figure D.12 under different cases of elasticity of substitution.

Figure D.12: Estimated impact of daily temperature shocks on annual MRPK dispersion under CES and hicks-neutral productivity



Notes: The formula for computing TFP losses from MRPK dispersion changes when the elasticity of substitution between capital and labor changes. The baseline figure also has elasticity of substitution equals 1 under Cobb-Douglas, and the difference between the panel (c) and (d) is that the MRPK in (c) is calculated as labor-capital ratio, and in (d) is calculated as sales-capital ratio. $\sigma = 0.4$ is the IV estimates from LRX, and $\sigma = 0.5$ is the average estimates across specification from micro-macro.

D.8.2 CES with labor augmenting factor productivity

We now incorporate labor factor-augmenting productivity. To be able to still estimate $var(mrpk)$ we include a third production factor M_{it}, material input. Subject to the inverse demand and capital wedges, each firm i engages in monopolistic competition and optimally chooses its quantity of inputs and price to maximize profits:

$$\max_{K_{it},L_{it}} A_{it}\left[(K_{it})^{\frac{\sigma-1}{\sigma}} + (B_{it}L_{it})^{\frac{\sigma-1}{\sigma}} + (M_{it})^{\frac{\sigma-1}{\sigma}}\right]^{\frac{\sigma}{\sigma-1}} - wL_{it} - p^m M_{it} - (1+\tau_{it}^k)rK_{it}$$

$$\text{subject to} \quad Y_{it} = Y_t\left(\frac{P_t}{P_{it}}\right)^{\varepsilon},$$

where B_{it} is the labor-augmenting productivity and ε is the elasticity of demand. The three FOCs can be written as

$$P_t Y_t^{\frac{1}{\varepsilon}} \frac{\varepsilon - 1}{\varepsilon} Y_{it}^{-\frac{1}{\varepsilon}} A_{it}^{\frac{\sigma-1}{\sigma}} Y_{it}^{\frac{1}{\sigma}} (K_{it})^{\frac{-1}{\sigma}} = (1 + \tau_k) r$$
$$P_t Y_t^{\frac{1}{\varepsilon}} \frac{\varepsilon - 1}{\varepsilon} Y_{it}^{-\frac{1}{\varepsilon}} Y_{it}^{\frac{1}{\sigma}} A_{it}^{\frac{\sigma-1}{\sigma}} (B_{it} L_{it})^{\frac{-1}{\sigma}} B_{it} = w$$
$$P_t Y_t^{\frac{1}{\varepsilon}} \frac{\varepsilon - 1}{\varepsilon} Y_{it}^{-\frac{1}{\varepsilon}} Y_{it}^{\frac{1}{\sigma}} A_{it}^{\frac{\sigma-1}{\sigma}} (M_{it})^{\frac{-1}{\sigma}} = p^m$$

We take logs to the three pairs of ratios of the FOC conditions and obtain

$$\log L_{it} - \log K_{it} = \sigma \log(1 + \tau_k) + \sigma (\log r - \log w) + (\sigma - 1) \log B_{it}$$
$$\log M_{it} - \log L_{it} = \sigma (\log w - \log p^m) - (\sigma - 1) \log B_{it}$$
$$\log M_{it} - \log K_{it} = \sigma \log(1 + \tau_k) + \sigma (\log r - \log p^m)$$

From which we can cancel $\log B_{it}$ and obtain

$$\log(1 + \tau_k) = \frac{1}{\sigma} \log \frac{M_{it}}{K_{it}} + \log \frac{p^m}{r}.$$

Now similarly to the scenario above, we assume material prices and rental rates are the same across firms within a region-sector-year. Therefore the price ratio will be a constant and won't affect the variance calculation. We can calculate capital wedge dispersion with equation

$$var(\log(1 + \tau_{it}^k)) = \frac{1}{\sigma^2} var(\log \frac{M_{it}}{K_{it}}).$$

The dispersion of log MRPK is then computed via the variance of log material costs over capital stock within a region-sector-year.

Regression Results. The estimation results are shown in Figure D.13 under different cases of elasticity of substitution.

Figure D.13: Estimated impact of daily temperature shocks on annual MRPK dispersion

